FTD-HC-23-643-70

FOREIGN TECHNOLOGY DIVISION

THIS IS AN UNEDITED ROUGH DRAFT TRANSLATION BY JOINT PUBLICATIONS RESEARCH SERVICES

TECHNIQUE OF SHAPING HIGH-VOLTAGE NANOSECOND PULSES

By

G. A. Vorob'yev, G. A. Mesyats

UNCLASSIFIED

Security Classification

DOCUMENT CONTROL DATA - R & D

(Security classification of title, body of abstract and indexing annotation must be entered when the overall report is classified)

1. ORIGINATING ACTIVITY (Corporate author) Foreign Technology Division Air Force Systems Command U. S. Air Force	2a. REPORT SECURITY CLASSIFICATION UNCLASSIFIED 2b. GROUP

3. REPORT TITLE

TECHNIQUE OF SHAPING HIGH-VOLTAGE NANOSECOND PULSES

4. DESCRIPTIVE NOTES (Type of report and inclusive dates)

Translation

5. AUTHOR(S) (First name, middle initial, last name)

Vorob'yev, G. A.; Mesyats, G. A.

6. REPORT DATE 1963	7a. TOTAL NO. OF PAGES 163	7b. NO. OF REFS 150
8a. CONTRACT OR GRANT NO. b. PROJECT NO. 6010201 c. d. DIA Task No. T66-01-8A	9a. ORIGINATOR'S REPORT NUMBER(S) FTD-HC-23-643-70 9b. OTHER REPORT NO(S) (Any other numbers that may be assigned this report)	

10. DISTRIBUTION STATEMENT

Distribution of this document is unlimited. It may be released to the Clearinghouse, Department of Commerce, for sale to the general public.

11. SUPPLEMENTARY NOTES	12. SPONSORING MILITARY ACTIVITY Foreign Technology Division Wright-Patterson AFB, Ohio

13. ABSTRACT

This monograph is the first attempt at a systematic presentation of material on the technique of shaping high-voltage nanosecond pulses. A considerable portion of the book is made up of the authors' works started at the high-voltage laboratory of Tomsk Polytechnic Institute in 1957 on the initiative of the Doctor of Physicomathematical Sciences Professor A. A. Vovob'yov. Description of devices for obtaining and converting the high-voltage nanosecond pulses is preceded by an analysis of the basic processes taking place in a spark with account taken of Weizel and Rompe theories and of the theory of streamer discharge and transient processes in a discharge circuit. The book is designed for scientific workers and engineers in appropriate fields and for students of higher educational institutions.

DD FORM 1 NOV 65 1473

UNCLASSIFIED

Security Classification

14 KEY WORDS	LINK A		LINK B		LINK C	
	ROLE	WT	ROLE	WT	ROLE	WT
Nanosecond Pulse Spark Discharge Discharge Circuit						

UNEDITED ROUGH DRAFT TRANSLATION

by Joint Publications Research Services

TECHNIQUE OF SHAPING HIGH-VOLTAGE NANOSECOND PULSES

By: G. A. Vorob'yev, G. A. Mesyats

English pages: 163

Source: Tekhnika Formirovaniya Vysokovol'tnykh Nanosekundnykh Impul'sov 1963, pp. 1-167

UR/0000-63-000-000

PREPARED BY:

TRANSLATION DIVISION
FOREIGN TECHNOLOGY DIVISION
WP-AFB, OHIO.

TECHNIQUE OF SHAPING HIGH-VOLTAGE NANOSECOND PULSES

/Book by G. A. Vorob'yov and G. A. Mesyats; Moscow, Tekhnika Formirovaniya Vysokovol'tnykh Nanosekundnykh Impul'sov, Russian, 1963, pp 1-167/

CONTENTS

CONTENTS (Continued) Page

UDC 621.374

This monograph is the first attempt at a systematic presentation of material on the technique of shaping high-voltage nanosecond pulses. A considerable portion of the book is made up of the authors' works started at the high-voltage laboratory of Tomsk Polytechnic Institute in 1957 on the initiative of the Doctor of Physicomathematical Sciences Professor A. A. Vorob'yov.

Description of devices for obtaining and converting the high-voltage nanosecond pulses is preceded by an analysis of the basic processes taking place in a spark with account taken of Weizel and Rompe theories and of the theory of streamer discharge and transient processes in a discharge circuit.

The book is designed for scientific workers and engineers in appropriate fields and for students of higher educational institutions.

FOREWORD

The progress of science calls for new requirements in regard to the pulse technique. From the pulses of millisecond duration, which were used in telegraphy, the pulse technique passed on to the microsecond pulses for the purposes of power engineering, radio engineering and radar and at the present time it deals with pulses of nanosecond duration (1 nanosecond=10^{-9} second) and shorter pulses. The nanosecond pulse technique may be divided into the technique of generating low-voltage pulses with an amplitude of a few hundred volts and lower and the technique of obtaining pulses with an amplitude of one, ten and hundred kilovolts.

Many works in the periodical press and also the monographs [1, 2] have been devoted to the methods of generating low-voltage short pulses. On the other hand, considerably fewer works have been devoted to the obtaining of high-voltage pulses of nanosecond duration in spite of the fact that the first investigations in this direction appeared 30-40 years ago [3-6]. This was explained on one hand by the fact that until 1950-1960 science and engineering did not show great interest in such pulses, and on the other hand — by the great difficulties encountered in obtaining and recording them. The harmonic spectrum of the nanosecond pulses extends up to super-high frequencies. Therefore, to generate and transmit these pulses it is necessary that the equipment used provide a wide frequency passband and at the same time be able to withstand high voltages without breakdown.

A number of areas in science and engineering can be named in which the high-voltage nanosecond pulses find an ever wider application.

In the acceleration technique [2, 7] these pulses are used for the injection of electrons into an accelerator, for a fast ejection of the accelerated particles, for obtaining a short-duration beam of charged particles, for investigation of the process of electron capture in the accelerator for a precise measurement of the energy of the particles, etc. Obtaining of short x-ray pulses necessary for pulsed testing of photomultipliers, for investigations in ballistics, etc. may also be included here.

In nuclear physics [2, 8] the high-voltage nanosecond pulses are

used for measuring the diffusion constants of neutrons, for the study of materials with a short lifetime, etc.

In radar [9, 10] the short pulses are used to determine short distances to targets with high accuracy.

In high-speed photography the high-voltage pulses of nanosecond duration together with electro-optical shutters and electronic optical converters are used for the investigation of super-fast processes. In particular, a discharge in gases is investigated in this manner: the rate of the development of electron avalanches [11, 12], expansion of the spark-discharge channel at the initial stage [13], the process of plasma formation during a spark discharge and explosion of the wire [14, 15].

In the physics of dielectrics and semiconductors the high-voltage pulses with a steep leading edge are used for the investigation of the kinetics of the breakdown process in solid, liquid and gaseous dielectrics, and also in semiconductors [16-19].

When using the short high-voltage pulses the strength of electric insulation increases by several times. Because of this, it is possible to reduce the dimensions of high-voltage installations [20, 21]. The use of these pulses for carrying out some of the high-voltage tests is also well known [22-24].

Hydrogen thyratrons and spark dischargers are used as commutators in the high-voltage nanosecond-pulse generators. The use of thyratrons is limited by a comparatively low anode voltage (about 30 kilovolts), a small operating current (less than 1 kiloampere), by large dimensions and by the commutation time (of the order of 10^{-8} second). Spark dischargers have considerable advantages in this respect. It is known that there are dischargers with an operating current of up to 10^6 amperes [25] and a voltage of 10^6 volts [26]. Under certain conditions the commutation time of the dischargers amounts to 10^{-10} second [27]. This explains the fact that the main attention is devoted in the book to generators with spark dischargers and that a description of some of the regularities of the gas discharges is given. Data on the generators with thyratrons are available in the other books [1, 2], and the special features of the operation of pulsed thyratrons and their properties are described by T. A. Voronchev [28].

In the book the chapters 1 and 5 were written by the authors together with the exception of Par. 1.2 written by Yu. P. Usov and Par. 5.3 written by G. A. Mesyats and V. V. Kremnev; the chapters 2, 3 and 4 were written by G. A. Mesyats and chapter 6 — by G. A. Vorob'yov.

CHAPTER 1. SOME OF THE REGULARITIES OF THE BREAKDOWN OF GASES

Introduction

The operation of high-voltage nanosecond-pulse generators with spark dischargers is highly affected by processes taking place in the discharge gap. The process of the preparation of the discharge from the instant of the application of the triggering pulse until the start of the formation of conductive channel is connected with the operating time and operating stability of the discharger. The speed of the formation of a channel with high conductance in the gap determines the steepness of the leading edge of the pulse. The maximum frequency of a stable operation of a pulse generator is determined by the time for restoring the electric strength of the gap. In addition to this, when using the dischargers it is important to know the factors on which the breakdown voltage of the spark gap depends.

Par. 1.1. Formation of Gas Discharge. Breakdown Voltage

Gas breakdown consists of three successive stages: the discharge-formation stage, the final stage and the arc stage (in the case of a large current in the discharge circuit). A channel with high electric conductivity is created between the electrodes during the discharge-formation stage. The current at this stage is small and the voltage on the electrodes remains nearly unchanged in the course of the stage. During the final stage a channel with a conductance approaching metal conductance is created between the electrodes, and the voltage on the electrodes rapidly drops to a very low value. The course of this stage determines the commutation characteristic of the discharger. During the other stage the flowing current depends on the parameters of the discharge circuit.

The formation of a gas discharge will be briefly examined in this paragraph.

At the beginning of the 20th century Townsend [12] developed a theory of discharge in gases, which with a subsequent correction makes it possible to describe some of the discharge processes in gases. The discharge process is represented qualitatively by the following pattern. Original electrons

formed in the immediate proximity to the cathode are accelerated by the electric field in the direction toward the anode. Upon the accumulation of sufficient energy the electrons colliding with the gas molecules and atoms ionize them and the number of free electrons increases in avalanche-like manner. Finally, the electron avalanche reaches the anode and is absorbed by it.

Positive ions formed during the impact ionization move toward the cathode and upon approaching it pull out electrons which form new electron avalanches. Consequently, pulling-out of the electrons from the cathode by the positive ions sustains the discharge.

Current density in the electron avalanches at the anode

$$j_a = j_0 \frac{e^{\alpha S}}{1-\gamma(e^{\alpha S}-1)}, \qquad (1.1)$$

where α is impact-ionization coefficient indicating the number of ionizations per one centimeter of the electron path; γ is coefficient indicating the average number of electrons pulled out from the cathode by one positive ion; j_0 is current density accounted for by the photoeffect from the cathode under the action of an extraneous ionizer not connected with the gas discharge.

At the present time it has been determined that the emergence of electrons from the cathode in the gas gap is connected not only with the ion bombardment of the cathode but is caused by many other processes called gamma processes, and first of all by the ultraviolet radiation of the excited gas molecules or atoms.

The quantity in the denominator of the expression (1.1) indicates the number of electrons pulled out from the cathode by ions which had formed in the gas gap as a result of ionization initiated at the cathode by one electron. The discharge is called self-maintaining if it does not become extinct when $j_0=0$. This is observed when

$$\gamma(e^{\alpha S}-1)=1. \qquad (1.2)$$

If $\gamma(e^{\alpha S}-1)>1$, then each following avalanche exceeds the preceding avalanche. This process called the step-up of the avalanches continues until electrical conductivity brought about by an avalanche proves to be sufficient for the next stage to run its course -- the final stage. The process of transition to this stage is not described in Townsend theory. It becomes clear from the foregoing that the time for formation of Townsend discharge is determined by the motion time of the electron avalanche and by the reverse motion of ions through the interelectrode gap, multiplied by the number of step-ups. Inasmuch as in a gas the mobility of ions is three orders lower than the mobility of electrons, the motion time of ions in the gas gap determines the time for formation of Townsend discharge, which according to theoretical eval-

uation should amount to 10^{-5}-10^{-3} seconds. This time was observed in the case of the breakdown of a discharged gas. However, with the atmospheric pressure the discharge time in an air gap with a length of one centimeter proved to be equal to 10^{-7} second [12, 29]. This fact which showed the untenability of Townsend theory played an important role in the further development of the studies on gas discharge. Observation of gas discharge in an ionization chamber [12, 29] showed that moving at a velocity of the order of 10^7 cm/sec the electron avalanche gradually expands and at a certain instant of time a sharp increase of ionized space is observed with this space covering at a very high speed all of the interelectrode space. This is followed by a complete breakdown. This rapid process, which is a continuation of the avalanche process, was called streamer.

The development of a streamer discharge appears to be as follows. The moving electrons produce not only the impact ionization but also the excitation of gas molecules and atoms. While reaching the normal state the excited molecules or atoms emit light quanta which bring about a stepped photoionization with an appearance of free electrons called photoelectrons and being of great importance in the development of a streamer.

After reaching the anode the electron avalanche is absorbed by it and leaves positive ions near its surface. Ionic charge creates an additional field with a strength E_1. Photoelectrons which had appeared near the anode move toward the positive volume charge in a field having the strength $E_1 + E$ where $E=\frac{U}{S}$ is field strength brought about by the applied voltage U. If the strength E_1 is sufficiently high, then after reaching the positive volume charge the photoelectrons will have time to create high-power avalanches which compensate the charge of the ions that are at the anode. This will lead to the creation of a conductive plasma. The new positive ions brought about by photoelectron avalanches, and newly appeared photoelectrons act in a manner similar to that described, and a plasma column called positive streamer rapidly extends in the direction toward the cathode. Meek [20] formulated the following condition for the initiation of the streamer: $E_1=kE$ where $k=0.1$ to 1 but its value has not been determined exactly.

If a higher voltage is applied to the gas gap, then Meek's condition may be satisfied when the avalanche has not yet reached the anode. In this case the streamer will appear in the interelectrode space and will spread toward the cathode and anode. The streamer spreading toward the anode is called negative.

In an inhomogeneous field the streamer spreads from the electrode with a large curvature. The velocity of the spread of the streamer in a homogeneous field amounts to $1.5 \cdot 10^8$ (positive) and to $7.9 \cdot 10^7$ cm/sec (negative); in a highly inhomogeneous field it is $2.5 \cdot 10^7$ (positive) and $2 \cdot 10^6$ cm/sec (negative).

On the basis of experiments with ionization chamber Raether [20] derived the following empirical equation for the condition for the initiation of the streamer:

$$\alpha x = 20, \tag{1.3}$$

where x is the path covered by the electron avalanche.

In the breakdown of large interelectrode gas gaps (of the order of tens of centimeters and more) with a highly inhomogeneous field when the average discharge gradients drop to 4-5 kv/cm, streamers do not create a conductive path between the electrodes and do not produce a breakdown. In this case the discharge is brought about by the leader process a description of which may be found in a book by I. S. Stekol'nikov [30].

On the basis of the latest investigations of the discharge time, discharge voltage and development of electron avalanches in ionization chamber the researchers [20] reached the conclusion that in the breakdown of gases in a homogeneous field at a constant voltage the formation of the discharge is brought about by the "step-up" of the avalanches according to Townsend. The breakdown voltage can be determined from the condition (1.3) with account taken of the relationship $\alpha = f(E)$. It turns out that the breakdown voltage is a function of the product of the multiplication of the pressure p by the interelectrode distance S, which was found earlier by Paschen and now bears the name law of Paschen. In Figure 1.1 are shown Paschen curves for certain gases. The curves have a minimum. The left branch of the curves is characterized by an increase of U_{pr} [$U_{pr}=U_{breakdown}$] with a decrease of pS. The increase of U_{pr} is limited to the phenomena characteristic of vacuum breakdown. For the right branch, U_{pr} increases with an increase of pS. In the work by Loeb [12] is cited an analytical dependence $U_{pr}=f(pS)$ which is an approximation of Paschen curve. With very large values of pS this dependence represents an almost straight line:

$$U_{пр} = A\,pS. \tag{1.4}$$

With a pS somewhat lower than the linear mode the dependence $U_{pr}=f(pS)$ has for many gases the following form:

[$U_{пр}=U_{pr}=U_{breakdown}$] $\qquad U_{пр} = A_0 pS + B_0\sqrt{pS}.$ (1.4')

where A, A_0 and B_0 are quantities constant for a given gas.

For certain gases (N_2, CO_2, etc.) a deviation from the law of Paschen is observed in the direction of a drop of the breakdown voltage with an increase in the gas pressure and the more so, the higher the pressure. Large deviations from the law of Paschen are observed in the case of an inhomogeneous field when an electrode with a large curvature has positive polarity.

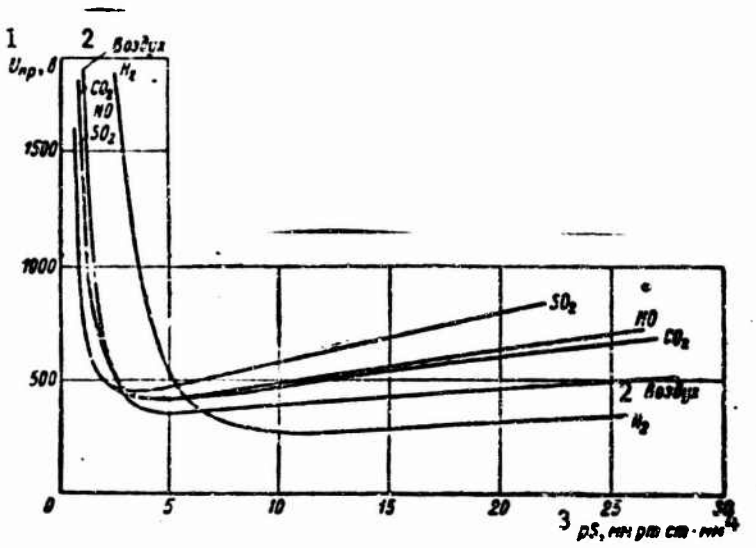

Figure 1.1. Relationship of breakdown voltage in different gases to pS in the case of a uniform field between the electrodes of the gap.

Key: (1) $U_{breakdown}$, volts (3) pS, mm of mercury column
(2) Air (4) mm

In a homogeneous field achieved by the use of flat electrodes with rounded edges it is possible to measure the breakdown voltage with accuracy to tenths of a percent. As a rule this voltage does not differ in the case of a breakdown at the commercial-frequency direct and alternating voltages. Experimental data satisfy well the equation (1.4'). Thus, according to Meek [20], for air at the atmospheric pressure

$$U_{пр} = 21{,}22S + 6{,}08\sqrt{S} \text{ кв}. \qquad (1.4'')$$

if S is measured in centimeters.

In the case of using spherical electrodes with small values of S/D (D is the diameter of the electrode) the values of U_{pr} approach the values for the case of a homogeneous field. With an increase of S/D, electric strength decreases and reproducibility of the results declines. With an $S/D \leqslant 0.5$ the accuracy of measuring the U_{pr} = 3% and with an $S/D \geqslant 0.75$ the results turn out to be poorly reproducible. The relationships at different values of D are cited in many works in the form of tables [21, 22, 31].

Table 1.1

ρ	0,7	0,75	0,8	0,85	0,9	0,95	1,0	1,05	1,1
k	0,72	0,76	0,81	0,86	0,9	0,95	1,0	1,05	1,09

With a change in the gas density $\rho=\frac{0.386p}{t+273}$ (p — mm of mercury column, t — °C), $U_{pr}=kU$ where U is breakdown voltage under normal atmospheric conditions (p=760 mm of mercury column, t=20°C); k is the coefficient dependent on the value of ρ (Table 1.1) [20]

If moisture does not become condensed on the electrodes an increase in the moisture content of the gas is accompanied in the case of a homogeneous field by an increase in the value of U_{pr} approximately by 0.1% for each millimeter of mercury column of the partial pressure of the moisture vapors. Moistness increases U_{pr} to a higher degree in the case of an inhomogeneous field.

An increase in gas pressure leads to an increase in electric strength. With pressures of the order of tens of atmospheres U_{pr} depends to a high degree on the condition of the surface and on the material of the electrodes. The material of the cathode has an especially great effect. The breakdown voltage increases successively with a change in the material of the cathode as follows: aluminum, copper, iron, stainless steel.

Polished electrodes aged by many discharges are used to obtain high values of U_{pr}.

The breakdown voltage in an inhomogeneous field depends on the polarity of electrode having a large curvature. For electrodes of the point-plane type the interelectrode distance of which is equal to a few centimeters the breakdown gradient at a positive polarity of the point is equal to 7.5 kv/cm, and at a negative polarity — to 20 kv/cm. With large interelectrode distances (tens and hundreds of centimeters) the breakdown gradients decrease to 4-5 kv/cm for a positive point and to 7-9 kv/cm for a negative point. Intermediate values of the breakdown voltage result for electrodes of the point-point type.

Table 1.2

(1) Газ	He	H_2	O_2	N_2	Cl_2
(2) $2U_{пр.}$, кв	1	3,5	5	6.5	9

Key: (1) Gas (2) $U_{breakdown}$, kv

In table 1.2 are given the breakdown voltages for different gases (a homogeneous field, pS=100 mm of mercury column · cm).

Some gases the composition of the molecules of which contains the atoms of ' ·ids have high values of electric strength exceeding by two and more times ; electric strength of the air. But most of these gases cannot be used since they have a high boiling point, are chemically active in regard to the surrounding materials and decompose under the effect of discharges with a formation of harmful substances.

B. M. Gokhberg and associates [29, 33, 34] were successful in isolating from among many gases two gases which satisfy the above-mentioned conditions. These are freon (CCl_2F_2) and elegas (SF_6). Freon has an electric strength 2.5 times higher than that of the air, its boiling point is 28°C. With a pressure of several atmospheres at room temperature freon changes into a liquid. Elegas has somewhat better properties. Its electric strength is close to the electric strength of freon, its boiling point is 62°C. Elegas is more inert than freon.

Addition of freon or elegas to the air and nitrogen increases electric strength of the latter two more than in proportion to the percent of the addition. These mixtures liquefy at higher pressures than pure freon and elegas. The breakdown voltage of the spark gap located in a closed vessel may change with an increase in the number of breakdowns of this gap. In the work [20] it is noted that the breakdown voltage of the air gap decreases as a result of formation of nitric oxide. When moisture is present, nitric acid may form which forms a conductive bridge between the electrodes on the walls of the vessel. A rise of the breakdown voltage is sometimes observed in a closed vessel after several breakdowns of CSF_8. This is explained by decomposition of the gas molecules into CF_4 and SF_6; as a result of this its pressure rises [20].

An appreciable drop of the static breakdown voltage is observed in the case of an intensive irradiation of the cathode of a spark discharger with ultraviolet rays. When using pulsed sources of irradiation (from a spark discharge) this effect is used for triggering the commutating spark dischargers and for the synchronization of high-voltage circuits. The effect of the breakdown-voltage drop was measured during the irradiation of the cathode of the main gap with a nearby auxiliary spark which appeared during an undamped discharge of a large-capacitance capacitor. A change in the irradiation intensity is usually accomplished by changing the distance l between the source of illumination and the main gap or by using shields which absorb ultraviolet radiation. In the works [20, 30] it is shown that the breakdown-voltage drop

$$\eta = \frac{U_{np} - U}{U_{np}} 100\% \qquad (1.5)$$

in the case of short distances l from the source of intensive ultraviolet irradiation to the main gap may reach 25 percent. With an increase of the distance l the value of η decreases.

A decrease of η with an increase of l is explained by the fact that a larger l is characterized by a more intensive absorption of ultraviolet rays by the air and, consequently, by a smaller photocurrent from the cathode i_0 the appearance of which lowers the breakdown voltage. It was determined experimentally [20] that the value of η increases in direct proportion to the increase of $\sqrt{i_0}$. On the basis of Townsend theory of gas discharge during a steady-state irradiation the decrease of η may be explained by the increase of the space-charge field of positive ions. In accordance with the experiment the calculated relationship $\eta=f(\sqrt{i_0})$ is rectilinear.

The most important quantity characterizing the effect of breakdown-voltage drop during irradiation with an auxiliary spark is the time between the breakdown of the auxiliary spark gap and the main spark gap, the stability of this time and the relationship of the spark gaps to various factors which affect the breakdown of a spark gap in the air under normal conditions.

These problems were investigated in a greater detail in the works [35, 36] and are set forth in Par. 5.5.

Par. 1.2. Delay Time of Discharge in Gases

If pulsed voltage is applied to a spark gap, then its breakdown occurs not immediately after reaching a static breakdown voltage in the gap but after a certain time called discharge delay time t_3. This time may be divided into static delay time, or the time between the instant of the application of a voltage sufficient for the breakdown of the gap, and the appearance of "effective" initiating electrons, and into the time for the formation of the spark discharge.

The ratio of the voltage U at which the breakdown of the gap takes place, to the static breakdown voltage U_{pr} is called relative overvoltage

$$\beta=\frac{U}{U_{pr}}.$$

The quantity $\beta_2=\beta-1$ is called absolute overvoltage and is sometimes expressed in percent. It is obvious that if $t_3>0$, then $\beta>1$. From the simplest Townsend theory (without taking the ionic volume charge into account) the probability of the appearance of a discharge starting in the time interval dt upon the expiration of t seconds after the application of voltage is equal [12] to:

$$W(t)\,dt = W n_0 e^{-W n_0 t}\,dt, \qquad (1.6)$$

where n_0 is the number of primary electrons released in one second from the cathode surface; W is the probability that each one of n_0 electrons will

create an avalanche capable of bringing about a discharge. The equation (1.6) leads to the following expression for statistical delay:

$$[t_{ст}=t_{st}=t_{statistical}] \qquad t_{ст}=\frac{1}{Wn_0}. \tag{1.7}$$

Each one of n_0 primary electrons leaving the cathode brings about $(e^{\alpha S}-1)$ ionizations during its motion toward the anode. The number of electrons released from the cathode by ions created by one of the primary electrons is called ionization-build-up coefficient M equal to

$$M=\gamma(e^{\alpha S}-1), \tag{1.8}$$

where γ is the number of electrons released from the cathode by one electron. In each separate case the coefficient M may be equal to 0, 1, 2, etc. but its average value will not necessarily be an integer. When $M<1$ the avalanche process and, as shown in Par. 1.1, the equality $M=1$ is the condition for breakdown according to Townsend theory. In doing so, the quantity W is the probability that with a voltage higher than the breakdown voltage the process of the initiation of new avalanches will not be discontinued. Making use of the theory of probability and taking into consideration that $\gamma \ll 1$, it can be shown that

$$M=\frac{\ln(1-W)}{W}. \tag{1.9}$$

Knowing the discharge conditions, M can be determined from the expression (1.8), W can be found from the expression (1.9), and then, evaluating n_0 from the conditions of the experiment the statistical delay time can be determined using the expression (1.7).

When breakdown bears streamer character statistical delay time depends on the product of the multiplication of the probability W_e that the original electron may lead to the creation of an electron avalanche, and the probability W_{st} that the avalanche creates a breakdown streamer

$$[W_{ст}=W_{st}=W_{streamer}] \qquad t_{ст}=\frac{1}{n_0 W_e W_{ст}}. \tag{1.10}$$

Under the action of the earth's radioactivity and cosmic rays from 10 to 20 electrons form under normal conditions in one cubic centimeter of air in one second. With such a small number of original electrons the statistical delay time is long. The number of original electrons n_0 increases nearly in proportion to the gas pressure so that a higher pressure decreases the statistical delay. Ultraviolet radiation of an appropriate mercury lamp, of a spark or corona discharge, radiation of radioactive materials, and the x-rays may be used for artificial ionization. Illumination of the cathode with ultraviolet light brings about a photocurrent from the cathode and

sharply increases the number of original electrons. In doing so, the probability of the formation of an avalanche by each one of these electrons approaches unity since each photoelectron starts moving away from the cathode under the action of the field between the electrodes. With a photocurrent density of 10^{-12} amp/cm^2 the number of electrons released from 1 cm^2 of the cathode surface in one second is equal to $6 \cdot 10^6$. A very intensive irradiation of the cathode (a photocurrent density of 10^{-9}-10^{-10} amp/cm^2) leads to the formation of the initial volume charge in the gas gap and reduces the breakdown voltage. For a discharge gap equal to 1 cm a photocurrent density of 10^{-12} amp/cm^2 does not as yet produce an appreciable distortion of the field by the volume charge, and statistical delay becomes sufficiently short. The photoelectric effect brought about by the spark discharge is many times higher than in the case of a mercury lamp [20].

In the irradiation of the gas gap by radioactive materials, statistical delay time is appreciably longer than in the ultraviolet irradiation of the cathode since alpha particles and gamma rays bring about an ionization of gas, nonuniform in time, in the entire volume.

Statistical delay time of the first discharge may be considerably longer than that of the following discharges in those cases when the number of unrecombined electrons after the first discharge is large. This phenomenon is characteristic of inert gases but it also can be observed in nitrogen and hydrogen. Increase in the number of original electrons is also explained by the possibility of field emission brought about by surface charges on a poisoned cathode. It is possible that these surface charges are brought about by photons from the preceding discharges.

With a heated cathode, thermionic emission sharply decreases statistical delay time and if it is reduced nearly to zero, then the time elapsed between the instant of the application of voltage sufficient for a breakdown, and the instant of breakdown is equal to the time for forming the discharge. For a Townsend discharge this can be calculated approximately by the methods set forth in the works [37-39]. In these works it was assumed that secondary electrons are formed as a result of bombardment of the cathode by positive ions. However, it is known that secondary electrons also appear under the action of discharge radiation in gas. Raether [40, 41] took both of these factors into account and calculated the time for the formation of a spark discharge in a homogeneous field on the basis of an assumption that it is determined chiefly by the time necessary for the growth of the avalanche to the dimensions at which the avalanche starts changing into a streamer. The streamer which has formed develops much faster than the avalanche. Therefore, its growth time may be neglected. In his evaluations Raether assumed that the transition of an avalanche into a streamer takes place with the condition (1.3).

A more exact approximation was carried out by Fletcher [17] who calculated for the first time the details of the space charge distribution in

an avalanche. He assumed that at the initial stage of development of the avalanche the distribution of the charge is determined chiefly by the diffusion of electrons with the concentration of electrons and positive ions being so low that the space-charge field may be neglected. The rates of increase of the concentrations of electrons n_- and of positive ions n_+ are described by the following equations:

$$\frac{\partial n_-}{\partial t} = \alpha v n_- - D\nabla^2 n_- + v\frac{\partial n_-}{\partial z}. \tag{1.11}$$

$$\frac{\partial n_+}{\partial t} = \alpha v n_-, \tag{1.12}$$

where v is the drift velocity of an electron in the direction of a field having the strength E along the axis z, and D is diffusion coefficient.

When owing to ionization the densities of electrons and positive ions increase the space-charge field starts changing the distribution of electrons. Fletcher suggested an approximate method of determining the conditions under which this process takes place. In his opinion, distribution does not change in the time t after the appearance of avalanche. If however, the time is larger than t, then the space-charge field becomes proportional to the number of electrons N and inversely proportional to the radius of the avalanche r_L, which would be true in the case of a spherical distribution of the charges. The radius r_L is determined by integrating the drift velocity brought about by the space-charge field E_L.

Therefore

[r_L=L=avalanche]

$$E_a = E_t \frac{N}{N_t}\left(\frac{r_t}{r_a}\right)^2. \tag{1.13}$$

where $E_L=E_t$ and $N=N_t$ at the instant of time t. For the space-charge field Fletcher found the following expression:

$$E_a = \frac{3}{16}\alpha^2 E\left(\frac{N}{N_t}\right)^{1/2}. \tag{1.14}$$

where $a=\frac{4D}{v}$.

The critical size of the avalanche N_{cr} at which the field in the avalanche becomes equal to zero is calculated from the conditions of equality of the space-charge field E_L to the external field E. According to the expression (1.14) this is possible when

[$N_{kp}=N_{cr}=N_{critical}$]

$$N_{kp} = \frac{256}{9}\cdot\frac{N_t}{(a\alpha)^2}. \tag{1.15}$$

The time for the formation of discharge t_r found from the assumption that

it is determined chiefly by the growth of the avalanche to the critical size is equal to

$$[t_p = t_r = t_{discharge}] \qquad t_p = \frac{1}{v\alpha} \ln N_{sp} \qquad (1.16)$$

To determine the numerical value of t_r Fletcher made use of the quantity $a = 3 \cdot 10^{-4}$ cm calculated from Raether's data [42]. In addition to this, he assumed v to be equal to $0.706\sqrt{E} \cdot 10^6$ cm/sec, which leads to an avalanche velocity observed by Raether [42] in fields approaching the minimum breakdown value, and extrapolated for higher fields.

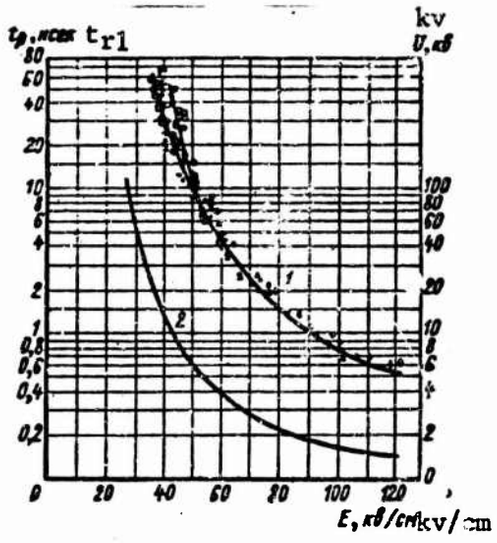

Figure 1.2. Relationship of the time for the formation of discharge t_r to the field strength E (1) and of the critical strength E_{cr} to the breakdown voltage U (2).

Theoretical curves of the relationship of the formation time to the field strength E at which a breakdown of the gap occurs is shown in Figure 1.2. Also shown there for comparison are the experimental points. The results of Fletcher's calculations indicate that the discharge formation time at an $E \geqslant 50$ kv/cm is a function of the field strength alone and does not depend on the length of the gap or applied voltage. This conclusion was confirmed by experiment. It follows from Figure 1.2 that with the large values of E the time t_r becomes equal to 10^{-9} second or less. An experimental study of the discharge formation time in the region of 10^{-9} second is also cited in the works [43-45]. To achieve larger values of E (or β) in the gap it is necessary that the duration of the leading edge t_f of the voltage applied to the gap be smaller than the expected value of the time t_r. In the experiments carried out by Fletcher [17] $t_f = 3 \cdot 10^{-10}$ second. Therefore, in the calculations he assumed the leading edge of the pulse to be ideally steep ($t_f = 0$).

The relationship of the discharge formation time t_r in the air under normal conditions to the distance between the electrodes S in a range of 0.2-4 mm with an overvoltage β=1.1 to 1.15 is determined in the work [46]. A multi-avalanche discharge with a discharge time of 10^{-6} to 10^{-5} sec appeared for an S=0.2 to 1.5 mm. With larger distances the time t_0 decreased unevenly by two orders and thenceforth depended in direct proportion to the magnitude of the gap S. With an intensification of irradiation of the gap with ultraviolet rays the intensity of the electron avalanches increased and the distance at which discontinuity in the relationship $t_r=f(S)$ was observed decreased. With the further increase of irradiation intensity this relationship was linear. The authors explain such a behavior of the relationship $t_r=f(S)$ by the transition of Townsend discharge into a streamer discharge. Consequently, to obtain a small value of t_r it is necessary to create in the discharge gap conditions for the realization of a single-avalanche streamer mechanism of the discharge.

In Figure 1.2 is shown the relationship of the critical field A to the magnitude of the voltage (the right Y-axis) at which after passing through the entire gap one avalanche reaches critical dimensions and leads to a breakdown. Several avalanches are necessary for the breakdown of a gap with a smaller E. This increases the t_r.

In conclusion, on the basis of the formula (1.10) we will obtain several relationships for t_r with different relationships between t_r and t_f.

1. Suppose $t_f \ll t_r$. With normal conditions in the air [20, 41]:

$$v=0.706(E)^{\frac{1}{2}}10^5 \text{ cm/sec.} \tag{1.17}$$

$$\text{With } \frac{E}{p}=44 \text{ to } 176 \text{ volts/cm/mm of mercury column [32]} \tag{1.18}$$

$$\alpha=A(E-B)^2$$

where $A=1.54 \cdot 10^{-7}$ cm/v^2, B=24,400 v/cm. A pressure p equal to 760 mm of mercury column was used. Since the value of N_{cr} has little effect on the result, an $N_{cr}=10^3$ may be used in the calculations [17, 20]. Substituting expressions (1.17) and (1.18) into the expression (1.16) we find

$$t_p=\frac{1690}{\sqrt{E}(E-24\,400)^2}, \tag{1.19}$$

or

$$t_p=\frac{1690\,S^{3/2}}{\sqrt{U_a}(U_a-24\,400\cdot S)^2}. \tag{1.20}$$

where U_a is the amplitude of the voltage pulse at which a breakdown of the gap occurs.

To determine the t_r Rose [14] suggested an empirical formula also found from the expression (1.16):

$$t_p \approx \frac{1.4}{(\beta-1)^2}. \tag{1.21}$$

2. Suppose $t_f < t_r$.

If the time t_r is measured from the start of the application of the voltage, then [17]:

$$[t_\phi = t_f = t_{\text{leading edge}}] \qquad t_p = t_1 + t_2 + t_\phi. \tag{1.22}$$

where

$$t_2 = \frac{1}{\alpha v}\int_0^{t_\phi} a(t)\, v(t)\, dt. \tag{1.23}$$

and t_1 is determined by formula (1.19) or (1.20). If the voltage on the leading edge of the pulse increases in accordance with rectilinear law, then

$$U = \frac{U_a}{t_\phi} t \tag{1.24}$$

or

$$E = \frac{U_a}{t_f S} t.$$

Substituting the expression (1.24) into the equalities (1.17) and (1.18), and substituting then the expressions obtained for v and α into the formula (1.23), we will find the t_2.

We will finally find the following for t_r:

$$t_p = \frac{1690\, S^{1.4}}{\sqrt{U_a}\,(U_a - 24\,400\, S)^2} + \frac{2t_\phi}{7} \times \\ \times \frac{U_a^2 - 6.71 \cdot 10^4\, U_a S + 14 \cdot 10^8 S^2}{(U_a - 24\,400 S)^2} + t_\phi. \tag{1.25}$$

3. We will examine now a case when the breakdown occurs on the leading edge of the pulse, i.e. $t_r < t_f$.

We will determine the time t_r from the start of the application of the voltage until the breakdown of the gap [14] from the following formula:

$$t_p = t_1 + t_2. \tag{1.26}$$

We will determine the value of t_1 from Raether's condition (1.3), and t_2 — from the expression (1.20) if the following is substituted in the place of U_a [14]:

$$U_e = \frac{t_1 + 3t_f}{4t_f}.$$

The final expression will asume the following form:

$$[U_a = U_e] \qquad t_p = (1.14\sqrt{S} + 2.44S)\cdot 10^{1}\frac{t_\Phi}{U_e} + \frac{1690\,S^{5/4}}{\sqrt{U_e}(U_e - 24\,400S)^{3/4}}. \qquad (1.27)$$

It follows from the equalities (1.20), (1.25) and (1.27) that the time t_r can be regulated steplessly from single nanoseconds to tens of nanoseconds with a constant value of U_a by varying the length of the spark gap S. In doing so, with a sufficient intensity of ultraviolet irradiation the value of t_r proves to be very stable [17, 44]. This phenomenon can be utilized in high-voltage nanosecond pulse technique [44, 46, 47]. Some of the networks making use of this effect are shown in Paragraphs 4.2 and 5.6.

Par. 1.3. Processes in Spark in the Period of Spark Discharger Commutation

In the period of discharger commutation the spark resistance varies from a very large value determined by the developed streamer, to a value approaching zero. The rate of the transition of the discharger from a nearly nonconductive state into a conductive state determines the duration of the leading edge of the pulse appearing on the load. This process of the transition of discharger from a nonconductive state into a conductive state may be characterized by a curve of the relationship of the voltage $U_k(t)$ [$U_k = U_{commutation}$] or resistance $R_1(t)$ [$R_1 = R_{spark}$] to time. It is customary to call the curve $U_k(t)$ characteristic of the commutator commutation. The duration of the commutation is characterized by the time between two fixed points U'_k and U''_k on the commutation curve (Figure 1.3).

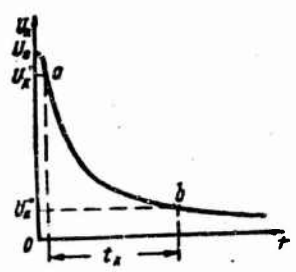

Figure 1.3. Characteristic of a spark discharger commutation.

Usually a $U'_k=0.9\ U_0$ is used and U''_k — equal to 0.2 or 0.1, according to the character of the curve $U_k(t)$. If there is a region of a delayed voltage drop on the commutation characteristic (to the right of the point b), then the former value of the U''_k is used, and if there is no such region, then the latter value of U''_k is used.

To determine the spark resistance in time, Toepler [3, 49] suggested the following empirical formula

$$R_1=\frac{kS}{q}$$

where S is the length of the spark gap; k is a constant characterizing the gas; q is the amount of electricity flowing through the spark gap.

Since $q=\int_0^t i\,dt$, then

$$R_u=\frac{kS}{\int_0^t i\,dt}.$$

$$[R_u=R_1=R_{spark}] \qquad (1.28)$$

Making use of the formula (1.28), Toepler [50], Krutzsch [51], Beindorf [6], Sahner [52] and others [3, 22] calculated the parameters of the leading edge of a pulse obtained in a network with a spark discharger as a commutator.

It is difficult to make practical use of the relations obtained with the aid of the formula (1.28) to determine the parameters of a pulse since the quantity k is actually not a constant but depends on the time [53], breakdown voltage and load resistance [5].

The relationship (1.28) obtained by Toepler is purely empirical. Therefore, theoretical evaluation of k is impossible. However, in spite of the approximate character of this formula certain dependences of parameters of the leading edge of a pulse, for example of the maximum steepness $\left(\frac{dU}{dt}\right)_m$, on the pressure and inductance [54] agree satisfactorily with the experimental data. However, this dependence on the breakdown voltage is expressed more markedly than that found from Toepler's formula.

The characteristic of discharger commutation depends both on the parameters of the discharge circuit and on the conditions in the spark gap. Two types of spark discharge are differentiated. Belonging to the first type are sparks the maximum current of which varies from a few amperes to tens of amperes — a low-power discharge. Belonging to the second type is a high-power discharge in which the current in the spark channel reaches hundreds and thousands of amperes. The first type of discharge appears when the storage capacity is small or when current-limiting resistances or inductance are inserted in the discharge circuit. In the case of a high-power discharge, capacitors with a value of the order of microfarads and more with low inductances and resistance of the discharge circuit are used as the storage devices.

In a low-power discharge the voltage drop and the increase of the current in a spark in the air under normal conditions takes place in a time of the order of 10^{-8} second [55-57] and stops at a level of a few tens of volts. This corresponds approximately to the potential difference between electrodes in the case of an arc discharge. Sometimes there is a step on the commutation curve [29, 58] the origin of which remains unclear up to the present time [59]. In the case of a high-power spark the voltage drop in the spark gap under normal conditions in the air also takes place in a time of the order of 10^{-8} second [30, 59, 60]. However, unlike a low-power breakdown the rapid voltage drop stops at a level of $U_s \approx (0.1 \text{ to } 0.2)U_0$ [U_s=voltage drop], after which the rate of the voltage drop is slowed down. The value of U_s increases in proportion to the U_0 and decreases with an increase of the resistance and inductance in the circuit.

As already noted, to obtain high-voltage pulses with a steep leading edge it is necessary to accelerate the process of creating conductance in the discharger, i.e. to decrease the commutation time. It was shown as far back as the work of Rogowski and Tamm [61] that the commutation time sharply decreases with an increase of the voltage in the discharger higher than the static breakdown voltage. Gänger [62], Rose [14], Fletcher [17] and others [16, 22] reached the same conclusion. Rose [14] created special conditions in the discharge circuit in order to obtain a minimum commutation time. In doing so, the inductance of the circuit was equal to $6 \cdot 10^{-10}$ henries. In a discharger filled with nitrogen, at a breakdown voltage of 5 kv, which corresponded to a relative overvoltage $\beta \approx 3.6$, the commutation time was $t_k = 5 \cdot 10^{-10}$ sec. The relationship of the commutation time to the field strength at which a breakdown of the gap occurs [63] is shown in Figure 1.4.

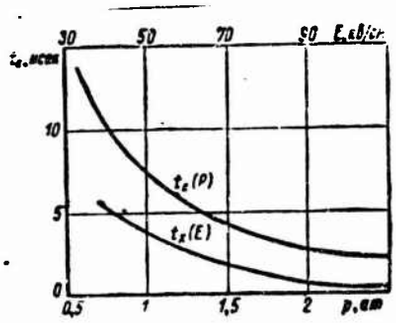

Figure 1.4 Relationship of the commutation time t_k to the pressure p and field strength in the gap E.

In the works by Beindorf [6], I. S. Stekol'nikov [35], Khün [59] and others [4, 63, 64] it is shown that commutation time decreases with an increase of the pressure in the discharger above the atmospheric pressure. In Figure 1.4 is given a curve of the relationship of commutation time to the air pressure [64]. The time t_k was determined between the levels of (0.9 to

0.2) U_0. Thus, the available experimental data indicate that commutation time decreases with a rise of the pressure in the discharger and of the overvoltage in the spark gap.

Table 1.3

v, %	0	3	9	16
t_k, nsec	7	14	20	21

It is shown in the work [65] that the commutation time t_k of a discharger depends on the shape of the electrodes. With the electrodes of the point--point type the value of t_k is approximately twice as large as with the sphere--sphere electrodes. Ultraviolet irradiation of the discharger affects the time t_k. The relationship of the value of t_k in the air under normal conditions to the percent drop of the breakdown voltage v, brought about by ultraviolet irradiation of the discharger [66] is shown in Table 1.3. The commutation time in a discharger filled with oil is shorter than in an air discharger under normal conditions [66]. Therefore, oil-filled dischargers are used in some devices to obtain a short-duration leading edge of a pulse [5, 67].

Weizel and Romple [20, 68-70] determined the spark resistance by examining the main processes taking place in the spark-discharge channel. In doing so, it was assumed that during the time of the existence of the spark channel, effects brought about by the presence of electrodes were negligibly small in comparison with the processes of the transfer of charges in a discharge region distant from the electrodes. The discharge current i and electric field strength E are connected by the relationship

$$i = \pi r^2 e n_e b_e E, \tag{1.29}$$

where n_e is concentration; b_e -- mobility of electrons; e — electron charge.

During commutation, which under our conditions lasts less than 10^{-8} sec, no substantial expansion of the discharge channel takes place [13, 61]. In addition to this, at high pressures it may be considered that mobility of electrons does not depend on electric field strength and so the equality (1.29) directly connects the quantities i, E and n_e.

The equation of energy balance in the spark channel may be written as follows

$$iE = W_S + W_T + \frac{du}{dt}, \tag{1.30}$$

where W_T is energy loss in a unit of time owing to thermal conduction; W_S — energy loss for radiation; u — internal energy of the spark channel.

Internal energy of a spark channel consists of the energy of the progressive motion of atoms, ions and electrons, of energy spent for ionization, and for molecular gases also of the energy of the excitation of oscillatory and rotational states and of the bond dissociation energy. It is assumed that electron gas receiving energy owing to the field transfers it to the heavy particles of the plasma so slowly that in the time intervals being examined neither the kinetic energy of ions, atoms or molecules nor the degree of excitation of the oscillatory or rotational states hardly change. The processes of molecular dissociation may be neglected. Consequently, internal energy in a discha ge channel is completely spent for ionization processes. It is also assumed that energy losses for the thermal conduction W_T and radiation W_S are also absent. It is easy to see that all of the assumptions listed are valid only for discharges of short duration in high electric fields.

Internal energy is defined by the expression

$$u = \pi r^2 n_e \frac{3}{2} k T_e + \pi r^2 n_e e u_i. \qquad (1.31)$$

where the first term represents kinetic energy of the electrons and the second — energy lost by electrons in the process of ionization (k is Boltzmann constant and T_e is electron temperature).

It follows from the expression (1.29) that conductance

$$F = \frac{I}{E} = \pi r^2 n_e b_e e. \qquad (1.32)$$

Both the internal energy and conductance are proportional to electron concentration with the proportionality constants depending little on the temperature T. If this dependence is neglected, then conductance may be approximately expressed in the following form

$$F = a' u, \qquad (1.33)$$

where

$$a' = \frac{b_e e}{3/2 k T_e + e u_i}. \qquad (1.34)$$

Since $b_e = \beta_e \lambda$ and $\lambda = \frac{1}{p}$, the expressions (1.33) and (1.34) may be written as follows:

$$F = \frac{a}{p} u, \qquad (1.35)$$

$$a = \frac{e \beta_e}{3/2 k T_e + e u_i}. \qquad (1.36)$$

where p is gas pressure; λ — electron free path length; β_e — factor of proportionality connecting b_e and λ.

If W_S and W_T equal to zero are taken [59, 60] and the equations (1.30) and (1.35) are solved simultaneously, eliminating the internal energy u, we will obtain

$$F^2 = \frac{2a}{p}\int_0^t i^2 dt. \tag{1.37}$$

From the expression (1.37) we will find the spark resistance R_1

$$R^2_1(t) = \frac{p S^2}{2a\int_0^t i^2 dt}. \tag{1.38}$$

Conditions on the basis of which formula (1.38) are reproduced most satisfactorily only during the stage of a rapid voltage drop in the spark. In doing so, the faster this stage progresses, the more the pattern described corresponds to reality. In the operation of spark dischargers, conditions are specially created in the high-voltage nanosecond devices to obtain a commutation time $t_k < 10^{-8}$ second.

Investigations of the applicability of the formula (1.38) for analyzing the processes in a spark were conducted in the direction of checking the time constancy of the coefficient a. Khün's [59] investigations did not confirm the time constancy of the coefficient "a" for discharges in the air and hydrogen. The main reason for this discrepancy consists in that the investigations of the spark were conducted with the times of 10^{-7} to 10^{-6} sec when the basic premises used in deriving the formula (1.38) were no longer observed. In addition to this, the breakdown of the gap investigated in the work [59] was initiated by an auxiliary spark which, as shown above, highly affects the length of the commutation time.

S. I. Andreyev and M. P. Vanyukov [53] investigated the time dependence of "a" in the air under normal conditions and its relationship to the resolving power of oscillograph equal to 10^{-9} sec. It follows from the data they obtained that during the first 10 nanoseconds the coefficient "a" changes insignificantly and the following "a" may be assumed

$$a = (1 \text{ to } 1.3)\ \text{cm}^2 \cdot \text{atm}/\text{v}^2 \cdot \text{sec}.$$

Unfortunately, the coefficient "a" has not as yet been determined experimentally for the other gases. Theoretical evaluation of the quantity "a" may be done using the formula (1.36).

Par. 1.4. Restoration of Electric Strength of the Spark Gap

In obtaining the high-voltage pulses with a high repetition rate it is important to know how fast the electric strength of a discharger is restored after a spark discharge.

When current no longer flows through a spark a column of heated and highly ionized gas remains in the channel, in which the processes of diffusion and recombination bringing about a decrease of electrical conductvity of the spark channel with time take place. However, the voltage on the discharger electrodes increases at the same time owing to the charging of the shaping element of the network from a charging device with this voltage slowing down the restoration of electric strength of the gap. If the breakdown voltage of the spark channel becomes restored faster than the voltage on the electrodes increases, then the shaping element of the network will become charged to the full voltage and the network will be able to produce the next pulse. If the increasing voltage on the electrodes reaches the breakdown voltage sooner than the shaping element is fully charged, then an uncontrolled breakdown will appear.

If the repeat-operation voltage at which the controlled operation of the discharger stops is found by means of a simultaneous construction of the curve of voltage rise on the discharger $U_r(t)$ [U_r=$U_{discharger}$] and the curve of the restoration of the breakdown strength $U_v(t)$ [U_v=$U_{restoration}$] and is defined by the ordinate point of their tangency or intersection.

Many works a review of which is given in the work [20] are devoted to the investigation of the process of restoration of electric strength of the gap after a spark discharge.

A. V. Rubchinskiy [72] investigated in detail the restoration of electric strength after a spark discharge in hydrogen, nitrogen, oxygen, air, inert gases and their mixtures at voltages of up to 10 kv, pressures up to one atmosphere and interelectrode distances of up to 20 mm. The discharge-current pulses reached 1,000 amperes with a different duration of them. The steepness of the voltage applied to the discharger is equal to 0.5-1 kv/microsecond. Electric strength is restored fastest of all in hydrogen and slowest of all in nitrogen. The difference in the rate of strength restoration in hydrogen and nitrogen is very great. For example, 50 percent of original strength is restored in hydrogen in 1,600 microseconds and in nitrogen in 4,000 microseconds. No substantial differences in the rate of strength restoration are observed in pure inert gases. The dependence of the restoration rate on the pressure is little marked in all gases. The steepness of the $U_v(t)$ characteristic is very highly affected by various admixtures to the pure gases. For example, an addition of 0.1 percent of hydrogen to argon increases the restoration rate nearly twofold. An admixture of oxygen to argon also has a similar effect. In addition to this, the lower the rate of the voltage applied to the discharger, the more effective the action of an admixture of oxygen. An addition of nitrogen to argon slows down the restoration of the strength. Nitrogen proved to be more sensitive to the admixtures than the inert gases. Four thousand microseconds are necessary to restore 50 percent of the original strength in pure nitrogen, and in nitrogen with an admixture of 1 percent of hydrogen — only 1,300 microseconds.

The shape and polarity of the electrodes have a considerable effect on the rate of restoration. When the point is the anode the restoration of

strength in nitrogen and hydrogen takes place faster than in the case of flat electrodes or when the point is the cathode. The material of the electrodes has no substantial effect on the shape of the curves $U_v(t)$. Investigation of the effect of duration and amplitude of a pulse of current flowing through the gap indicates that with an increase of the duration of the flow of current through the discharger the rate of the restoration of the strength decreases to a higher degree than with an increase of the amplitude.

On most of the curves $U_v(t)$ investigated in the work [72] there are two sections differing in the slope: initial section with a high rate and a flattened section where the rate of strength restoration is considerably lower. In the opinion of A. V. Rubchinskiy [72] the initial steep section of the curve $U_v(t)$ is determined by the breakdown strength of the ion layer which forms at the cathode under the action of voltage applied to the gap, and the following flattened section is connected with an increase of gas density in the discharge column as the gas cools.

With a decrease of the concentration of charges the thickness of the ion layer grows and U_v increases. When the concentration of the charges becomes so small that under the action of the voltage applied to the gap this layer extends over the entire gap, the second section of the curve $U_v(t)$ starts. Since the cooling process of the gas continues slower than the decrease in the concentration of the charges, the second section of the restoration curve has a flatter shape than the first. Calculations showed a qualitative correspondence of the experimental and theoretical curves $U_v(t)$ for all gases except nitrogen and argon. The influence of oxygen and hydrogen admixtures on the increase of the steepness of $U_v(t)$ in nitrogen and argon may be explained by the tendency of hydrogen and oxygen to the formation of negative ions. Recombination of negative ions with positive proceeds faster than the recombination of electrons with positive ions. Therefore, an addition of hydrogen and oxygen to argon and nitrogen accelerates the fall-off of the concentration of the charges in the gap and restores its strength. In addition to this, the molecules of the impurity may break down the metastable molecules of the basic gas which reduce the breakdown strength of the gas owing to stepped ionization.

In addition to the methods examined, gas or magnetic blowing [20, 21, 31], a discharger with a number of gaps larger one, etc. may be used to accelerate the process of restoration of the strength of the gap after a spark breakdown.

It is clear from the foregoing that the pulse repetition rate depends on the time for the restoration of the breakdown strength of the gap. However, the characteristic $U_v(t)$ is not the only characteristic of the frequency properties of a discharger. It is also necessary to know the characteristic of the voltage rise on the discharger $U_r(t)$ which should lie lower than $U_v(t)$ and not touch or intersect it. It is especially important to have a flattened initial section of $U_r(t)$. It is of interest to note that this is helped by

the low after-discharge resistance of the discharger, which for a certain time after the discharge stays approximately equal to zero. The last circumstance prevents the voltage rise on the discharger since nearly all of the charging voltage will be applied for a certain time to a charging resistor (or inductance). The lowering of the rate of increase in the initial portion of the characteristic $U_r(t)$ is helped by the charge of the shaping capacitance through the inductance (especially in the case of a resonant charge) unlike a charge through a resistor [7]. In addition to this, a charge passing through an inductance increases the efficiency of the generator in comparison with a circuit arrangement with a charging resistor.

Owing to a long time for the restoration of the discharger strength the pulse repetition rate in pulse generators has a value of the order of 10^3 cps with the currents in a pulse of up to 1 kiloamp and voltages of the order of ten kilovolts.

CHAPTER 2. ANALYSIS OF PROCESSES IN DISCHARGE CIRCUIT WITH A COMMUTATING DISCHARGER

Introduction

Before passing on to an analysis of processes in a discharge circuit and their effect on the shape of a voltage pulse we will introduce the basic notations of the pulse parameters (Figure 2.1a). Here t_f is duration of the leading edge of a pulse; t_{sr} — duration of the cut; t_i — pulse duration; U_a — pulse amplitude; Δ — voltage horn.

Par. 2.1. Discharge Circuit of a Pulse Generator

The substitution network of the discharge circuit of a generator of nanosecond pulses is shown in Figure 2.2 where U_0 is the voltage of the shaping element; C_n — the load and wiring capacitance; C — shaping capacitance; R_n — nonlinear resistance of the commutator; L — discharge-circuit inductance; R_d — damping resistance and internal resistance of the shaping element.

Depending on concrete conditions the parameters of a substitution network may assume different values (including zero values and infinitely large values). Unlike the microsecond pulse networks, in the discharge circuit of a nanosecond network the pulse shape is considerably affected by the variation of the commutator resistance R_k in time, which decreases in the course of the commutation time from infinity to a value approaching zero.

In the general case an exact calculation of the parameters of the leading edge of a pulse in a network with a commutator is made difficult owing to mathematical difficulties. Calculation may be carried out with certain assumptions; for example, the commutation characteristic of the discharger is specified. In doing so, a source of emf with a zero internal resistance instead of the commutator resistance is inserted in the substitution network of the discharge circuit. The time dependence of this emf is

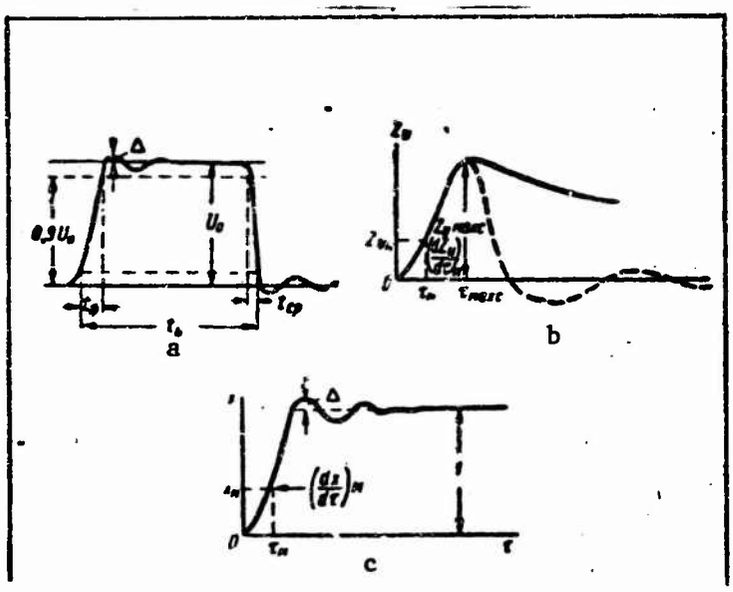

Figure 2.1. Determination of pulse parameters (a); voltage pulse on the load R_n (b); pulse on the capacitance C (c).

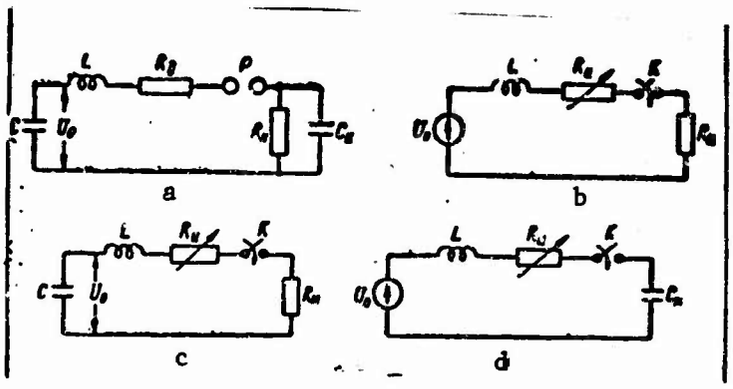

Figure 2.2. General substitution network (a); substitution network with account taken of the circuit inductance (b); substitution network with account taken of the value of the capacitance of the shaping capacitor (c) and network with account taken of the spurious parameters of the L,C_n discharge circuit (d).

described by the commutation characteristic $U_k(t)$ which changes insignificantly with a change in the active and reactive parameters of the circuit [35, 52]. Therefore, with a variation of these parameters in a certain range the characteristic $U_k(t)$ may be considered invariable.

We will examine the effect of parameters of the discharge circuit and commutation time on the duration of the leading edge of a pulse in the case of invariable voltage on the shaping element ($C=\infty$). It follows from the diagram in Figure 2.2b that with a unit voltage on the shaping element the transfer characteristic of the circuit on the terminals of the load has the following form

[$Z_H=Z_n$]
$$h'(p)=\frac{Z_n(p)}{Z(p)}. \qquad (2.1)$$

where $Z_n(p)$ is the load impedance; $Z(p)$ — aggregate impedance of the circuit, including $Z_n(p)$.

If the commutator is replaced by a source of emf $e=-U_k(t)$, then the aggregate relative emf is equal to

[$e_э^*=e_e^*$]
$$e_э^*=1-\frac{U_k(t)}{U_0}. \qquad (2.2)$$

The characteristic $e^*_e(t)$ always bears a monotonic increasing character. If h(p) is also a monotonic increasing function, then the duration of the leading edge of the pulse on the load [73] is equal to

[$t_\phi=t_f=t_{\text{leading edge}}$]
$$t_\phi=\sqrt{t_k^2+t_{0\phi}^2} \qquad (2.3)$$

where t_k is the commutation time of the discharger; t_{0f} — the duration of of the leading edge with the condition that

$$e_e^*(t)=0 \mid t<0;$$
$$e_e^*(t)=1 \mid t\geqslant 0.$$

In the general case the value of t_{0f} can be determined with good approximation directly from the transfer characteristic h(p). If

$$h(p)=\frac{1+a_1p+a_2p^2+\ldots+a_mp^m}{1+b_1p+b_2p^2+\ldots+a_np^n}, \qquad (2.4)$$

where $m\leqslant n-1$, then according to [73]

$$t_{0\phi}=\lambda\sqrt{2(a_2-b_2)+b_1^2-a_1^2}, \qquad (2.5)$$

where λ is a factor which depends on the method of determining the t_{0f}.

In practice, in all of the arrangements of the discharge circuit used hereafter $\lambda=2.2$ if the duration of the leading edge is determined between the levels of 0.1-0.9 of the pulse amplitude.

An important conclusion follows from the formula (2.2) that t_f is not dependent on the form of a function approximating the commutation characteristic but depends only on the value of t_k. In the simplest case, when $Z_n=R$ and $Z(p)=Lp+R$, the value of $t_{0f}=2.2\frac{L}{R}$. If $t_k<t_{0f}$, then it follows from the expression (2.3) that

$$t_\phi \approx \frac{t_k}{2}+2.2\frac{L}{R}. \qquad (2.6)$$

Thus to decrease the duration of the leading edge it is necessary to decrease the commutation time and the time constant of the discharge circuit $\frac{L}{R}$.

Formula (2.3) may be used approximately also in the case when the function $h(t)$ is not monotonic, if the voltage horn at the vertex of $h(t)$ is less than 10 percent [74]. However, in doing so, it is necessary to determine t_f not by the formula (2.5) but directly from the curve $h(t)$.

Usually the commutation characteristic is determined experimentally and approximated by some suitable function, usually by the exponential

$$U_x(t)=U_0e^{-\alpha t}. \qquad (2.7)$$

For an exact calculation of the pulse parameters with account taken of the conditions in the discharger and of the circuit parameters it is necessary to know the resistance of the commutator R (in our case this is the spark resistance R_1). It is impossible to calculate the transient in the circuit in Figure 2.2a with account taken of nonlinear resistance of the spark according to Weizel and Rompl [1, 37]. Actually, there is even no need for this since all of the pulse generators used have only three different substitution networks of the discharge circuit, a detailed analysis of which will be given in the following three paragraphs.

Par. 2.2. Determination of Parameters of the Leading Edge of a Pulse With Account Taken of the Inductance of the Discharge Circuit

To obtain rectangular pulses with a large current the substitution network of the generator has the following parameters: $C=\infty$, $C_n=0$, $R_d=0$. The discharge circuit of a generator with a shaping line has such a substitution network (see Figure 2.2b) and also a circuit with a shaping capacitor for which the R_nC is several orders larger than the duration of the leading edge of the pulse t_f.

Differential equation for the current of the discharge circuit with account taken of the spark resistance R_i according to the formula (1.38) has the following form

$$L\frac{di}{dt} + R_0 i + \frac{i}{\sqrt{\frac{2a}{pS^2}\int_0^t i\,dt}} = U_0. \tag{2.8}$$

In the place of i and t we will introduce new variable quantities:

[R_{sp}=R_i=R_{spark}]

$$x = \frac{iR_0}{U_0}; \quad \tau = \frac{t}{\theta}; \quad \theta = \frac{2pS^2}{aU_0^2}. \tag{2.9}$$

where p is gas pressure; S — the length of the spark gap; "a" — a constant characterizing the gas. The variable x is a relative pulse voltage across the resistance R_{sp}. We will substitute i and t expressed by x and τ into (2.8) and introduce the coefficient

$$A = \frac{aU_0^2 L}{2pS^2 R_0}. \tag{2.10}$$

In doing so, we will obtain

$$x + \frac{x}{2\sqrt{\int_0^\tau x^2 d\tau}} + A\frac{dx}{d\tau} = 1. \tag{2.11}$$

It follows from the expression (2.11) that $x=f(\tau)$ depends only on one parameter A and has no exact solution except for the case when A=0. In doing so,

$$\tau = \frac{1}{2}\ln\frac{x}{1-x} + \frac{3-2x}{4(1-x)^2} + k_0. \tag{2.12}$$

The integration constant k_0 is determined from the condition that τ=0, x=0.01 and is equal to 1.537. Numerical solution of the equation (2.11) for nonzaro values of A was carried out by Sahner [52], and the curves $x=f(\tau)$ for different values of A are shown in Figure 2.3a.

Making use of the curves $x=f(\tau)$ it is possible to calculate the commutation characteristics of the discharger with different coefficients A (see Figure 2.3b). It may be seen from the figure that the commutation characteristic depends little on the value of A. This characteristic may be conditionally divided in the region of a rapid voltage drop in the discharger gap and the region of a slow drop where this drop is protracted. The same shape of commutation characteristics is observed experimentally in the case of large currents in the spark (a high-power discharge). Such a behavior of the commutation characteristics draws the transition region of the leading edge toward the top of the pulse and increases the duration of the leading edge.

The τ_f vs A characteristic determined from the curves in Figure 2.3a is well approximated by a straight line when $0 \leqslant A \leqslant 25$

$$\left.\begin{aligned} &\tau_\phi = 10.5 + 2.2\,A \\ \text{or} \qquad &\\ &t_\phi = \frac{pS^2}{aU_0^2} + 2.2\,\frac{L}{R_n}. \end{aligned}\right\} \qquad (2.13)$$

This formula is analagous to the expression (2.6).

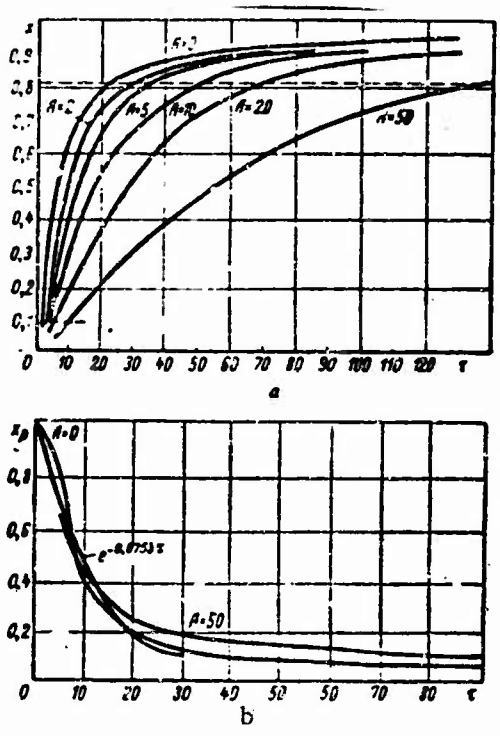

Figure 2.3. Time dependence of the relative voltage $x=\frac{U}{U_0}$ across the resistance R_n (a) and commutation characteristics of the discharger $x_r=f(\tau)$ for different A (b); the equivalent exponential $x_r=e^{-0.0753\tau}$ is also shown here. $x_r=\frac{U_k}{U_0}$.

Making use of the equation (2.11) we will calculate the maximum steepness of the leading edge of the pulse. For this purpose we will denote the

second term of the equation (2.11) by y. In doing so,

$$\int_0^{\tau} x^2 d\tau = \frac{x^2}{4y^2}. \tag{2.14}$$

We will differentiate the equality (2.14) with respect to τ. We will substitute into the resulting expression the y and $\frac{dy}{d\tau}$ found from the equation (2.11). If it is taken into account that for the maximum steepness $\frac{d^2x}{d\tau^2}=0$, then

$$2x_m(1-x_m-Ax'^3_m)-x'_m(1-Ax'_m)=0. \tag{2.15}$$

The values of the voltage x_m and the steepness x_m' pertain to the point with the maximum value of the steepness. The maximum steepness cannot as yet be determined from the equality (2.15) since x_m is not known. It may be seen from Figure 2.3a that in the region of maximum steepness the relationship $x=f(\tau)$ approaches rectilinear relationship. Therefore, it is sufficient to determine the value of x_m approximately in order to find $\left(\frac{dx}{d\tau}\right)_m$ with high accuracy. We will assume that the value of x_m does not depend on A. In that case, after determining it for any one value of A (for example, A=0), this value may be considered valid for the other values of A.

Making use of the equation (2.11) it is possible to show that with

$$A=0 \quad x_m=\tfrac{1}{3}.$$

If we substitute this value of x_m into the equation (2.15) and transform somewhat the equality obtained, we will obtain the following

$$4A\left(Ax'_m-\frac{3}{4}\right)^3-8\left(Ax'_m-\frac{3}{4}\right)^2-4\left(Ax'_m-\frac{3}{4}\right)+\frac{3}{2}=0. \tag{2.16}$$

Solution of the equation (2.16) and substitution of A and x_m' with their values from the equality (2.9) and (2.10) lead to the following formula

$$\left(\frac{dU}{dt}\right)_m=\frac{27}{256}\cdot\frac{aU_0^3}{pS^2}|1-\varphi(A)|. \tag{2.17}$$

The following empirical formula may be used when $0\leqslant A\leqslant 25$

$$\varphi(A)=-0.157A+0.0108A^2-0.00017A^3. \tag{2.18}$$

It may be seen from the formulas (2.17) and (2.18) that to increase the steepness and decrease the leading edge of the pulse it is necessary to decrease the parameter A.

Verification of the correctness of assumptions made in the derivation of the formula (2.17) may be carried out by means of a comparison with the exact values of $\left(\frac{dU}{dt}\right)_m$ calculated in the work [52] for some of the values of A.

Comparison of the results shows a good agreement of the formula (2.17) with the exact data when $A \leqslant 25$ (discrepancy in the results does not exceed 5 percent).

Par. 2.3. Effect of the Value of the Shaping Capacitor on the Pulse Parameters

If the time constant of $R_n C$ is congruent with the commutation time of the discharger, then it is necessary to calculate the voltage drop in the capacitor C attributable to its discharge. In this case, the effect of C_n may be neglected and it may be considered that $C_n=0$. If it is necessary to damp the oscillations at the pulse tail, then a resistance R_d is connected in series with R_n. In the calculations we will consider that R_n is the sum of the damping and load resistance (see Figure 2.2c). In a generator with such a circuit it is possible to obtain a duration of the leading edge of the pulse shorter than the commutation time t_k owing to a certain discharge of the capacitor during the commutation. However, in this case the pulse amplitude $U_a < U_0$, and a shorter pulse duration (see Figure 2.1b) can be obtained than the commutation time. If $R_i=0$ and $L=0$, then the pulse will have a sawtooth shape with the following duration at a level of 0.1

$$t_1=2.3\ R_n C.$$

We will pass on to an analysis of the processes taking place in the discharge circuit (see Figure 2.2c). Differential equation for current in the circuit has the following form

$$i(R_a+R_n)+L\frac{di}{dt}=U_c. \tag{2.19}$$

If instead of the R_i, its value from the formula (1.38) is substituted into the equality (2.19) and the following series of new constant and variable quantities are introduced:

$$B=\frac{R_n C}{\theta};\quad k=\frac{\sqrt{LC}}{\theta};\quad \theta=\frac{2pS^2}{aU_0^2}; \tag{2.20}$$

$$\tau=\frac{t}{\theta};\quad Z=\frac{i\theta}{CU_0};\quad x=\frac{U_c}{U_0};\quad Z=-\frac{dx}{d\tau}, \tag{2.21}$$

then we will obtain

$$\frac{Z}{y}+BZ+k\frac{dZ}{d\tau}=x. \tag{2.22}$$

Here $y=\frac{\pi r^2 Su}{0.5\,U_0^2 C}$ is a quantity proportional to the inner energy of the discharge channel. The following relationship exists between Z, y and τ:

$$2Z^2 = y\frac{dy}{d\tau}. \tag{2.23}$$

In this case the relationship between Z, y and x has the following form

$$Z = -\frac{1}{4}\cdot\frac{d(y^2)}{dx}. \tag{2.24}$$

It follows from the expression (2.21) that $\frac{d}{d\tau} = -Z\frac{d}{dx}$.

We will eliminate Z and τ from the equality (2.22), and integrate with respect to x the right and left members of the equation obtained. In doing so, we will determine the integration constant on the basis of the following conditions: $\tau=0$, $y=0$, $x=1$. After all transformations we will obtain a differential equation which describes the relationship between plasma energy in the discharge channel y and the voltage across the capacitor x:

$$\left.\begin{aligned} &2\sqrt{\varphi} + B\varphi + \frac{k^2}{8}\left(\frac{d\varphi}{dx}\right)^2 + 2x^2 - 2 = 0, \\ &\varphi = y^2. \end{aligned}\right\} \tag{2.25}$$

The equation (2.25) was obtained by Weizel [69] for analyzing the process of plasma formation during a discharge and he solved it for certain particular values of B and k.

The relationship between Z and τ is defined in a parametric form in terms of x

$$Z = -\frac{1}{4}\cdot\frac{d\varphi}{dx}, \quad \tau = 4\int\frac{dx}{d\varphi/dx} + \text{const.} \tag{2.26}$$

Later on, we will be concerned not with the current Z but with the voltage across the resistance R_n, equal to

$$Z_U = ZB.$$

In this case the expression (2.26) assumes the following form

$$Z_U = -\frac{B}{4}\cdot\frac{d\varphi}{dx}; \quad \tau = -B\int\frac{dx}{dZ} + \text{const.} \tag{2.27}$$

The equation (2.25) cannot be solved exactly in the general form. However, when k=0 it changes into an ordinary quadratic equation with respect to $\sqrt{\varphi}$. After finding $\varphi(x)$ and substituting it into the expression (2.27) we will find the following:

$$\tau = \frac{1}{2}\ln(x_1 - 1) - \frac{B\sqrt{1+2B}}{2(\sqrt{1+2B}-1)}\ln(\sqrt{1+2B} - x_1) -$$

$$- \frac{B\sqrt{1+2B}}{2(\sqrt{1+2B}+1)}\ln(x_1 + \sqrt{1+2B}) + \text{const}; \qquad (2.28)$$

$$Z_U = x\left(1 - \frac{1}{x_1}\right),$$

where

$$x_1 = \sqrt{1 + 2B(1 - x^2)}. \qquad (2.29)$$

The integration constant can be determined from the condition that $\tau=0$, $Z_U=0.01$. An analysis of the relationships (2.28) and (2.29) indicates that the curve $Z_U(\tau)$ has a maximum. From the condition $\frac{dZ_U}{dx}=0$ we will determine $Z_{U\,max}$ and the value of x_{max} corresponding to it

$$x_{max} = \sqrt{\frac{(1+2B) - (1+2B)^{2/3}}{2B}}, \qquad (2.30)$$

$$Z_{U\,Max} = \left(1 - \frac{1}{\sqrt[3]{1+2B}}\right)\sqrt[3]{\frac{1+2B}{2B}}. \qquad (2.31)$$

If we substitute the value of x from the equation (2.30) into the equality (2.28), then we will determine the time τ_{max} with which Z_U assumes the maximum value. The quantity τ_{max} cannot be a technical characteristic of the leading edge of the pulse since at the beginning the leading edge has a rapid increase which changes into a very slow rise. Therefore, it is important to determine the maximum steepness Z'_{U_m} of the leading edge. For this purpose, we will determine y from the expression (2.22), square it, take a derivative of y^2 with respect to τ and taking the equality (2.23) into account we will obtain an equation in which we will take a $\frac{d^2Z}{d\tau^2}=0$. Then we will obtain the following

$$Z_m = \frac{k\,Z'^2_m - Z'_m x - Z'_m}{2(B\,Z_m + k\,Z'_m - x_m)^3} \qquad (2.32)$$

where the subscript "m" indicates values corresponding to a point with the maximum steepness of the leading edge. In order to determine the maximum steepness Z'_m from the expression (2.32) it is necessary to know the values of Z_m and x_m when B are specified. It is impossible to determine Z_m and x_m in the general case when $k\neq 0$.

To determine x_m and Z_m when $k=0$ we will perform on the equation (2.22) the same operations as in the derivation of the formula (2.32), and then take from the left and right members the derivative with respect to τ and assume a $\frac{d^2Z}{d\tau^2}=0$. In doing so, after substituting Z with Z_U we will obtain:

$$2\left[2(x_m - Z_{Um})^3 - \frac{Z_{Um}}{B}\right](x_m - Z_{Um})^3 =$$

$$= 6(x_m - Z_{Um})^2\left[\frac{Z_{Um}\cdot x_m}{B} + 2Z_{Um}(x_m - Z_{Um})^3 - \frac{Z^4_{Um}}{B}\right] +$$

$$+ \frac{2Z_{Um}}{B}(x_m - Z_{Um})^3 - \frac{Z^3_{Um}}{B^2}. \qquad (2.33)$$

Since $Z_{U\,m} < 0.25$ (see Par. 2.2) and $x_m \leqslant 1$, then the expression (2.33) can be simplified by proceeding from a concrete value of B. For example, with $B \geqslant 5$

$$x_m \approx 4Z_{Um}. \qquad (2.34)$$

The second relationship for the determination of connection between x_m and $Z_{U\,m}$ can be provided by formula (2.29). In this case we will obtain

$$x \approx 1 - \frac{7}{36B}. \qquad (2.35)$$

It follows from these expressions that with $B \geqslant 5$, $Z_{U\,m} \approx \frac{1}{4}$ and $x_m \approx 1$, i.e. the voltage across the capacitor C hardly changes. Consequently, with $B \geqslant 5$, formula (2.17) which was obtained with a replacement of the capacitor C with a source of infinite power (see Par. 2.2), can be used to determine the maximum steepness of the leading edge of the pulse.

In order to have an idea of the steepness of the leading edge of the pulse when $0 < B < 5$, we will determine $Z_{U\,m}$ and x_m when $B \ll 1$. In doing so, the expression (2.29) will assume the following form

$$Z_{U\,m} \cong Bx_m(1 - x_m^2).$$

Substituting this value of $Z_{U\,m}$ into formula (2.33) and neglecting small quantities we obtain

$$15x^4_m - 12x^2_m + 1 = 0$$

or

$$x_m = 0.8399 \approx 0.84; \quad Z_{Um} = 0.247B. \qquad (2.36)$$

If the obtained values of x_m and $Z_{U\,m}$ are substituted into formula (2.32) having first substituted Z_m with the quantity $Z_{U\,m}$, we will obtain

$$\left(\frac{dZ_U}{d\tau}\right)_m = 0.342B. \qquad (2.37)$$

i.e. with a decrease of B the maximum steepness decreases and in the limit with $B \to 0$ it also tends to zero. The reason for this phenomenon consists in a large decrease of the pulse amplitude when B are small. With the values of $B<5$ the pulse maximum becomes more explicit and the pulse shape approaches a peaked shape. Therefore, the duration of the leading edge can be determined by the value of τ_m from the formulas (2.28) and (2.30).

We will dwell in a greater detial on the effect of the value of k on the pulse parameters. We will determine the condition for aperiodicity of the capacitor discharge. In the limit with $\tau \to \infty$ the voltage on the capacitor $x \to 0$, $\frac{d\varphi}{dx} \to 0$. Substituting these values of x and $\frac{d\varphi}{dx}$ into formula (2.25) we will determine the limit value of the quantity φ_∞ and then

$$y_\infty = \sqrt{\varphi_\infty} = \frac{\sqrt{1+2B}-1}{B}. \tag{2.38}$$

If the expression obtained is substituted into the equation (2.22) and Z is expressed in terms of x, we will obtain the following equation of the asymptote of the curve $x(\tau)$

$$k^2 \frac{d^2x}{d\tau^2} + B\left(1 + \frac{1}{\sqrt{1+2B}-1}\right)\frac{dx}{d\tau} + x = 0. \tag{2.39}$$

$$\text{With} \qquad k < \frac{1}{4}(1 + 2B + \sqrt{1+2B}) \tag{2.40}$$

the asymptote becomes aperiodic and, consequently, the curve $x(\tau)$ will not have zero and negative values in the interval $0 < \tau < \infty$. With an ideal commutator (i.e. with $R_1=0$) the condition of discharge aperiodicity has the following form

$$R > 2\sqrt{\frac{L}{C}} \tag{2.41}$$

or

$$k < \frac{B}{2}.$$

If the condition (2.41) is observed, then the condition (2.40) will also be observed, and with an increase of B the condition (2.40) approaches (2.41). This is explained by a decrease of the effect of the spark resistance.

We will determine the effect of k on the pulse amplitude. When k=0 the pulse amplitude can be determined by the formula (2.31). From the equation (2.25) we will express φ in terms of x, $\frac{d\varphi}{dx}$, B and k and will take a derivative of φ with respect to x. Taking the equality (2.27) into account we will assume that at the point where $Z_U = Z_{U\,max}$ the derivative $\frac{d^2\varphi}{dx^2}=0$. In doing so, we will obtain

$$Z_{UMAX} = x_{MAX}\left[1 - \frac{1}{\sqrt{1 - \frac{2k^2}{B} \cdot Z^2_{UMAX} + 2B(1 - x^2_{MAX})}}\right]. \tag{2.42}$$

In order to determine the pulse amplitude it is necessary to know x_{max} when $k \neq 0$. When the values of B are large the curve $Z(x)$ has a flat maximum. Therefore, in order to know $Z_{U\,max}$ it is sufficient to determine x_{max} only approximately. Formula (2.30) obtained for k=0 may be used for its approximate determination. The validity of the formula (2.42) for B=1, B=4 and $k=\sqrt{2}$ to $10\sqrt{2}$ was verified by the graphs shown in Weizel's work [70]. This verification showed that the largest error is about 4 percent. Thus, the use of the formulas (2.42) and (2.30) for the determination of the pulse amplitude gives a good correspondence with the results of exact calculations.

We will reduce formula (2.42) to a form more convenient for use by substituting the parameter k with the parameter $A=\frac{k^2}{B}$ (see Par. 2.2) and substituting x_{max} from the expression (2.30). In doing so, we will obtain

$$Z_{U\,MAX}=\sqrt{\frac{1+2B-(1+2B)^{2/3}}{2B}}\times \times\left[1-\frac{1}{\sqrt{(1+2B)^{2/3}-2A\cdot Z^2_{U\,MAX}}}\right]. \tag{2.43}$$

Par. 2.4. Determination of the Pulse Parameters With Account Taken of the Load Capacitance

The load and wiring capacitance C_n in the substitution network of a discharge circuit have to be calculated in the generators to obtain rectangular pulses when the load resistance R_n is high. In doing so, a resistance R_d is inserted in the circuit to damp the oscillations at the top of the pulse. The capacitor C is replaced with a source of infinite power having a voltage U_0 (see Figure 2.2d).

If the duration of the leading edge of the pulse on the load

$$t_\phi \ll R_\Sigma C_\Sigma. \tag{2.44}$$

then the current during the commutation period $i_{R_n} \ll i_{C_n}$ and, consequently, the effect of the resistance R_n on the process in the circuit may be neglected and it may be considered that $R_n=\infty$.

If the discharger is to be considered an ideal commutator (i.e. $R_1=0$), then the value of the damping resistance R_d found from the condition that $\Delta \leqslant 4$ percent (see Figure 2.1c) is determined from the relationship

$$R_\partial \geqslant \sqrt{2\frac{L}{C}\left(1-\frac{L}{2R_\Sigma^2 C}\right)}. \tag{2.45}$$

When the equality (2.45) is observed the duration of the leading edge of the pulse between the levels of 0-1 is found from the following formula

$$t_\phi = \frac{3\pi}{2\sqrt{2}} \cdot \frac{\sqrt{LC}}{\sqrt{1+\frac{R_\phi}{R_n}}}. \qquad (2.46)$$

We will analyze the effect of spark resistance on the pulse parameters when the condition (2.44) is satisfied. For the sake of analogy with the calculation given in Par. 2.3 we will omit the subscripts "n" and "d" aft r the C and R.

Differential equation of the current in the circuit (see Figure 2.2c) will be written as follows:

$$Ri + R_n i + L\frac{di}{dt} + U_c = U_0. \qquad (2.47)$$

After the transformations of the equation (2.47) similar to those carried out in the derivation of the equation (2.22) we will obtain the following

$$\frac{Z}{y} + BZ + k^2\frac{dZ}{d\tau} + x = 1. \qquad (2.48)$$

The same notations have been used as in the preceding paragraph. The differences consist only in the connection between Z, x and τ, and also between Z, y and x. In this case

$$Z = \frac{dx}{d\tau}, \qquad (2.49)$$

$$Z = \frac{1}{2}y\frac{dy}{dx}. \qquad (2.50)$$

The equation (2.47) may be reduced to the following form

$$2\sqrt{\varphi} + B\varphi + \frac{k^2}{8}\left(\frac{d\varphi}{dx}\right)^2 + 2x^2 - 4x = 0. \qquad (2.51)$$

where $\varphi = y^2$.

After determining the relationship $\varphi(x)$ from the equation (2.51) the relative voltage on the capacitor $x(\tau)$ with which we are concerned will be written as follows:

$$\tau = 4\int \frac{dx}{d\varphi/dx} + \text{const.} \qquad (2.52)$$

Like the equation (2.25) the equation (2.51) is not solved in the general form. An idea of the curve $x(\tau)$ (see Figure 2.1c) will be sufficiently complete if the voltage horn at the vertex of the pulse Δ and the steepness

of the leading edge $\frac{dx}{d\tau}$ are known. First we will find the condition with which $\Delta=0$. For this purpose, it is necessary to determine yce ($\frac{d\varphi}{dx}=0$, $x=0$) from the expression (2.51), substitute it into the inequality (2.40) and find aperiodicity condition of the curve $x(\tau)$. As in the preceding case, it turns out that this condition is the inequality (2.40). However, fulfillment of the condition (2.40) is not always expedient since this leads to a decrease of the steepness of the leading edge of the pulse. If $k=\frac{B}{\sqrt{2}}$ or $R=\sqrt{2}\frac{L}{C}$, then the steepness is higher than with the condition (2.40) and the horn Δ_1 is equal to 4 percent even in the most unfavorable case when $R_i=0$.

We will determine the maximum steepness of the leading edge of the pulse $\left(\frac{dx}{d\tau}\right)_m$ for $k=0$. For this purpose, with $k=0$ we will find φ from the equation (2.51), take a derivative of φ with respect to x, after which taking into account the expressions (2.48), (2.49) and (2.51) we will obtain

$$\frac{dx}{d\tau}=\frac{1-x}{B}\left(1-\frac{1}{\sqrt{1-2Bx^2+4Bx}}\right). \qquad (2.53)$$

If a derivative of $\frac{dx}{d\tau}$ with respect to x is taken and it is equated to zero, then we will determine the value of x_m at which steepness assumes the maximum value

$$x_m=1-\sqrt{\frac{(1+2B)-(1+2B)^{1/2}}{2B}}. \qquad (2.54)$$

Substituting this expression into the formula (2.53) we determine $\left(\frac{dx}{d\tau}\right)_m=f(B)$. To determine $\left(\frac{dx}{d\tau}\right)_m$ when $k\neq 0$ we will substitute $\frac{d\varphi}{dx}=\frac{1}{k}\cdot\frac{dx}{d\varphi}$ into the equality (2.51). Next, we will express φ in terms of B, k, x and $\frac{dx}{d\tau}$, we will take a derivative of φ with respect to x and equate the terms containing x'' to zero:

$$\left(\frac{dx}{d\tau}\right)_m=\frac{1-x_m}{B}\left(1-\frac{1}{\sqrt{1-2Bk^2\left(\frac{dx}{d\tau}\right)_m^2-2Bx_m^2+4Bx_m}}\right). \qquad (2.55)$$

If $x_m=f(B, k)$ is known, then $\left(\frac{dx}{d\tau}\right)_m$ is determined by solving the transcendental equation (2.55). The value of x_m can be determined approximately by proceeding from the following. The $\frac{dx}{d\tau}$ vs x characteristic has a flat

maximum when $x=x_m$. Therefore, steepness in the region close to x_m depends little on x. It is sufficient to find only an approximate value of x_m in order to determine $\left(\frac{dx}{d\tau}\right)_m$ with high accuracy.

It is possible to find the value of x_m approximately considering that with one and the same B x_m is not dependent on k, determine x_m with $k=0$ by formula (2.54) or find x_m considering that $R_1=0$.

As the numerical solution of the equation (2.51) indicates, with $B\leqslant 5$ the best results are obtained in determining x_m by the first method. In Table 2.1 are given the values of $\left(\frac{dx}{d\tau}\right)_m$ obtained with an exact and approximate determination of x_m when the equality $k=\frac{B}{\sqrt{2}}$ is observed.

Table 2.1

B	0	1	2	4
$\left(\frac{dx}{d\tau}\right)_m$	0,3849	0,2033	0,1433	0,0927*
	0.3849	0,2041	0,1431	0,0920**

* Определяется из первого условия.
** Точное значение x_m.

Key: (1) Determined from the first condition (2) Exact value of x_m

As it follows from Table 2.1 the difference between the exact and approximate values of the maximum steepness does not exceed one percent.

To determine the maximum steepness of the leading edge of the pulse with the conditions of $k=\frac{B}{\sqrt{2}}$ and $B\leqslant 5$ the following empirical formula obtained from the formulas (2.54) and (2.55) may be recommended:

$$\left(\frac{dU}{dt}\right)_m=\frac{\sqrt{3}aU_0^2}{9S^2p}\left[1-0{,}6876\frac{\sqrt{2LC}}{\theta}+0{,}2493\left(\frac{\sqrt{2LC}}{\theta}\right)^2-\right.$$
$$\left.-0{,}0312\left(\frac{\sqrt{2LC}}{\theta}\right)^3\right]. \qquad (2.56)$$

where U_0 is the voltage of the source; $\theta=\frac{2S^2p}{aU_0^2}$.

Formulas for calculating the pulse parameters according to the conditions in the discharge gap and circuit parameters were obtained in Par. 2.2-2.4. It follows from formulas (2.13), (2.17), etc. that to decrease the duration of the leading edge of the pulse it is necessary, with other conditions being constant, to decrease first of all the values of the spurious parameters L and C. But if L and C are negligibly small, then the duration of the leading edge t_f will be determined by the spark resistance. In doing so, to decrease t_f it is necessary to decrease the time constant of the discharger

$$\theta=\frac{2S^2p}{aU_0^2}$$

We will examine the methods of decreasing the θ. As it follows from the equation (1.4), for the right branch of Paschen curve the breakdown voltage increases with an increase of pS. In a certain range of pressures U_0= =const when pS=const. We may write $pS=p_0S_0$ where p_0 is pressure corresponding to normal conditions and usually taken to be equal to one atmosphere; S_0 is the length of the spark gap at the atmospheric pressure and the breakdown voltage U_0.

Then we obtain

$$S=\frac{S_0}{p},$$
$$\theta=\frac{2S_0^2}{ap\,U_0^2}. \qquad (2.57)$$

Consequently, to decrease the θ it is necessary to increase the pressure in the discharger p with the U_0 being constant. This conclusion agrees with the experimental data cited in Par. 1.3.

A very rapid increase of the breakdown voltage with a decrease of pS is observed in the left branch of Paschen curve (see Figure 1.1). If it is assumed approximately that

$$U_0=n-mp$$

where n and m are certain constant quantities, then

$$\theta=\frac{2pS^2}{a(n-mp)^2}. \qquad (2.58)$$

With an invariable pS the denominator tends to "an" with a decrease in the pressure p while the numerator continues to decrease. This leads to a decrease of θ. This conclusion is in qualitative correspondence with the results of investigations of low-pressure dischargers [75].

If a pulse breakdown of the discharger takes place when p=const and the voltage is higher than the static breakdown voltage U_{pr}, then

$$U_0 = \beta U_{np}$$

and

$$\theta = \frac{2pS^2}{aU_{np}^2\beta^2}.$$

[np = pr = breakdown] (2.59)

Consequently, with an increase of overvoltage β in the gap the value of θ decreases, which leads to a decrease of the duration of the leading edge of the pulse. This is confirmed by experimental data given in Par. 1.3.

If in the expression for θ the numerator and denominator are divided by S^2 and a p=1 atmosphere is taken, then we will obtain

$$\theta = \frac{2}{aE^2}, \quad (2.60)$$

where E is electric field strength at which a breakdown of the gap takes place.

It follows from formula (2.60) that the value of θ can be controlled by selecting a gas with different coefficients "a" and the strength E. In addition to this, the value of E changes with a different shape of the electrodes. In the case of electrodes with a nonuniform field in the gap the average value of E is smaller than in a uniform field. Consequently, θ should increase with an increase in the degree of nonuniformity of the field in the discharger. In the work [65] it is shown with the point-to-point electrodes the commutation time t_k exceeds the t_k with the sphere-to-sphere electrodes.

A decrease in the value of θ at a constant pressure p with a decrease in the length of the spark gap should be expected from formula (2.60) since in this case electric strength of the gases E increases. In Table 2.2 are given the values of the field strength E at which a breakdown of the gap in the air takes place according to the length of the gap S in a uniform field [29, 76].

Table 2.2

S, cm	1	0.1	0.06	0.01	0.006	0.001	0.0005
E, kV/cm	31	45	53	97	125	400	700

With a decrease of S from 1 to 0.01 the value of E increases approximately threefold while the value of θ (and consequently also the commutation time t_k) decreases in this process by nearly one order. This conclusion is confirmed by experimental data [63]. However, this effect may be utilized only with low pulse amplitudes.

The relative parameters of the pulse depend on the coefficients which unite θ and the circuit parameters. For the substitution network (see

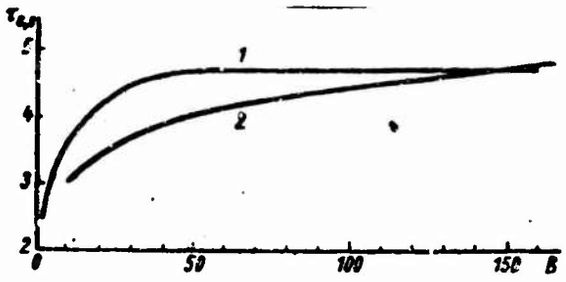

Figure 2.4. Curves of the relationship of the time $\tau_{0.8}$ to the value of B: 1 — experimental; 2 — theoretical.

Figure 2.2b) such a coefficient is A, and for the networks in Figures 2.2c and d — B and k. It is of interest to verify this experimentally. In Figure 2.4 are shown the curves of the relationship of the duration of the leading edge at a level of 0.1-0.8 to the coefficient B for the substitution network in Figure 2.2c. The value of the parameter B was controlled by varying the p, R_n, C and U_0. The discharger was in an air-filled coaxial metal chamber. An L=0 could be considered in all experiments. Also shown here is a curve obtained theoretically from formulas (2.28) and (2.29) by eliminating x with an a=1. Experimental points lie around the curve which runs close to the theoretical curve. Thus, in the first approximation it may be considered that the value of t_f depends only on the final value of B regardless of the character of the variation of this coefficient.

CHAPTER 3. METHODS OF DECREASING THE DURATION OF THE LEADING EDGE OF A HIGH-VOLTAGE PULSE

Par. 3.1. Capacitive Correction of the Leading Edge of a Pulse

In a generator with a shaping line, insertion of a noninductive capacitor (Figure 3.1a) parallel to the shaping line can be used to decrease the

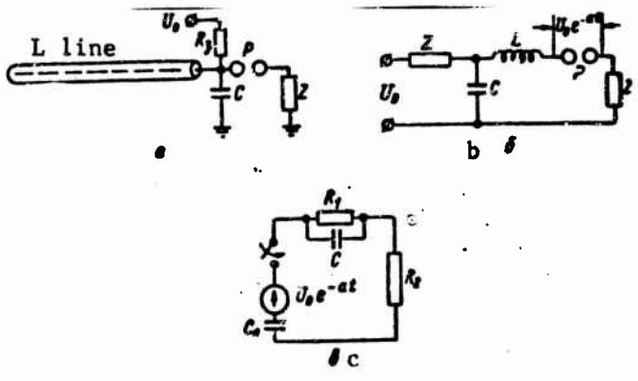

Figure 3.1. Diagram of capacitive correction of the leading edge of a pulse in a generator with a shaping line (a), substitution network (b) and substitution network of the discharge circuit of a generator with shaping C_0 and correcting C capacitors (c).

duration of the leading edge. The substitution network of this device with account taken of the inductance of the discharge circuit is shown in Figure 3.1b. We will replace the commutation characteristic with the following exponential

$$U_1(t) = U_0 e^{-a_0 t}. \qquad (3.1)$$

In the case of unit voltage, the voltage across the load may be written in operator form according to the dimensionless operator $q=\frac{p}{a_0}$ as follows:

$$h(q)=\frac{Bq+1}{(q+1)[q(B+b)+2]}. \qquad (3.2)$$

where

$$B=a_0ZC,\ b=\frac{a_0L}{Z}. \qquad (3.2')$$

When $\frac{(B+b)^2}{8Bb}>1$ the original h(t) has the following form

$$h(\tau)=\frac{1}{2}\left[1+2\frac{B-1}{Bb-B-b+2}e^{-\tau}-\frac{Bb-b+B}{Bb-b-B+2}\times\right.$$
$$\left.\times e^{-\delta\tau}\frac{\operatorname{sh}(\omega\tau+\varphi)}{\operatorname{sh}\varphi}\right]. \qquad (3.3)$$

where

$$\delta=\frac{B+b}{2Bb};\quad \omega=\frac{1}{2Bb}\sqrt{(B+b)^2-8Bb};\quad \tau=a_0t;$$
$$\operatorname{th}\varphi=\frac{2Bb\omega}{B(b-b+B)}. \qquad (3.3')$$

The factor $\frac{1}{2}$ in the expression (3.3) indicates that in a network with a shaping cable the pulse voltage decreases by one half in comparison with the charging voltage.

When $\frac{B+b}{8Bb}<1$ the hyperbolic sines and tangents in the equality (3.3) are substituted with trigonometric sines and tangents, and in the expression for ω the sign under the root is changed to the opposite sign. The characteristics $h(\tau)$ for b=0 ard different values of B are shown in Figure 3.2a.

With an increase of B the duration of the leading edge decreases but with large B a spike Δ appears at the vertex, which distorts the shape of the pulse. The maximum of this spike may be found from the equation $\frac{dh(\tau)}{d\tau}=0$. In Figure 3.2b are shown the curves of the relationship of the duration of the leading edge τ_f to B and b. We will determine the optimum value of the parameter B at which $\Delta\approx 5$ percent. For this purpose we will substitute $\tau=\tau$ and $h(\tau)=\frac{1}{2}[1+\Delta(\tau)]$ into the equation (3.3) and find the curve of the correction boundary B=f(b) (see Figure 3.2b). The optimum value of the capacitance C may be found from this curve. When $0\leqslant b\leqslant 2$ the value of

$$C\approx 0{,}63\frac{t_k}{Z}-0{,}19\frac{L}{Z^2}. \qquad (3.4)$$

With L=0 and the optimum value of C the duration of the leading edge decreases by more than one half. It follows from Figure 3.2b that the effectiveness of correction decreases with an increase of L. When $L>t_kZ$ correction hardly decreases the duration of the leading edge of the pulse.

A decrease of the duration of the leading edge of a pulse using the arrangement described is possible in a network with a shaping line. However,

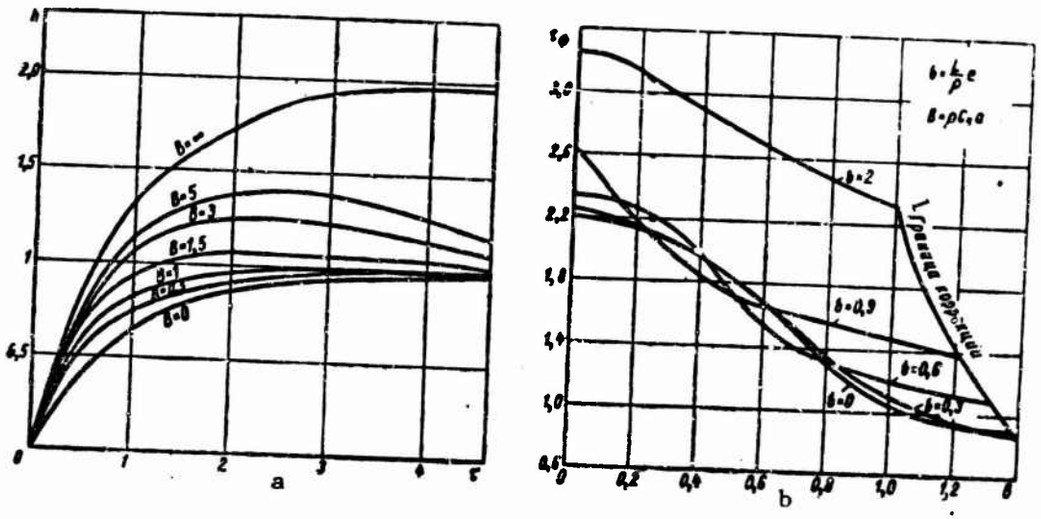

Figure 3.2. Voltage across the impedance Z in relation to τ and B (a), and duration of the leading edge of the pulse on Z in relation to B and b (b).

Key: (1) Correction boundary

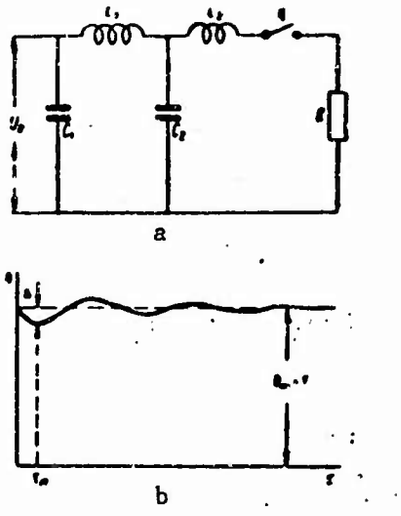

Figure 3.3. Substitution network of a discharge circuit with a compensating capacitance (a) and voltage characteristic across R in the case of an ideal commutator (b).

correction network with a large shaping capacitance when it can be replaced with a source of infinite power (see Figure 3.1c) follows directly from the substitution network (see Figure 3.1b) when L=0.

When $R_1=R_2$ the analysis of this network will be the same as in the network in Figure 3.1b. In addition to this, owing to a decrease of the pulse amplitude by one half the t_f decreases by more than one half.

When using a corrective capacitor the duration of the cutoff increases owing to a protracted discharge of the capacitor.

If it is necessary to obtain high-voltage pulses with a steep leading edge, flat top and long duration, then paper oil-filled capacitors with a large capacitance are used. The self-inductance of these capacitors (see Par. 5.4) is high. This prevents the obtaining of a short leading edge. In addition to this, sometimes small dimensions of a discharge circuit cannot be used, for example due to the necessity of observing insulation distances in the case of very high voltages. Because of this, the inductance of the circuit will be high and, accordingly, the duration of the leading edge of the pulse will be long.

The effect of spurious inductance on the duration of the leading edge of the pulse may be decreased by inserting a noninductive capacitor between

the high-voltage electrode of the commutator and the grounded lead of the load (Figure 3.3a).

In Figure 3.3a L_1 is inductance the effect of which has to be eliminated, and L_2 is inductance remaining in the circuit.

If $L_1 \gg L_2$ and $C_1 \gg C_2$, then in the first period after the operation of the commutator for the load the primary current will be provided by the capacitor C_2 and not by the shaping capacitor whose current will be limited by the high inductive reactance $L_1 p$. If a sufficiently large value of C_2 was selected and it does not have time to discharge considerably in the period of shaping the leading edge, then the duration of the leading edge of the pulse in the case of constant load will be determined only by the inductance L_2. However, oscillations may appear on the top of the pulse in this case (see Figure 3.3b). To evaluate these oscillations we will examine the transient in the circuit shown in Figure 3.3a. The voltage across the resistance R for an ideal commutator with unit voltage on the shaping capacitor has the following form in the operator form

$$h(q) = \frac{Bq^2 + 1}{Bbq^3 + Bq^2 + (b+1)q + 1}. \qquad (3.5)$$

where

$$q = \frac{L_1}{R} p; \quad B = \frac{C_2 R^2}{L_1}; \quad b = \frac{L_2}{L_1}. \qquad (3.5')$$

It follows from the condition (3.5) that when the values of B are large

$$h(q) \approx \frac{1}{bq + 1}. \qquad (3.5'')$$

or

$$h(t) \approx 1 - e^{-t \frac{R}{L_2}}. \qquad (3.5''')$$

Consequently, the duration of the leading edge of the pulse $t_f = 2.2 \frac{L_2}{R}$ with account taken of the commutation time t_k can be determined from the equation (2.3) since the transfer characteristic h(t) tends to a monotonic characteristic when B are large.

The value of B has to be determined from the condition for permissible dip Δ at the top of the pulse. In doing so, we will determine the characteristic $h(\tau)$ for the case of oscillatory process in the circuit. In the case of aperiodic process the capacitor C_2 has time to become already discharged on the leading edge of the pulse. We will determine Δ when $b \ll 1$

$$h(\tau) = 1 - \frac{2}{\sqrt{4B - 1}} e^{-\frac{\tau}{2B}} \sin \frac{\sqrt{4B-1}}{2B} \tau, \qquad (3.6)$$

where

$$\tau = t\frac{R}{L_1}$$

The distortion of the top is brought about by the second addend of this equality, i.e.

$$\Delta(\tau) = -\frac{2}{\sqrt{4B-1}} e^{-\frac{\tau}{2B}} \sin\frac{\sqrt{4B-1}}{2B}\tau. \qquad (3.7)$$

If a derivative $\frac{d\Delta(\tau)}{d\tau}$ is taken in this equation and equated to zero, then the highest amplitude of the spike $\Delta(\tau)=\Delta_m$ corresponds to the smallest value of $\tau=\tau_m$ found from this equation. To decrease Δ_m it is necessary first of all to decrease the amplitude $\frac{2}{\sqrt{4B-1}}$, i.e. to increase B. The following formula may be used to determine the value of Δ when $\Delta_m \leqslant 10$ percent

$$\Delta_m \approx \frac{1}{\sqrt{B}} = \frac{\sqrt{L_1}}{\sqrt{C_1 R}}. \qquad (3.8)$$

In doing so, the value of τ_m is determined from the formula $\tau_m = \frac{\pi\sqrt{B}}{2}$ or

$$t_m = \frac{\pi}{2}\sqrt{L_1 C_1}. \qquad (3.9)$$

The relationships (3.8) and (3.9) were obtained for $b \leqslant 1$. However, a detailed analysis of the original of the representation (3.5) indicates that in all of the cases used in practice ($\Delta_m < 10$ percent; $b \leqslant 0.5$) these relationships give a good approximation. This analysis is complicated and is not given here.

With the aid of compensation method the duration of the leading edge of the pulse (when $R_1=0$) can be decreased for the network shown in Figure 2.2b by

$$\frac{t_{f1}}{t_{f2}} = \frac{L_1 + L_2}{L_1} = \frac{1+b}{b} \text{ times},$$

and for network in Figure 2.2d by

$$\frac{t_{f1}}{t_{f2}} = \frac{\sqrt{C_n(L_1 + L_2)}}{\sqrt{L_2 C_n}} = \sqrt{\frac{1+b}{b}} \text{ times}.$$

In concluding this paragraph we will examine the problems of the correction of pulse shape by selecting the value of the shaping capacitor.

It was pointed out in Par. 1.3 and 2.2 that the steepness of the commutation characteristic of the discharger changes with time with the steepness being very marked at the start of the commutation and sharply decreasing at the end. If a line is used as a shaping device, then with small spurious parameters of the discharge circuit the leading edge of the pulse will iterate the commutation characteristic. In this process the duration of the leading edge between the levels of 0.1 and 0.9 will be long with the greatest portion of the leading edge being between the levels of 0.9 and 0.8 of the amplitude. Another important drawback of a network with a shaping cable is the decrease of the pulse amplitude by one half in comparison with the charging voltage.

We will introduce the following coefficient for the characteristic of the region of transition from the leading edge of a pulse to its top

$$\alpha=\frac{t_{0.8}}{t_{0.9}}$$

where $t_{0.8}$ is the time for the increase of the voltage on the leading edge of the pulse from 0.1 U_a to 0.8 U_a, and $t_{0.9}$ — from 0.1 U_a to 0.9 U_a.

In a network with a shaping cable with A=0 the coefficient $\alpha\approx0.33$ (see Figure 2.3a) whereas for and ideal rectangular pulse $\alpha=1$. By selecting the value of the shaping capacitor the α may be increased and t_f decreased by means of a small decrease of the amplitude in comparison with the charging voltage. This method of correction is based on the circumstance that in the period of slow voltage drop on the commutation characteristic the voltage in the capacitor also drops owing to a partial discharge. Because of this, the transition from the leading edge to the top of the pulse takes place more sharply. In Table 3.1 are given experimental data on the effect of the value of the shaping capacitor on the pulse parameters when the air pressure in the discharger p=1 atmosphere, charging voltage U_0=15 kv, the load resistance is 75 ohms and inductance of the discharge circuit is less than 10^{-8} henries. With the time t_m the pulse voltage assumes the maximum value equal to U_a, and with the time $t'_{0.9}$ it drops on the pulse tail to 0.9 U_a.

Table 3.1

1 Формирующий элемент	Кабель РК-3	С-2000 пф 3	С-1000 пф	С-500 пф	С-250 пф
U_a, кв kv	15	13,4	13	11,3	8,6
$t_{0.8}$, мксек пвес	7,5	6,8	6,4	6,3	5,6
$t_{0.9}$, мксек	21	8,3	7,5	7,1	6,9
$t'_{0.9}$, мксек	—	47	27,8	19,1	12,8
α	0,36	0,82	0,85	.,89	0,81
t_m, мксек	∞	32	20,3	15,4	10,9

Key: (1) Shaping element (2) Cable RK-3 (3) pf=picofarads

It follows from Table 3.1 that when C=2,000 picofarads the pulse amplitude is only 11 percent lower than the charging voltage. The coefficient α approaches unity and the leading edge of the pulse is nearly three times shorter than in a network with a shaping cable. The shape of a pulse obtained in a network with a capacitor is not always acceptable owing to the slow voltage drop on the tail. By using circuits for shortening the pulse duration it is possible to obtain pulses approaching in shape the rectangular pulses. We will assume that the voltage drop at the top of the pulse is ten percent relative to the amplitude voltage. For the case examined in Table 3.1 $t_f=t_{0.9}=t_f=8.3$ nanoseconds, $t_i=t_{0.9}+t'_{0.9}=55.3$ nanoseconds. It is assumed that the duration of the cutoff $t_{sr}\approx t_f$ (see Figure 2.1a). The duration of the leading edge will amount only to 1/7 of the duration of the entire pulse. In most cases this satisfies the requirements demanded of the rectangular pulses.

In Par. 2.3 it was shown that with a small inductance of the discharge circuit all parameters of the pulse depend on the value of $B=R_n C \frac{U_0^2}{2pS^2}$. On the basis of the data in Table 3.1, to obtain a pulse approaching in shape a rectangular pulse it is necessary to have a $B \geqslant 100$ or

$$C \geqslant \frac{200 p S^2}{\alpha U_0^2 R_n}. \qquad (3.10)$$

Par. 3.2. "Peaking" Spark Discharger

To decrease the duration of the leading edge of a pulse a spark discharger P is sometimes used, which is inserted in series with a long line, usually a cable (Figure 3.4a), over which the pulse propagates. The latter creates considerable overvoltage in the discharger and upon its breakdown the leading edge of the pulse is shortened. Overvoltage is created owing to a delay of the breakdown of the gap of the discharger P and owing to a doubling of the pulse voltage, as in an open line.

These dischargers were given the name "peaking" dischargers. At the present time they are used to obtain pulses with a leading edge of the order of 10^{-10} seconds and an amplitude of tens of kilovolts (see Par. 5.7).

An equivalent network of the discharge circuit of the "peaker" for the period of the conversion of the leading edge of the pulse is shown in Figure 3.4b. The network has no self-inductance of the discharge circuit since the peaker chamber is usually well matched with the cables L_1 and L_2. For the simplicity of the calculation we will asume that voltage on the leading edge of the primary pulse increases in accordance with the following linear law

$$U=\frac{U_0}{t_{\phi_1}} t, \qquad (3.11)$$

and the voltage at the top of the pulse remains equal to U_a (Figure 3.5) for and infinitely long time.

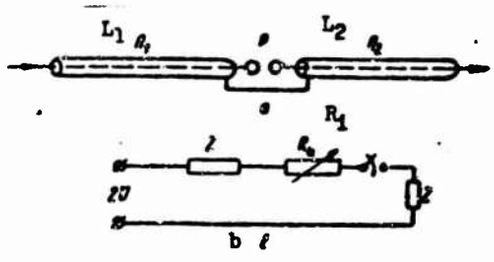

Figure 3.4. The circuit diagram of the peaking spark discharger (a) and the substitution network of the discharge circuit (b).

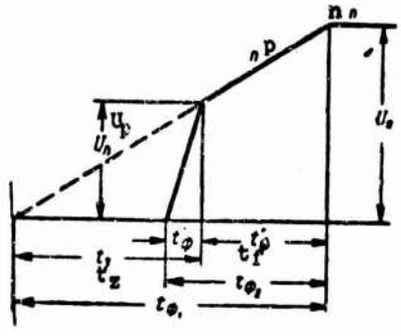

Figure 3.5. On the calculation of peaking of the leading edge of a pulse.

The duration of the leading edge of the pulse at the output t_f (see Figure 3.5) depends on the overvoltage which is brought about by the delay time of the breakdown of the peaker t_z. The latter depends on the duration of the leading edge t_f. With other conditions being equal the time t_z [t_{delay}] depends on the length of the gap S and bears a statistical character. The longer the t_z the higher the voltage U_p at which the gap breaks down and the shorter the length of the leading edge of the pulse t_{f_2}, and vice versa. It follows from Figure 3.5 that if with the shortest of the possible t_z the breakdown occurs at the point n, then regardless of the value of t_z the breakdown voltage remains equal to U_a. The smallest value of t_z is equal to t_r — the discharge-formation time. Therefore, the condition

[$t_p = t_r$ = discharge-formation time] $\qquad t_{\varphi_1} = t_p \qquad (3.12)$

corresponds to the highest stability of the value of t_{f_2}.

We will show that when condition (3.12) is satisfied the value of t_{f_2} turns out to be minimal. Indeed, if the breakdown of the gap takes place at the point n, then taking into account the doubling of the voltage due to the reflection of the wave from the peaker and taking into consideration that p=1 atmosphere, we obtain (see Par. 2.2)

$$t_{\phi_1} = m \frac{S^2}{a(2U_a)^2} . \tag{3.13}$$

where m depends on the method of determining the duration of the leading edge of the pulse.

If the length of the gap S is increased and consequently that of t_z also, in such a manner that the breakdown takes place at the point n", then the breakdown voltage will not change but t_{f_2} will increase owing to a decrease of the overvoltage. If S is decreased so that with $t_z=t_r$ the breakdown would occur at the point n', then t_{f_2} will also increase owing to the increase of t''_f and of the voltage in the gap in the period of the commutation of the discharger. Thus, the value of S at which t_{f_2} is minimal is also determined from the condition (3.12). Henceforth we will indicate this value of S by S_m.

In the breakdown on the leading edge of the pulse the discharge-formation time is determined by formula (1.26) which with the condition (3.12) will assume the following form for our case

$$[U_0 = U_e] \qquad t_{\phi_1} = \frac{(1.14\sqrt{S_m} + 2.44S_m)\cdot 10^6}{U_a} t_{\phi_1} + \frac{1690 S_m^{3/2}}{\sqrt{2U_a}(2U_a - 2.44\cdot 10^6 \cdot S_m)^2} . \tag{3.14}$$

where

$$U_e \approx U_a \frac{t_1 + 3t_{f_1}}{4t_{f_1}}$$

The value of t_1 is determined from Raether condition (1.3). With the pulse amplitudes U_a=5 to 50 kv the characteristics $S_m=f(t_{f_1})$ found from the condition (3.14) may be approximated with the curves of the following form

$$S_m = \eta U_a t_{\phi_1}^{\delta} . \tag{3.15}$$

where $\eta=1.9 \cdot 10^{-2}$; $\delta=0.21$ if U_a is expressed in kilovolts and t_{f_1} in nanoseconds.

To determine the relationship of t_{f_2} to t_{f_1} we substitute the values of S_m from the expression (3.15) into the equation (3.13)

$$t_{\phi_1} = \eta_1 t_{\phi_1}^{\delta_1}. \tag{3.16}$$

where

$$\eta_1 = \frac{m^{\delta_1}}{4^{\delta_1}}; \quad \delta_1 = 2. \tag{3.16'}$$

It follows from the expression (3.16) that the value of t_{f_2} is dependent on t_{f_1} and is not dependent on the pulse amplitude. To decrease t_{f_2} it is necessary to decrease t_{f_1} with the pressure in the discharger being constant.

The peaking efficiency $k_e = \frac{t_{f_1}}{t_{f_2}}$ decreases with a decrease of t_{f_2}. According to the work [78], to obtain a pulse with U_a=20 kv and t_{f_2}=0.6 nanosecond the value of $k_e \approx 3$.

It follows from the equality (3.16) that with atmospheric pressure in an air peaking discharger, to obtain a pulse with a duration of the leading edge $t_{f_2} \leqslant 10^{-9}$ seconds it is necessary to have a t_{f_1} of the same order as t_{f_2}. To create a generator of primary pulses with such a short leading edge is very difficult. Sometimes the pressure in the discharger is increased to increase the t_{f_1}.

By increasing the pressure of nitrogen in the discharger to 100 atmospheres with U_a=20 kv and t_{f_2}=0.3 nanosecond Fletcher [27] increased the peaking efficiency k_e approximately to 60.

To increase k_e it is possible to make use of the method of successive peaking of the leading edge of the pulse when several peaking dischargers connected with lengths of cable are installed. If a pulse with a leading edge of t_{f_1} comes over the line L_1, then in the line L_n we will obtain

$$t_{\phi_n} = \eta_1^n t_{\phi_1}^{n\delta_1}. \tag{3.17}$$

where n is the number of dischargers.

The method of successive peaking may be used even when the value of t_{f_1} is of the order of several microseconds. With such a great length of the leading edge of the pulse the overvoltage during the breakdown of the gap P_1 will not exceed unity.

It follows from Figure 3.5 that

$$t_{\phi_1} = t'_f + t_{\phi_1} - t_s \qquad (3.18)$$

where

[$U_n = U_p$ = overvoltage]

$$t_s = \frac{U_a}{2U_a} t_{\phi_1}. \qquad (3.19)$$

The value of t'_f is approximately equal to t_k — to the commutation time of the discharger in the case of a static breakdown. With p=1 atmosphere the value of $t_k = t_{k0} \approx 10^{-8}$ second and depends little on the breakdown voltage and with $p > 1$ atmosphere the time $t_k \approx \frac{t_{k0}}{p}$.

If in the formula (3.19) the voltage U_p is substituted with its value expressed by the product of pS (Paschen curve), then

$$t_{\phi_1} \approx \frac{t_{k_0}}{p} + t_{\phi_1}\left(1 - \frac{A p S}{2U_a}\right). \qquad (3.20)$$

It follows from the expression (3.20) that if by varying the pS the second term in parentheses approaches 1, then $t_{f_2} \to \frac{t_{k0}}{p}$. This is achieved by increasing the S until the beginning of stable breakdowns of the gap. Consequently, even with p=1 atmosphere, by controlling the S the t_f can be decreased to 10^{-8} second with the aid of the first peaker. The further decrease of t_f takes place after the subsequent peakings.

Investigations showed that with the use of three peakers the duration of the leading edge of a pulse with an amplitude of U_a=30 kilovolts decreases from $0.8 \cdot 10^{-6}$ to 10^{-9} second. Thus the peaking efficiency $k_e \approx 800$.

Practically any primary pulse has a duration limited either by a voltage drop owing to the discharge of the shaping capacitor or by the length of the shaping cable. Therefore, statistical variations in the breakdown of a peaking discharger will vary the duration and amplitude of a pulse. To stabilize the operation of a peaking discharger it is necessary to use ultraviolet irradiation of the cathode or other methods of eliminating the statistical lag.

Par. 3.3. Artificial Lines With Nonlinear L and C Elements

One of the effective means of increasing the steepness of the leading edge of the pulses is the use of lines with nonlinear inductance or capacitance. There are materials in which a decrease of magnetic inductivity takes place with an increase of the current or a decrease of specific inductive capacitance with an increase of electric field strength. If a line is made up of such materials, then the propagation velocity of an electromagnetic wave increases with an increase of the voltage. In a propagating wave the points

with a large voltage will be "overtaking" the points with a smaller voltage and the length of the leading edge of the pulse will decrease.

We will examine the propagation of a plane linearly polarized wave in a homogeneous isotopic nonlinear medium [79]. We will consider that in a wave propagating along the axis z magnetic field is oriented along y and electric field — along x. If a change in the fields takes place sufficnetly slowly, then the connection of magnetic field strength H with magnetic induction B and of electric field strength E with electric induction D is not time-dependent and is defined by the following functions

$$B_y = B(H_y); \quad D_x = D(E_x). \tag{3.21}$$

If we limit ourselves only to the nonlinearity of the first relationship in this expression and consider the second a linear $D = \varepsilon E$, then the solution of Maxwell equations will assume the following form

$$H = f\left[Z \pm \frac{ct}{\sqrt{\varepsilon\mu(H)}}\right]; \quad E = \pm \int_0^H \sqrt{\frac{\mu(H)}{\varepsilon}}\, dH, \tag{3.22}$$

where c is the velocity of light in vacuum; $\mu(H) = \frac{dB}{dH}$, and $f(\xi)$ is an arbitrary function defined fro boundary conditions.

Solution of the equation (3.22) describes traveling waves each point of the profile of which moves at a velocity which depends on the magnitude of magnetic field strength at this point $v = \frac{c}{\sqrt{\varepsilon\mu(H)}}$. If $\mu(H)$ is a decreasing function of H, then the points of the wavefront where H is larger in absolute value, will propagate at a higher velocity. Because of this, the wavefront of the magnetic field strength H will decrease and the droop will stretch out. Starting with a certain instant t an infinite derivative will appear in the function H(t, Z). This indicates the appearance of an electromagnetic shock wave. Theoretically in this case $t_f = 0$; however, in practice the value of t_f is always larger than zero and is determined by the properties of the medium in which the wave propagates. The condition relative the characteristic B(H) is satisfied, for example, in ferrite magnetized to saturation by a longitudinal (in relation to the direction of the wave propagation) uniform magnetic field H_0.

I. G. Katayev [80] suggested using the phenomenon described in an artificial line with nonlinear L or C to increase the steepness of the leading edge of the pulse. In doing so, pulses with an amplitude of several kilovolts and duration of the leading edge of (0.3 to 0.5) 10^{-9} sec were obtained in a line with inductances wound on ferrite cores and with linear capacitances with the field in the ferrite being 500-700 oersteds. When using

a line employing ferroelectrics it is possible to obtain pulses with a leading edge of only a few nanoseconds owing to the small breakdown strength of the ferroelectrics which prevents an increase of E and a decrease of ε. The work [80] shows the feasibility of using nonlinear capacitances of n-p junctions for the purposes indicated. However, in the latter case it is possible to obtain pulses with an amplitude of several tens of volts.

We will dwell in a greater detail on the operation of a line with ferrite coils L(I) and capacitances C_0=const (Figure 3.6). An analysis of the operation of such a line was carried out by I. G. Katayev.

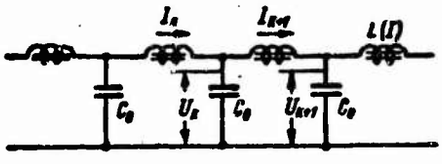

Figure 3.6. Diagram of an artificial line with nonlinear inductances.

If there is no mutual induction between the cells and the following conditions are observed

$$\left.\begin{aligned} |I_n - I_{n+1}| &\ll I_n, \\ |U_n - U_{n+1}| &\ll U_n. \end{aligned}\right\} \tag{3.23}$$

then by analogy with the formula (3.22) two simple waves will exist in the line:

$$\left.\begin{aligned} I &= f(t \pm Z)\sqrt{L(I)C_0}, \\ U &= \pm \int_0^I \sqrt{\frac{L(I)}{C_0}}\, dI. \end{aligned}\right\} \tag{3.24}$$

It follows from the relationships obtained that the propagation velocity of the wave depends on the current. Therefore, in the process of propagation in a nonlinear long line the wave becomes deformed as in a continuum. With a decreasing characteric L(I) the wavefront will be becoming steeper as it moves in the line. If the character of the characteristic L(I) does not change, then a break appears on the wavefront which leads to a sharp decrease of t_f in comparison with the input wave.

If the field in the ferrite is uniform (for example, the core has the form of a toroid or thin rod) and the cores were brought up to saturation by and external constant magnetic field H_0, then when the current of the wave is larger than a certain critical current the characteristic L(I) has a droop-

ing character. It can be shown that the following relationship is observed after the formation of discontinuity

$$\tau_{z.s} < \tau_s < \tau_{p.s}$$

where $\tau_{z.s}$, $\tau_{p.s}$, τ_s are the time constants of the cell beyond discontinuity, before discontinuity, on discontinuity respectively. The shortest possible duration of the shock-wave front depends on the relaxation time of the ferrite τ_0 and the time constant of the cell τ_s. With the condition that $\tau_s \ll \tau_0$ for a ferrite core with a rectangular hysteresis loop the current-time relationship on the shock-wave front has the following form

$$I = I_a \frac{e^{\frac{\lambda p_0 I_a}{M} t}}{\sqrt{e^{\frac{2\lambda p_0 I_a}{M} t} + 1}}. \qquad (3.25)$$

where λ is relaxation frequency; p_0 — coefficient dependent on the parameters of the coil (for example, for a toroid $p_0 \approx 0.4 \frac{n}{D_{sr}}$ where n is the number of turns and D_{sr} — the average diameter of the toroid); M — magnetic moment of a unit of volume of saturated ferrite; I_a — amplitude of the wave of current

$$[t^2_c = t^2_s] \qquad I_a = k_0 \frac{C_0 M}{(\tau^2_c - C_0 L_0)}. \qquad (3.26)$$

In the last expression the value of k_0 depends only on the dimensions and design of the coil, L_0 is the inductance of a coil without ferrite.

It follows from the expression (3.25) that the duration of the leading edge between the levels of 0.1 and 0.9 of the amplitude value amounts to

$$t_\phi = 3 \frac{M}{p_0 I_a \lambda}. \qquad (3.27)$$

The delay time of one cell found from the formula (3.26) amounts to

$$\tau_c = \sqrt{L_0 C_0 + k_0 \frac{M C_0}{I_a}}. \qquad (3.28)$$

Wave impedance of a long line does not depend on I but depends on I_a

$$Z = \sqrt{\frac{L_0}{C_0} + k_0 \frac{M}{I_a C_0}}. \qquad (3.29)$$

Therefore, conditions for matching remain the same as in an ordinary line.

Oscillations brought about by spin precession are superimposed on the shock wave in some cases. The duration and frequency of these oscillations

depend on the quality of the ferrite and on the degree of saturation. Oscillations increase with an increase of the cell's time constant τ_s.

It follows from the equality (3.27) that the duration of the leading edge decreases with an increase of the current amplitude. However, with an increase of I_a the oscillations on the top of the wave increase. To eliminate these oscillations it is necessary to decrease τ_s.

In the work [81] is shown the feasibility of creating two discontinuities in a line the inductance L(I) of which has a falling and an ascending section. The last circumstance may be utilized for shaping rectangular pulses.

CHAPTER 4. METHODS OF OBTAINING AND CONVERTING PULSES IN DEVICES WITH LONG LINES

Introduction

Long lines find wide application for shaping short high-voltage pulses. Cable lines are used for shaping, delaying, shortening of the duration and increasing the amplitude of the pulses. They are also used as noninductive loads.

In analyzing the network attempt was made to determine its basic characteristics without taking into account the attenuation of the waves in a cable since the last problem is examined separately in Par. 5.2. In accordance with this, wave impedance of a line Z, propagation velocity of the waves v and delay time per unit of length T are expressed by the well known formulas:

$$Z=\sqrt{\frac{L}{C}};\quad v=\frac{1}{\sqrt{LC}}=\frac{c}{\sqrt{\varepsilon\mu}};\quad T=\sqrt{LC}. \tag{4.1}$$

where c=300 meters/microsec is velocity of light; ε and μ are respectively specific inductive capacitance and magnetic inductivity of the medium surrounding the line.

Par. 4.1. Shaping of Pulses With the Aid of Sections of Long Lines

We will examine the diagram of a transmission line. In Figure 4.1a is shown the source of emf E with internal impedance Z_1. The source of emf is located at the point x=0 and supplies a line of the length l having wave impedance Z. The line terminates at the arbitrary impedance Z_2. The voltage at a certain arbitrary point A which is at a distance x from the start of the line may be written in operator form as follows [2]:

$$U_{-}(p)=a\frac{1+\rho_e e^{-2pT(l-x)}}{1-\rho_0\rho_e e^{-2pT(l-x)}}E, \tag{4.2}$$

where

$$\alpha=\frac{Z}{Z_1+Z};\quad \rho_2=\frac{Z_2-Z}{Z_2+Z};\quad \rho_0=\frac{Z_1-Z}{Z_1+Z}- \tag{4.2'}$$

are coefficients of reflections from the end and the start of the lines.

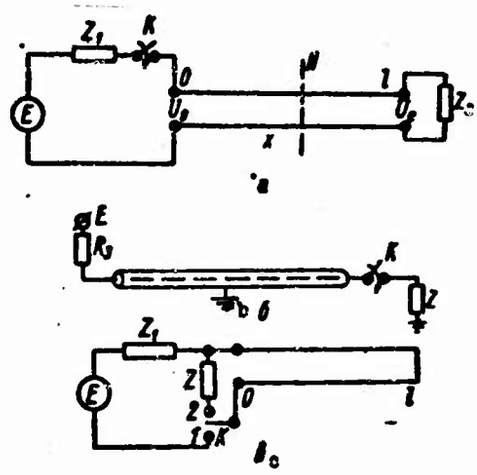

Figure 4.1. The simplest networks for shaping the pulses with the aid of long lines: pulse shaping network in a general form (a) with an open shaping line ($R_z \gg z$) and with a short-circuited shaping line (c).

Input impedance of a line terminating at an arbitrary load Z_2 is equal to

$$[Z_{вх}=Z_{vkh}=Z_{in}] \qquad Z_{вх}=\frac{1+\rho_2 e^{-2p\tau l}}{1-\rho_0 e^{-2p\tau l}}. \tag{4.3}$$

The voltage across Z_1 will be written as follows:

$$U_{Z_1}(p)=\frac{(1-\alpha)-\rho_2(\rho_0+\alpha)e^{-2p\tau l}}{1-\rho_0\rho_2 e^{-2p\tau l}}E. \tag{4.4}$$

We will examine certain particular cases which follow from the formulas (4.2)-(4.4).

1. If $Z_1=Z$, $Z_2=0$, then

$$U_x(p)=\frac{1}{2}\cdot E\left[1-e^{-2p\tau(l-x)}\right]. \tag{4.4'}$$

Using the inverse Laplace transform it is possible to show that

$$U_x(t) = \frac{1}{2}[E - E(t - 2T l_x)]. \qquad (4.5)$$

where $l_x = l - x$.

When E=const a rectangular voltage pulse with an amplitude $U_a = \frac{E}{2}$ and duration $t_i = 2Tl_x$ defined by a double length of short-circuited section will appear at the point A. The value of the load resistance inserted at the point A must satisfy the condition that $R_n \gg Z$ [$R_n = R_{load}$] in order not to disturb the matching of the line.

Sending to the input of the line a pulse with a finite rate of the rise of the leading edge, for example

[$T_s = T_v$ = time constant] $\qquad E(t) = E(1 - e^{-\frac{t}{T_s}})$, $\qquad (4.6)$

we will obtain, after shortening, a pulse which from the instant of voltage rise to the instant of the fall-off (i.e. in the course of the time t_i) will be described by the equation (4.6). If the time constant $T_v < \frac{Tl_x}{5}$, then it may be considered that input voltage became completely stable in the time t_i. Then, with $t \geqslant t_i$ the cutoff of the pulse will be expressed by the following relationship

$$U_c(t) = \frac{1}{2} E e^{-\frac{t - Tl_x}{T_s}}. \qquad (4.7)$$

If in the time t_i the E(t) does not reach a value approaching a steady-state value, then the cutoff is described by the following equation

$$U_c(t) = \frac{1}{2} E e^{-\frac{t}{T_s}} (e^{\frac{Tl_x}{T_s}} - 1). \qquad (4.8)$$

In the cases examined the pulse amplitude turns out to be smaller by one half than that of the input signal. This is explained by the insertion at the input of the line of the impedance $Z_1 = Z$ which is necessary to quench a pulse reflected from the short-circuited end of the line. If a $Z_1 = 0$ is taken, then no decrease of the pulse amplitude takes place and numerous pulses reflected from the start and end of the line will appear following the primary pulse.

Additional pulses appear when $Z_1 = Z$ if the voltage at the input of the line E(t) is a pulse of finite duration. For example, if the leading edge of a pulse is infinitely steep and the voltage on the top drops in accordance with the exponential

$$E(t) = Ee^{-\frac{t}{\tau_0}}. \qquad (4.9)$$

then the expression for the voltage of the additional pulse will assume the following form

$$[U_д = U_d = U_{\text{additional pulse}}] \quad U_д(t) = \frac{1}{2}E(1 - e^{-\frac{2Tl_x}{\tau_0}}). \qquad (4.10)$$

When $T_v \gg 2Tl_x$ the amplitude of the additional pulse will be determined from the following formula

$$U_д \approx E\frac{Tl_x}{\tau_0}. \qquad (4.11)$$

By varying l_x and T_v the amplitude of the additional pulse can be made as small as desired.

If a pulse of rectangular shape, for example with a duration τ_1, is sent to the input of the line, then following the primary pulse a pulse similar to the primary pulse but having opposite polarity will appear after the time $\tau_1 - 2Tl_x$.

2. We will examine now a case when $Z_1 = Z$, $Z_2 = \infty$, E=const. In this case the expression (4.4) will assume the following form

$$U_{z_1}(p) = \frac{E}{2}(1 - e^{-2pTl}). \qquad (4.11')$$

or after transformation

$$U_{z_1}(p) = \frac{E}{2}[1 - 1(t - 2Tl)]. \qquad (4.12)$$

In this case the expression for input impedance will assume the following form

$$Z_{вх} = Z\,\text{cth}\,pTl. \qquad (4.13)$$

The equation (4.12) describes a rectangular pulse with an amplitude E/2 and a duration of $2Tl$. It is easy to see that with the values of Z_1 and Z_2 indicated above the network in Figure 4.1a changes into a substitution network with a shaping line as shown in Figure 4.1b.

The condition of equality of the load impedance and of the wave impedance of the line is not always observed in such a generator. The ratio Z_1/Z may prove to be somewhat larger or smaller than unity. To analyze a pulse when $\frac{Z_1}{Z} \neq 1$ we will expand the denominator in the expression (4.4) into a series. The representation of the voltage across the load will assume the following form

$$U_{z_1}(p) = a_1E(1 - e^{-2pTl})[1 + \rho_0 e^{-2pTl} + \rho_0^2 e^{-4pTl} + \ldots]. \qquad (4.13')$$

Inverse transformation leads to the following expression for the voltage:

$$U_{z_1}(t) = a_1 E\{1 - 1(t - 2Tl) + \rho_0[1(t - 2Tl) - 1(t - 4Tl)] + \\ + \rho_0^2[1(t - 4Tl) - 1(t - 6Tl) - \ldots]\}, \qquad (4.14)$$

where

$$1(\Delta t) = 1 \text{ для } \Delta t > 0,\ 1(\Delta t) = 0 \text{ для } \Delta t < 0,$$
$$\Delta t = t - nTl,\ n = 2, 4, 6 \ldots;\ a_1 = \frac{Z_1}{Z_1 + Z}. \qquad (4.14')$$

It follows from the expression (4.14) that in the case of mismatching of the load impedance and of the wave impedance of the line the voltage pulse has a stepped shape. These steps have one and the same sign if $Z_1 > Z$, or periodically change the sign if $Z_1 < Z$. In the general case the expression for the value of the k-th step has the following form

$$U_k = E\frac{Z_1}{Z_1 + Z}\left(\frac{Z - Z_1}{Z + Z_1}\right)^{k-1}. \qquad (4.15)$$

where k=1, 2, 3 ...

When k=1 the value of U_k is equal to the pulse amplitude. The permissible ratio Z_1/Z is usually determined by the relative height of the second projection. If, for example, it is specified that U_2 must amount to not more than 5 percent of the amplitude, then Z_1/Z assumes the values of 0.9 or 1.1, i.e. the load impedance must be within the following range

$$0.9Z < Z_1 < 1.1Z.$$

In addition to the network in which voltage is used for charging the line there exists a network with a short-circuited line, which is charged with current [83] (see Figure 4.1c).

At first the line is connected to the power-supply source E and a current $I = \frac{E}{Z_1} = \text{const}$ is set up in it. At the instant t=0 the commutator K is moved from the position 1 into the position 2, the line is cut off from the supply source and is connected to the load impedance equal to the wave impedance Z. The wave process taking place in this case is similar to the process in a network with a shaping line charged with voltage but the role of the voltage waves in an open line is performed here by the current waves and vice versa. Consequently, a current wave will have an amplitude $i_a = \frac{I}{2}$ and the duration $t_i = 2lT$.

The amplitude of the voltage pulse on the load impedance may be found from the following formula:

$$U_a = I_a Z = \frac{EZ}{2Z_1}. \qquad (4.16)$$

The advantage which a short-circuited line has over an open line follows from this expression. When $Z_1 \ll Z$ it is possible to obtain a voltage pulse with an amplitude which considerably exceeds the voltage E of the power-supply source. However, owing to the difficulties connected with switching the commutator and with a prolonged flowing of the charging current large in magnitude, a network with a short-circuited shaping line is seldom used [83].

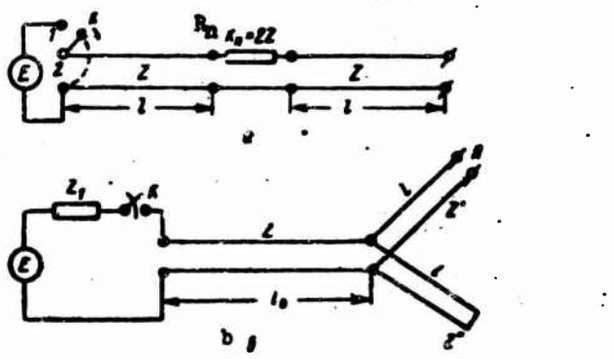

Figure 4.2. Pulse shaping networks with two (a) and three (b) lines.

The networks with the pulse shaping lines examined above are the simplest. The chief drawback of the first two networks is the small value of the ratio of the pulse amplitude to the voltage at the input of the network which is equal to $\frac{U_a}{E} = \frac{1}{2}$. More complex networks are used to increase this ratio. In Figure 4.2a is shown a network with a two-step shaping line [83]. Two identical lines with a wave impedance Z and a length l are charged to the voltage E. In the time Tl after moving the key K from the position 1 into the position 2 a voltage with an amplitude $U_a = E$ and duration $t_1 = 2lT$ forms on the resistance R_n.

In a network with a two-step line the shape of the pulse is somewhat less satisfactory than when using the usual shaping line since the process of pulse shaping takes a longer time ($3Tl$ instead of $2Tl$ in a network with one line). This leads to an attenuation and distortion of the pulse.

In Figure 4.2b is shown a pulse-shortening network formed by the connection of three lines. It is possible to show that if $Z_1 = Z$, $l_1 = l_2 = l$, $Z' = Z'' = 2Z$, the line l_2 is short-circuited and l_1 is open, then a pulse with

an amplitude $U_a=E$ and duration $t_i=2l/$ forms at the end of the open line (the point A). If E(t) is a pulse with a drooping vertex or a rectangular pulse, then additional pulses appear at the point A after the primary pulse. When using pulses with a drooping vertex it is necessary to use the formula (4.11) to eliminate the additional pulses.

In a network with three lines a pulse with an amplitude $U_a=2E$ may be obtained if a $Z_1=0$ is used. However, in this case a train of additional pulses brought about by the reflection of the wave from the start and end of the line will follow the primary pulse. This effect may be made use of only in the case when the reflected pulses are not interference.

An important drawback of the networks shown in Figure 4.1a and 4.2b is that in order to eliminate the additional pulses it is necessary to insert an impedance $Z_1=Z$ directly at the output of the generator, which is undesirable at high voltages since this leads to an increase of the spurious parameters L and C of the discharge circuit and to an increase of the duration of the leading edge of the pulse.

In Figure 4.3a is shown a network in which the suppression of additional pulses is accomplished by matching the end of the line [54]. If the network parameters are selected in such a manner that $Z_1=0$, $Z_2=Z$, $Z_3\gg Z$ and E=const, then upon the arrival of the wave into the line there will be no voltage between the points "a" and "b" until the wave reaches the point "a". When the wavefront reaches the point "a" the potential of this point will immediately increase to the value of E and voltage will be applied to the load Z_3 until the wavefront reaches the point "b". After this, the potentials of the points "a" and "b" will become equal and there will be no voltage between them. Thus, a rectangular pulse with a duration $t_i=lT$ and an amplitude $U_a=E$ appears on the load.

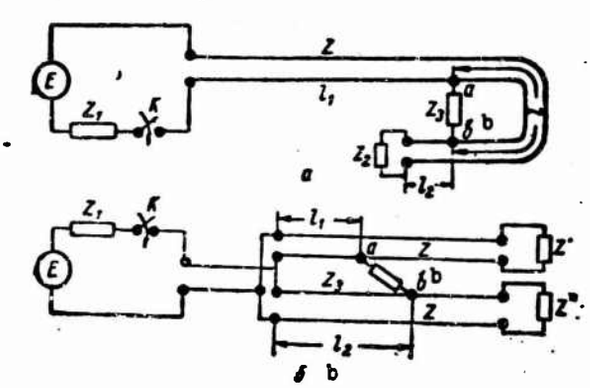

Figure 4.3. Networks with the suppression of reflected pulses at the end of the line.

In Figure 4.3b is shown a network [54] the principle of operation of which is similar to the principle of operation of a network with a loop. Two identical waves start propagating simultaneously over the lines 1 and 2 after closing the key K but in the first line the wave will reach the end of the load Z_3 (the point "a") faster than in the second since $l_1 < l_2$. In the time l_1 a voltage E (if $Z_1=0$) will be applied to the impedance Z_3 but as soon as the wave in line 2 reaches the point "b" both ends of the load Z_3 will prove to be energized by one and the same potential and the voltage across Z_3 will disappear. If $Z_3 \gg Z$, $Z'=Z''=Z$ and E=const, then a single rectangular pulse without the following reflections appears on Z_3. If the pulses propagating in the lines (see Figures 4.3a and b) have a finite steepness of the leading edge and a limited duration, then the evaluation of the parameters on the impedance Z_3 may be done using the formulas (4.7), (4.8), (4.10) and (4.11) having first substituted $\frac{1}{2}E$ with the value of E and $2l$ with the value of l.

Networks with a loop and a double line have certain new properties in comparison with the simplest networks. For example, if in the network shown in Figure 4.3a a $Z_1=Z$ is used and $Z_2=0$, then two pulses of the same polarity with an amplitude E/2 may be obtained on Z_3. If not one but several loops with load resistances are made in the line or if not one but several loads at certain distances from each other are connected in a network with a double line, then pulses shifted by different time intervals relative to each other can be obtained on these loads. The main drawback of these networks is the existence of a potential relative to the ground at both ends of the load in the period of shaping the pulse.

In a network with a shaping line, which has gained the widest use, the entire voltage in the spacing between the pulses is applied to the line. In the case of high voltages this leads to an increase of the insulation and dimensions of the cable.

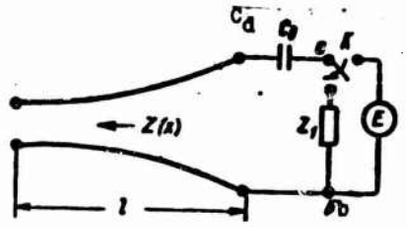

Figure 4.4. Network with a parabolic line and a capacitor for shaping rectangular pulses.

O. N. Litvinenko [92] suggests insertion of a capacitor with the capacitance C_d in series with a parabolic line (Figure 4.4). Wave impedance of a parabolic line varies in accordance with the following law:

$$Z(x) = Z(0)\left(1 - \frac{x}{a}\right)^2 . \qquad (4.17)$$

and input impedance in the case of an open end

$$Z_{in} = Z(0)\,\mathrm{cth}\,p\tau l - \frac{1}{p} \cdot \frac{Z(0)}{a} , \qquad (4.18)$$

where τ is the time of the wave motion from the start of the line to a point with the coordinate x; "a" is a parameter characterizing the degree of heterogeneity of the line.

It follows from the equation (4.18) that if a

$$C_d = \frac{a}{Z(0)}$$

is used, then the aggregate impedance of the capacitor and Z_{in} will be equal to the input impedance of a homogeneous line open at the end [see formula (4.13)]. Therefore, if a $Z_1 = Z(0)$ is used, then a pulse will be shaped on the impedance Z_1 as in the case of a homogeneous open line with the parameters $t_1 = 2t_z$, $U_a = \frac{E}{2}$. Since the capacitance of a parabolic line

[$C_n = C_{line}$]

$$C_n = \int_0^l C dx = \frac{a}{Z(0)} \cdot \frac{t_z}{a - t_z} . \qquad (4.18')$$

then the highest voltage in the shaping line $U_{line} = E\left(1 - \frac{t_z}{a}\right)$ where t_z is the total delay time of the shaping line. Such a shaping device cannot be used to obtain single pulses or pulses with a low repetition rate since the distribution of voltages in this case will be determined not by the values of the capacitances C_d and C_{line} but by the leakage resistance of the capacitor and the line.

Par. 4.2. The Use of Spark Dischargers to Decrease Pulse Duration

In pulse-shaping networks with long lines the matching impedances decrease the pulse amplitude and introduce high-frequency distortions (see Par. 5.3). Spark dischargers are often used to eliminate these impedances from the generators. In addition to this, networks with dischargers and impedances which have certain valuable properties are sometimes used. A diagram of a device with a discharger and lines is shown in general form in Figure 4.5a.

We will examine first a case when $Z_1 \gg Z$ and $Z_2 = \infty$. If the breakdown voltage of the gap of the discharger P is larger than E but smaller than 2E, then in the case of a direct passage of the wave E the gap will

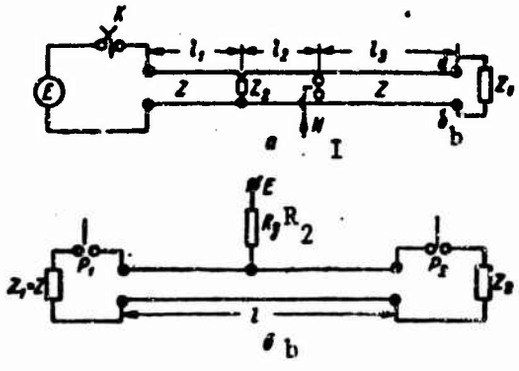

Figure 4.5. Networks of the generators with long lines and dischargers for obtaining short high-voltage pulses.

not break down but after the reflection of the wave from the end of the line (the points "a" and "b") the voltage on P becomes equal to 2E and it breaks down. The breakdown of the gap of the P brings about a wave -E which after reflection at the points "a" and "b" removes voltage from the line and the load as a result of which a voltage pulse with an amplitude 2E and dura- $2T\ell_3$ is shaped on Z_1. However, this pulse will be accompanied by additional pulses reflected from the discharger and from the end of the line ℓ_3. If a $\ell_3=0$ and $Z_2=\infty$ are used and the length of the gap of the discharger P is set to be such that it would not break down under the action of the voltage $2E\,\frac{Z_1}{Z_1+Z}$ alone but would break down upon the arrival of a synchronizing pulse I in the time t_z after the arrival of the wavefront, then a pulse with an amplitude $U_a=2E\,\frac{Z_1}{Z_1+Z}$ and a duration $t_1=t_z$ will be shaped on the impedance Z_1. When $Z_1 \gg Z$ we have a $U_a=2E$. A network is also usable when $\ell_2=0$ and $Z_1=Z$, $Z_2 \gg Z$ [48]. In this case the voltage pulse on Z_2 has the following parameters: $U_a=E$ and $t_1=t_z$.

In some experiments it is necessary that the duration of the cutoff t_{sr} be much shorter than the duration of the leading edge t_f. A network shown in Figure 4.5a may be used for this purpose if $Z_1=Z$, $\ell_3=0$, the discharger P has a short commutation time and the load impedance $Z_2 \gg Z$. If the discharger P breaks down at the top of the pulse, then a pulse with a duration $t_1=2\ell_2 T$ and an amplitude $U_a=E$ is formed on the impedance Z_2 with the duration of the cutoff being determined only by the commutation time of the discharger P,

and t_i — by the length of the section of the line l_2. To eliminate reflections in such a network it is necessary to match the generator end.

Thus, pulse duration and its stability are determined by the value of t_z. A delay in the operation of the discharger P for a considerable time t_z may be accomplished by means of circuits for delaying the synchronizing pulse which ignites the discharger P. As a rule, the initiation of this pulse coincides with the initiation of the operation of the commutator. Thus, it is possible to obtain pulses with a $t_i = 10^{-7}$ sec and longer. However, in obtaining the pulses with a duration of the leading edge $t_f < 10^{-8}$ sec, a pulse duration of the order to tens of nanoseconds and an amplitude of up to 100 kv it is possible to do without the synchronizing pulse by using as the t_z the time for forming a pulse breakdown of the gap. To eliminate the statistical lag it is necessary to irradiate the cathode with ultraviolet rays by means of a synchronizing light pulse. In addition to this, the value of t_z may be stabilized by a considerable overvoltage in the gap by means of a steep leading edge of the pulse. Under these conditions the value of t_z can be controlled by varying the length of the gap S with the pulse amplitude and the steepness of the leading edge being constant. For an ideally steep drop with a height U_a the relationship between t_z, U_a and S with atmospheric pressure in the air will be written as follows [see Par. 1.2]:

$$t_z = \frac{1690\, S^{1/6}}{\sqrt{U_a (U_a - 24\,000 S)^3}}. \qquad (4.19)$$

When the steepness of the leading edge of the pulse is finite, evaluation of the value of t_z may be carried out by using the formulas (1.25) and (1.27)

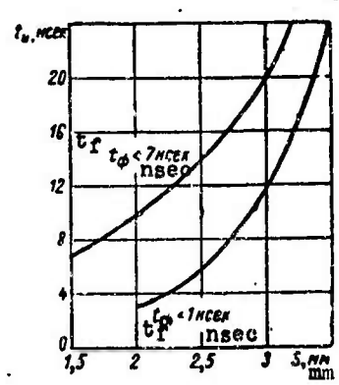

Figure 4.6. Relationship of the delay time of the discharger operation to the length of the spark gap with the pulse amplitude being 15 kv.

In Figure 4.6. is shown the relationship of the time $t_1 = t_z$ measured from the start of the application of the pulse until the breakdown of the gap

to the length of the spark gap with atmospheric pressure in the air and different lengths of the leading edge of the pulse. Since the breakdown of the gap S according to the pulse duration takes place with a different overvoltage, the duration of the cutoff determined by the commutation time t_k of the discharger P will increase somewhat with an increase of t_k.

Ultraviolet irradiation of the discharger cathode is usually done from an auxiliary spark gap the breakdown of which has to be synchronized with the arrival of a pulse for starting the commutator by means of a series connection of two dischargers with the line or by means of a network with a series connection of the dischargers (see Par. 5.6 and 5.7).

In conclusion we will examine a pulse-shaping network not critical in regard to the value of the load impedance (see Figure 4.5b). This network involving the use of thyratrons was proposed by Yu. V. Vvedenskiy [85]. Normally the line is charged to a voltage E through the charging resistance R_z. After the operation of the discharger P_2 at the instant $t=0$ a voltage $U_2' = E\frac{Z_2}{Z_2 + Z}$ appears on the impedance Z_2 and a wave $E\frac{Z}{Z_2 + Z}$ moves to the left. If in the period $\tau = lT$ of the motion of this wave over the line the discharger P_1 has time to operate at the instant of time $t=t_1$, then the wave on the impedance Z_1 will be damped and a wave $\frac{E}{2}$ brought about by the operation of P_1 will move to the right. After reaching the impedance Z_2 this wave will create on it a voltage $U_2'' = -\frac{EZ_2}{Z_2 + Z}$.

Consequently, the resultant voltage drop on Z_2 will be equal to 0. A rectangular pulse with an amplitude $U_a = E\frac{Z_2}{Z_2 + Z}$ and a duration $t_i = \tau - t_1$ will be shaped on the impedance Z_2. If the time t_1 between the operation of the dischargers P_1 and P_2 varies in a range of $t_1=0$ to $\pm\tau$, then pulse duration will be controlled in a range of $t_i=0$ to 2τ. The network can shape pulses on any load Z_1 from a no-load condition of the line to a short circuit. Short circuit is used to obtain large-current pulses of controllable duration [86].

Par. 4.3. Transforming the Short High-Voltage Pulses

Pulse transformers used in the microsecond range cannot be used for the transformation of high-voltage pulses of nanosecond duration owing to the inductance of the dissipation and spurious capacitances of the windings, which increase the leading edge and distort the shape of the pulse. Measures taken for increasing the passband of transformers make it possible to transform nanosecond pulses of only low voltage (of the order of 100 volts) [1, 27]. To

transform high-voltage pulses of nanosecond duration, long lines with variable wave impedance are used and also systems of homogeneous long lines connected in a special manner.

In essence the simplest transformer is a homogeneous long line with wave impedance Z and a length l if a load impedance $Z_1 \gg Z$ is connected to it at the end. In doing so, in the case of an input pulse with an amplitude E and duration t_i the pulse amplitude on the load proves to be equal to

$$U_a = 2E \frac{Z_1}{Z_1 + Z} \approx 2E.$$

However, with a mismatched generator end of the line the primary pulse will be accompanied by a train of additional pulses brought about by a successive reflection from the end and the start of the line. If a network with a line and a discharger is used, then these additional pulses can be shunted by the operation of the discharger at the proper time. With a series connection of the line section with a length $l_1, l_2, \ldots l_n$ and wave impedance $Z_1, Z_2, \ldots Z_n$ and the condition that $Z_2 > Z_1$, $Z_3 > Z_2, \ldots, Z_n > Z_{n-1}$ we will obtain the following for the pulse amplitude at the output of the line

$$U_a = 2^n E \frac{Z_1}{Z_1 + Z_1} \cdot \frac{Z_2}{Z_2 + Z_1} \cdot \frac{Z_3}{Z_3 + Z_2} \cdots \frac{Z_n}{Z_n + Z_{n-1}} \cdot \frac{Z'}{Z' + Z_n}, \qquad (4.20)$$

where Z' is the load impedance.

If, for example, $Z_j = 2Z_{j-1}$ $(j = 1, 2, \ldots n)$, then

$$U_a = \frac{2^{2(n-1)}}{3^n - 1} \cdot \frac{Z'}{Z' + Z_n} E. \qquad (4.20')$$

With an open end of the last line and with $n = 5$ the transformation ratio $\frac{U_a}{E} = 6.31$. If the delay per unit of length T of all sections of the lines is the same and the duration of the input pulse $t_i < l_k T$ where l_k is the length of the shortest section of the line, then a transformed pulse with a multiplicity of additional pulses brought about by the reflection from the start and end of each one of the sections will appear on Z'. This transformation method is used if the additional pulses can be shunted or if it is necessary to have pulses with a steep leading edge and a flat top at a certain distance from the start of the leading edge and the subsequent shape of the pulse is of no material importance. Such pulses are necessary, for example, for the investigation of delay processes of a phenomenon brought about by the action of high voltage. When using this transformation method an important limitation are the processes at the junction of the lines, which lead to an increase of the duration of the leading edge of the pulse. Lines with different geometrical dimensions are connected at the places of junction. This is equivalent to an insertion at this place of a certain capacitance which shunts the line (see Par. 5.1).

Lines with a variable wave impedance in which linear capacitance and inductance vary along the length of the lines are used to eliminate the drawbacks indicated. General theory of heterogeneous long lines is set forth in the work [2]. An exponential line [1, 2] in which inductance, capacitance and wave impedance vary along the length of the line x in accordance with the following law:

$$L = L_0 e^{\gamma x};\ C = C_0 e^{-\gamma x};\ Z = \sqrt{\frac{L}{C}} = Z_0 e^{\gamma x}. \qquad (4.20'')$$

where γ is a positive or negative constant quantity, finds the widest practical application. With a transformation ratio larger than two the usual heterogeneous lines have large dimensions. Therefore, they are used for matching the impedances [2].

Usually coaxial lines with a spiral inner conductor and variable wave impedance are used for transformation. The problems of investigation of spiral lines are set forth in the works [2, 87-89]. Spiral transformers are made with a rectangular and a round cross section. Kuchel and Williams [90] give the following formula for the determination of wave impedance of a round spiral transformer (Figure 4.7) when the ratio of the radius of the spiral to its pitch is larger than unity:

$$Z = \sqrt{\frac{\mu_0}{\varepsilon_0}} \cdot \frac{R_1}{\tau\sqrt{k}} \sqrt{\frac{1}{2}\left[1 - \left(\frac{R_1}{R_2}\right)^2\right] \ln \frac{R_2}{R_1}}. \qquad (4.21)$$

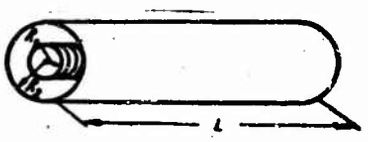

Figure 4.7. Design of a spiral round transformer.

where R_1 is the radius of the spiral; R_2 — the radius of the shield; τ — the pitch of the spiral; μ_0, ε_0 — magnetic inductivity and specific inductive capacitance of the free space; k — the relative specific inductive capacitance of the dielectric filling the space between the spiral and the shield. With the optimum ratio $\frac{R_2}{R_1} = 2.06$ [91]

$$Z = 0{,}44 \sqrt{\frac{\mu_0}{\varepsilon_0}} \cdot \frac{1}{\sqrt{k}} \cdot \frac{R_1}{\tau}. \qquad (4.22)$$

Having set the values of Z and R_1 at the start of the line it is possible

to determine the pitch of the spiral τ_{in} at the input of the transformer. Wave impedance at the start of the line Z_0 and at the end Z_l are connected by means of the transformation ratio $\varkappa$ by the following relationship:

$$Z_l = \varkappa^2 Z_0. \tag{4.23}$$

If the transformation ratio $\varkappa$ is specified, then the pitch of the spiral at the output of the line τ_{out} can be determined by the formula

$$[\tau_{вых} = \tau_{out};\ \tau_{вх} = \tau_{in}] \qquad \tau_{out} = \frac{\tau_{in}}{\varkappa^2}. \tag{4.24}$$

The length of a spiral exponential transformer can be determined by the following formula

$$l = \tau_{in}\left(\frac{1 - e^{-2\pi R_1 \gamma N}}{e^{2\pi R_1 \gamma} - 1}\right). \tag{4.25}$$

where N is the number of turns. The total delay time of the transformer is determined on the basis of a specified distortion of the top of the pulse (voltage drop on the top) Δ

$$t_3 = 50\frac{t_u \ln \varkappa}{\Delta}. \tag{4.26}$$

where t_i is duration of the pulse being transformed. It follows from the equation (4.26) that with invariable t_z and t_n the distortion of the top increases with an increase of the transformation ratio $\varkappa$. Formulas (4.21) through (4.26) make it possible to carry out an approximate calculation of an exponential transformer with a spiral winding of the inner conductor. As Yu. S. Belozerov [90] showed, the difference between the parameters of a transformer calculated by these formulas and those measured experimentally does not exceed 20 percent. On the basis of the works [1, 90, 91] it may be concluded that permissible distortions of a pulse result when $\varkappa < 3$. The highest voltage obtained in these works at the output of the transformer amounts to $U_a = 8.6$ kv with the pulse duration $t_n = 14$ nanoseconds).

The main obstacle to the use of spiral transformers with a variable wave impedance is the comparatively low frequency passband (of the order of 250-300 Mc) [91]. This is explained by the variation of inductance with frequency and by the effect of distributed capacitance between the turns. To increase the passband it is necessary to use rectilinear heterogeneous lines even though they have large dimensions.

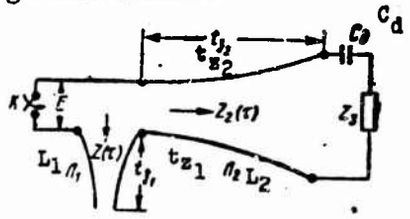

Figure 4.8. Network with two parabolic lines for obtaining and transforming the pulses.

O. N. Litvinenko [92] suggests the shaping of pulses by means of two parabolic lines L_1 and L_2 (Figure 4.8). Wave impedances of the shaping line L_1 and of the transforming line L_2 vary in accordance with the following law:

$$\left.\begin{aligned} Z_1(\tau) &= Z_1(0)\left(1-\frac{\tau}{b}\right)^2, \\ Z_2(\tau) &= Z_2(0)\left(1-\frac{\tau}{a}\right)^2. \end{aligned}\right\} \tag{4.27}$$

where $a<0$, $b>0$, τ is the time for the motion of the wave to any point on the line. If the following conditions are observed

$$Z_1(0)=Z_2(0)=Z(0);\ R_n=Z_2(t_{z_2});\ C_0=\frac{a+t_{z_2}}{Z_3}. \tag{4.28}$$

then the signal appearing at the input of the line L_2 will be transmitted without distortion to Z_3. When $a=b$, a rectangular pulse is shaped at the input of the L_2. In doing so, a voltage pulse also of a rectangular form will be shaped at the output of the line L_2

$$U=\frac{E}{2}\left(1+\frac{t_{z_2}}{b}\right)\left(1-e^{-2pt_{z_2}}\right). \tag{4.29}$$

It follows from this expression that the pulse duration

$$t_u=2t_{z_2} \tag{4.30}$$

depends only on the delay time t_{z_2}, and the transformation ratio

$$\varkappa=\frac{U}{E}=0.5\left(1+\frac{t_{z_2}}{b}\right). \tag{4.31}$$

The largest value of $\varkappa$ can be obtained with the smallest possible value of

$$b=a=t_{z_2} \tag{4.32}$$

(which corresponds to a short circuit of the line L_1).

To calculate this device it is necessary to set the longest pulse duration t_i, the maximum transformation ratio $\varkappa_m$ and the impedance Z_3. As a result of the calculation we can learn the law of variation of the wave impedances Z_1 and Z_2 and also of C.

It follows from the equations (4.30) and (4.32) that

$$a=b=\frac{t_i}{2}.$$

From the expression (4.31) we will determine the delay time of the line L_2

$$t_{z_n} = (2n - 1)\frac{t_n}{2} . \qquad (4.33)$$

and from (4.28) — the value of the capacitance

$$C_n = \frac{t_n \tau_n}{Z_0} . \qquad (4.34)$$

From the formulas (4.27) we will find the wave impedance at the start of the lines L_1 and L_2

$$Z(0) = \frac{Z_0}{\left(1 + \frac{t_n}{a}\right)^2} = \frac{Z_0}{4\tau_n^2} . \qquad (4.35)$$

The quantities "a", "b" and Z(0) completely define the law of variation of wave impedances of the lines.

To reduce the dimensions of the device described the lines L_1 and L_2 may be made spiral. The advantage of a network with two parabolic lines over an exponential transformer is that the shape of the pulse does not depend on the transformation ratio, and the feasibility of obtaining pulses of a strictly rectangular shape.

CHAPTER 5. HIGH-VOLTAGE NANOSECOND-PULSE GENERATORS

Par. 5.1. Discontinuities in Long Lines

Discontinuities appear in the lines in two cases: 1) upon connecting additional impedances to a line, upon connecting the lines with different wave impedance, in branching the lines, etc.; 2) in the case of a sharp change in the dimensions of conductors, in the case of connecting the base insulators, in the case of a break in the lines, etc. To calculate the effect of discontinuity of the first type on the shape of the wave a substitution network is ordinarily used which consists of a series-connected wave impedance of the line and a two-terminal network (Figure 5.1) simulating the remaining portion of the line and the connected impedance or a new line, and of a generator with a voltage $2U_{pad}$ where U_{pad} is the voltage of an incident wave having a random shape. The form of the two-terminal network depends on the method of inserting a discontinuity. For example, in inserting an impedance Z_1 or an additional line with such a wave impedance the two-terminal network consists of parallel-connected impedances Z and Z_1. In

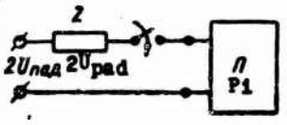

Figure 5.1. Substitution network for calculating the discontinuities of the first type.

a series connection the Z_1 and Z are connected in series. If an arbitrary impedance Z_1 is inserted at the end of a line, then this impedance will serve as a two-terminal network. In doing so, in the case of short circuit $Z_1=0$ and in the case of an open end of the line $Z_1=\infty$. It is necessary to

bear in mind that the substitution network is valid only for the time interval from th- rival of the wave to the place of discontinuity until the return from the d and the start of the line of those waves which were refracted and reflected at the place of disconuity. Superposition method may be used to calculate the effect of reflected waves.

Results obtained in super-high-frequency technique may be used in analyzing the discontinuities in transmission and their effect on the pulse shape. In doing so, it is necessary to know the highest frequency in the pulse spectrum, which has to be transmitted without a substantial change in the amplitude and phase. The upper cutoff frequency of the frequency characteristic corresponding to the point at which the amplitude falls to $\frac{1}{\sqrt{2}}$ of the amplitude at the center frequencies may be taken as the value of f_m. The connection between the f_m and duration of the leading edge t_f of the pulse, determined between the levels of 0.1-0.9 of the amplitude has the following form [2]

$$[t_\phi = t_f] \qquad f_m = \frac{0.4}{t_\phi}. \qquad (5.1)$$

The effect of discontinuity of the second type on the shape of a voltage wave is taken account of in the general case [2, 93, 94] by inserting instead of discontinuity a Pi or T-network whose parameters depend on the type of discontinuity and dimensions of the line. The simplest discontinuities may be substituted with a capacitance inserted parallel to the line.

We will examine some of the frequently encountered discontinuities.

The following are possible in the case of a sudden change in the radii of the conductors of a coaxial cable: a change in the diameter of the inner conductor alone (Figure 5.2a), a change in the diameter of the outer conductor alone (see Figure 5.2b) and a simultaneous change both of the inner and outer diameter (see Figure 5.2c). In all cases, discontinuity is taken account of by inserting the capacitance

$$C = FD$$

where D is the diameter of the outer conductor (in the second case it may be considered that $D = \frac{D_1 + D_2}{2}$); F is a factor whose relationship to the ratio of the diameters is shown in Figure 5.3 [94]. In the case of a break in the inner conductor of the line $\frac{d_1}{D} = 0$. The value of the capacitance C for the third case is determined from the results of the two preceding cases. In doing so, it is assumed that a sudden change exists first in the inner conductor alone, and then in the outer. The equivalent capacitance is found by the addition of the capacitances in the first and second determinations. It

is necessary to bear in mind that data given here may be used if the wavelength $\lambda > 5D$ where D is the largest one of the diameters of the line. The curves given in Figure 5.3 for the determination of F are designed for the calculation of overhead lines. In filling the cable with a dielectrict it is necessary to multiply the value of the capacitance C by the specific inductive capacitance ε. If a dielectric with ε fills only the

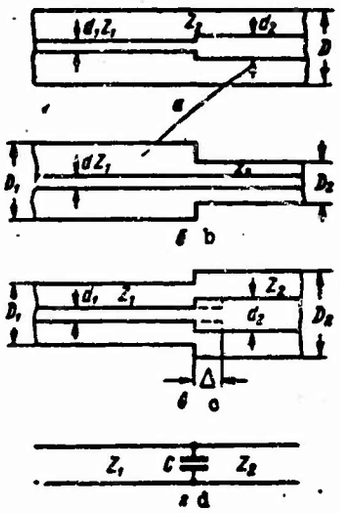

Figure 5.2. Discontinuities of the second type (a, b, c) and their substitution network (d).

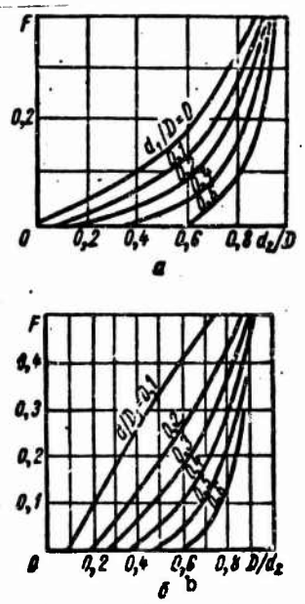

Figure 5.3. Graphs for calculating the capacitance C corresponding to the discontinuities shown in Figure 5.2a (a) and in Figure 5.2b (b).

line having an inner conductor of a smaller diameter, then the value of the capacitance C calculated with the aid of the graphs shown in Figure 5.3 should be multiplied by ε. In the case when dielectric fills a line with a large diameter of the inner conductor, it may be considered in the first approximation that the value of C found for an overhead line remains unchanged. For lines in which the diameter of the outer conductor changes it may be considered that upon filling the line of a larger diameter with a dielectric the value of C increases by ε times, and upong filling the line of a smaller diameter C does not change. If the dielectric fills only a portion of a coaxial line in which dimensions do not vary, then this is equivalent to a sudden change in the wave impedance.

In some cases a sudden change in the dimensions of a line may occur when its wave impedance is invariable. In this case it is necessary to observe the condition: $\frac{d_1}{D_1}=\frac{d_2}{D_2}$. Discontinuity at the place of the junction may be taken into account by inserting the capacitance C into the substitution network. The effect of the magnitude of this capacitance is reduced by shifting the inner conductor to a distance $\Delta=\frac{D_2}{10}$ from the place of discontinuity (shown by broken line in Figure 5.2c). This shift is equivalent to the insertion of a series inductance which compensates the effect of the capacitance C. In the case of high voltages in the line, electric strength of such a transition is small owing to the existence of acute angles. To increase the electric strength it is better to use a stepless conical transition element from one line to another (Figure 5.4a). It is expedient to select the length of this transition element from the following relationship

$$L > 2D. \tag{5.2}$$

A conical transition element is often used in making the discharge devices, peakers, etc. Therefore, we will examine conditions which determine the parameters of such a transition element in the case of a high voltage. The maximum voltage U_{max} between the conductors of a line with large diameters of the chamber and all parameters (R_0, r_0, ε, Z) of the cable are usually known. The values of the diameters D and d are determined from two conditions: 1) the chamber must stably withstand the maximum operating voltage U_{max}; 2) wave impedance of the chamber and of the cable must be the same. The following may be written on the basis of the first condition

$$\left[U_{макс}=U_{max};\ E_{\partial}=E_{d'}\right] \qquad U_{макс}=E_{\partial}\frac{d}{2}\ln\frac{D}{d}. \tag{5.3}$$

where $E_{d'}$ is permissible electric field strength which is determined by the strength of the overlap on the surface of the racks, by the pressure in the chamber and by the kind of the gas filler.

The second condition will be written as follows:

$$Z=\frac{60}{\sqrt{\varepsilon}}\ln\frac{D}{d}. \tag{5.4}$$

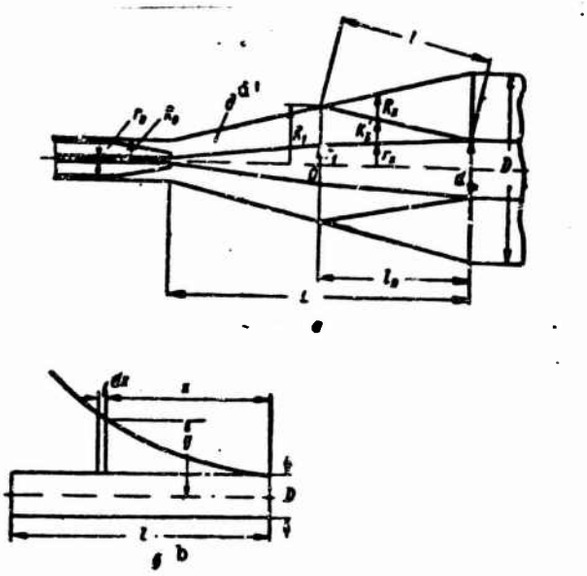

Figure 5.4. For the calculations of a coaxial conical transition element (a) and of the profile of the shield of a matched load (b).

The dimensions of the transition cone are determined with the condition that the wave impedance Z is constant and the necessary electric strength is provided. The dielectric d' is laid inside the section to increase the electric strength (see Figure 5.4a). The distance l is determined from the following condition

$$l \geqslant \frac{U_{max}}{E_{p.d}}$$

where $E_{p.d}$ is permissible strength determined by the overlap on the dielectric d' and by the pressure in the chamber. Taking the equality (5.2) into account we will find the following from Figure 5.4a

$$R_1 \approx \frac{2D-l}{4} + \frac{D^2}{32l}. \qquad (5.5)$$

We will determine r_1 from the formula (5.4)

$$r_1 = \left(\frac{2D-l}{4} + \frac{D^2}{32l}\right) e^{-\frac{60}{Z\sqrt{\varepsilon}}}. \qquad (5.6)$$

If the ε of the dielectric d' and of the cable insulation are the same, then the wave impedance of the cone to the left of the point 0 will be equal to Z if $\frac{R_1}{r_1} = \frac{R_x}{r_x}$.

We will now find the profile of the dielectric d' with the condition of keeping the wave impedance to the right of the point 0 constant. We will make use of the formula for wave impedance of a line with a two-layer dielectric

$$[\varepsilon_3=\varepsilon_e] \qquad Z=\frac{60}{\sqrt{\varepsilon_e}}\ln\frac{R_x}{r_x}. \qquad (5.7)$$

where ε_e is the equivalent specific inductive capacitance [87].

$$\varepsilon_e=\frac{\varepsilon_1\varepsilon_2\ln\frac{R_x}{r_x}}{\varepsilon_2\ln\frac{R'_x}{r_x}+\varepsilon_1\ln\frac{R_x}{R'_x}}. \qquad (5.8)$$

where R'_x is the radius of circumference of demarcation of the dielectrics; ε_1 — the permittivity of the gas filler ($\varepsilon_1=1$); ε_2 — the permittivity of the dielectric d'. We will find R'_x from the equations (5.8) and (5.7)

$$\ln R'_x=\frac{1}{\varepsilon_2-\varepsilon_1}\left(\frac{Z^2\varepsilon_1\varepsilon_2}{3600\ln\frac{R_x}{r_x}}+\varepsilon_2\ln r_x-\varepsilon_1\ln R_x\right). \qquad (5.9)$$

If the origin of coordinates is taken at the point 0, then

$$R_x=R_1+\frac{R-R_1}{l_0}x,$$

$$r_x=r_1+\frac{r-r_1}{l_0}x.$$

Substituting R_x and r_x into the equation (5.9) we will find R'_x in relation to x. In practice the substitution of the curve $R_x'(x)$ with a straight line introduces into the value of wave impedance the largest error of less than ten percent. In most cases such an error is permissible.

With an increase of the voltage U_m the diameters D and d of the chamber will increase. This may lead to the appearance of waves of higher orders. The frequency at which the appearance and transmission of the highest types of waves over a cable is possible is called critical. For the most dangerous wave of H_{11} the critical frequency is determined by the following formula

$$f_k=\frac{2c}{\pi\sqrt{\varepsilon}(D+d)}. \qquad (5.10)$$

where $c=3\cdot10^{10}$ cm/sec is velocity of light in free space. If it is considered that a pulse can be transmitted until $f_k\geqslant f_m$, then the relationship between the duration of the leading edge and the diameters D and d will assume the following form:

$$t_\phi \geqslant \frac{0.2\varepsilon}{c}(D+d) \qquad (5.11)$$

(for gases $\varepsilon=1$).

The connection between t_f, U_{max} and Z may be determined from the formulas (5.4) and (5.11) [95].

$$t_\phi \geqslant \frac{24\pi\left(e^{\frac{Z}{60}}+1\right)}{cZ}\cdot\frac{U_{max}}{E_\partial}. \qquad (5.12)$$

In the first approximation it may be considered that with an increase of the pressure p the permissible strength increases in proportion to p (see Par. 1.1)

$$[E_\partial = E_d] \qquad E_\partial = E'_\partial p. \qquad (5.13)$$

where E'_d is permissible field strength in the case of atmospheric pressure. Thus, we will ultimately obtain

$$t_\phi \geqslant \frac{24\pi\left(e^{\frac{Z}{60}}+1\right)}{cZE'_\partial}\cdot\frac{U_{max}}{p}. \qquad (5.14)$$

Consequently, to decrease the duration of the leading edge of the pulse being transmitted it is necessary to increase the pressure p in the chamber.

Data for the determination of E_d and $E_{p.d}$ may be found in the works [12, 20, 29, 96].

We will examine the methods of eliminating discontinuities brought about by the supporting elements made of a dielectric. A method of reducing the effect of reflections from the supports with a decrease of the diameter of the inner conductor at the place where the support is located has been developed in the work by Cornes [97]. The distortions of a pulse decrease with a decrease of the width of the support b and of the wave impedance Z' in the region of the support installation. In a general case, if a short section with a wave impedance Z' and a delay time T is inserted into a line with a wave impedance Z, then with a duration of the leading edge of the pulse $t_f > 2T$ and impedances Z' and Z close to each other in value, with a unit amplitude of the input pulse the amplitude of the reflected pulse [2]

$$[U_{отр} = U_{reflected}] \qquad U_{отр} = \frac{2T(Z'-Z)}{t_\phi(Z'+Z)}. \qquad (5.15)$$

In the works [98, 99] it is recommended to use supporting beads with a concave surface, and to eliminate the effect of lumped capacitance of the support on the shape of the pulse by means of special "recesses" in the inner conductor with the dimensions of these recesses being determined experimentally. In doing so, it is possible to obtain a reflection coefficient equal to 0.4 percent for frequencies of up to 1,200 Mc.

Sometimes a load impedance exactly equal to the wave impedance of the transmitting line cannot be taken, or a matched line with a wave impedance different from the transmitting impedance cannot be used as a load. In this case, reflected pulses appear owing to a discontinuity at the place of the connection of the line with the load.

The matching of the lines with the load may be accomplished by two methods: connection of resistances to the load so that the equivalent impedance of the entire device would be equal to the wave impedance of the line, and by connecting the lines with a steplessly varying wave impedance between the load and the transmitting line. It is not recommended to use the former method of matching owing to the large pulse-power losses in the additional resistances. In matching by the latter method the wave impedance of a heterogeneous line at the input must be equal to the wave impedance of the transmitting line, and at the output — to the load impedance.

Par. 5.2. Attenuation of Waves in Cable Lines

The most important task of the pulse technique is transmission of a generated pulse without distortion to the place of destination. Chiefly coaxial cables are used for this purpose since unlike the open lines they have advantages (wide frequency spectrum with a comparatively low attenuation, a small antenna effect, protection from external sources of interference, small dimensions and convenient make-up design with high voltages). The work [87] examines in a sufficient detail the problems of propagation of electromagnetic waves over the radio-frequency cables and gives the characteristics of the latter.

Propagation of an electromagnetic wave over a long line is characterized by the propagation factor

$$\gamma = \alpha + j\beta, \tag{5.16}$$

where α is attenuation factor and β — phase factor.

In the absence of ionization processes the attenuation of a wave is connected with the existence of the resistance r of the forward and return wires and the conductance g of the line insulation.

$$\alpha = \frac{r}{2}\sqrt{\frac{C}{L}} + \frac{g}{2}\sqrt{\frac{L}{C}}. \tag{5.17}$$

where L and C are inductance and capacitance of the line respectively. The resistance of a coaxial line

$$r = \frac{2\cdot 10^{-3}}{\sqrt{10}}\sqrt{f}\left(\sqrt{\frac{\mu_1}{\sigma_1}}\cdot\frac{1}{d} + \sqrt{\frac{\mu_2}{\sigma_2}}\cdot\frac{1}{D}\right) \text{ ом/м, ohms/meter} \tag{5.18}$$

where f is the frequency of the propagating signal; μ_1, μ_2 — relative

permeability; σ — specific electrical conductivity, m/ohm-mm^2; D, d — the outside and inside diameters of the wire respectively.

The presence of the factor $\sqrt{f}$ in the expression for r takes into account the surface effect on the inner wire and proximity effect on the outer wire of the cable.

If both wires are made of the same metal, then

$$r = \frac{2 \cdot 10^{-3}}{\sqrt{10}} \sqrt{\frac{f\mu}{\sigma}} \left(\frac{1}{d} + \frac{1}{D} \right)_{\text{ohms/meter}}^{\text{ом/м}} \qquad (5.19)$$

If the wires are twisted out of separate strands, then

$$r = \frac{2 \cdot 10^{-3}}{\sqrt{10}} \sqrt{\frac{f\mu}{\sigma}} \left(\frac{k_1}{d} + \frac{k_2}{D} \right)_{\text{ohms/meter}}^{\text{ом/м}} \qquad (5.20)$$

where k_1 and k_2 indicate by how many times the resistance of a twisted wire exceeds the resistance of a one-piece wire of the same gage. For the inner wire of a coaxial line $k_1 = k_s$, called the twist factor, increases with the increase of the number of parallel-twisted strands, and for a seven-wire conductor $k_s = 1.3$. For the outer wire $k_2 = k_{opl}$, called the braiding factor, depends on the make-up of the cable braiding.

The resistance of a coaxial line may be decreased if the outer surface of the inner conductor and the inner surface of the outer wire are coated with a layer of metal having a low resistivity, for example, with a layer of silver.

V. M. Gorbachev, N. A. Uvarov and L. D. Usenko [10] investigated the attenuation of nanosecond pulses in radio-frequency cables. Pulses with an amplitude of about 100 volts, $t_1 \approx 50 \cdot 10^{-9}$ sec and $t_f < 1$ nanosecond were sent to the input of the cable. The data of the experiment were compared with the data of the calculation which was based on taking into account only the resistance of the forward and return wire. For a unit voltage drop at the input of the cable the voltage [1] at a distance l from the input

$$h = 1 - F(x), \qquad (5.21)$$

where $x = \frac{\alpha l}{2\sqrt{\pi\tau}}$; F(x) — Cramp function which is equal to the following when the values of x are small

$$F(x) = \frac{2}{\sqrt{\pi}} \left(x - \frac{x^3}{1!3} + \frac{x^5}{2!5} - \frac{x^7}{3!7} + \dots \right); \qquad (5.22)$$

$\tau = t - \frac{l}{v}$; v — propagation velocity of the waves. In this case, the attenuation factor

$$\alpha = \frac{1}{4\pi} \sqrt{\frac{\mu}{\sigma} \cdot \frac{C}{L}} \left(\frac{k_1}{d} + \frac{k_2}{D} \right). \qquad (5.23)$$

Table 5.1

1 Тип кабеля	$\frac{d}{2}$, мм mm	$\frac{D}{2}$, мм	Z, ом ohms	C, пф/м 2	$k_{опл}$ 3	k_s 4	10^{-4}, $м^{-1}$ $м^{-1}$
РК-6	1,275	4,9	52	96	2,42	1,1	3,01
РК-3	0,635	4,8	75	68	2,43	1	3,02
РК-2	0,34	3,7	92	55	2,43	1	4,56
РК-50	0,15	3,4	167	25	2,63	1	5,25
РК-1	0,34	2,6	77	66	2,90	1	6,10
РК-19	0,34	1,5	52	96	3,80	1	12,1

Key: (1) Type of cable; (2) Picofarads/meter; (3) k_{opl}=braiding factor (4) k_s=twist factor.

The calculated values of α and experimentally determined values of k_{opl} for the cables investigated are given in Table 5.1.

The calculation and experimental data coincided well. This shows that with the voltage amplitude indicated, at the frequencies of 200-500 Mc (t_f of about 1 nanosecond) the power losses in the dielectric are small and their effect on the degree of attenuation of a wave may be neglected.

During the propagation of a high-voltage pulse over a cable ionization processes may occur in the cable insulation near the inner conductor. By analogy with the pulse corona on the overhead lines these processes produce a high attenuation. Unfortunately, appropriate experimental investigations are absent.

Par. 5.3. Resistances for High-Voltage Nanosecond Pulse Devices

Resistances used in the high-voltage nanosecond devices must satisfy the following requirements: the value of the resistance must not depend on the voltage and frequency in a certain range of them; the resistance must have low spurious inductance and capacitance and be thermally stable.

It is not always possible to satisfy these requirements. Therefore, the problem of the development of resistances for nanosecond high-voltage devices cannot be considered solved. We will examine some of the characteristics of these resistances.

Carbonaceous film resistances, metal-film and composition resistances are used as the nanosecond-range resistances. Wire resistances are not usable owing to high inductance.

A characteristic of the surface effect may be provided by the depth δ

of the penetration of current into the conductor, at which current density becomes 2.718 lower than the maximum density at the surface of the conductor. The depth δ is determined by the following formula

$$\delta = \sqrt{\frac{\rho}{\pi \mu f}}. \qquad (5.24)$$

where f is frequency; μ — permeability of the conductor; ρ — resistivity of the material of the conductor. Knowing the depth δ in relation to frequency it is possible to determine the degree of the change in the resistance at this frequency and the maximum permissible thickness Δ of the conducting layer. The dependence of the value of resistance on frequency does not show in practice for the entire frequency spectrum of the pulse if for the highest frequency f_m $\frac{\Delta}{\delta} \leqslant 0.1$. The value of δ for conductors at the frequencies corresponding to nanosecond pulses may reach tens of microns. Therefore, the conducting films must have a thickness of the order of units of microns, which does not encounter difficulties in making the resistances. The effect of the self-capacitance and self-inductance of a line shows when a high-frequency voltage acts on the resistance. The substitution network of the resistance at high frequency is analagous to the substitution network of a long line with losses. In addition to this, the resistance is affected by the capacitance between the end lead-outs of the resistance and their capacitance in relation to the ground. The values of the linear capacitance and inductance C_0 and L_0 are determined by the form factor of the resistance [101] (it is assumed that the resistance has a cylindrical form)

$$K_f = \frac{l}{\pi D}$$

where l is the length of the resistance and D — its diameter.

[$K_\phi = K_{f-}$]

$$C_0 \approx 10^{\frac{0.8}{K_\phi} - 1} \ n\phi/cм; \ \text{picofarads/cm} \qquad (5.25)$$

$$L_0 = 2(\ln 4\pi K_\phi - 1) \ cм/cм. \ \text{cm/cm} \qquad (5.26)$$

In the case of a spiral threading on the resistance, which is made to increase the resistance, the value of L_0 is determined by another formula:

$$L_0 = 0{,}9 \frac{n^2}{K^2_\phi} \ cм/cм, \qquad (5.27)$$

where n is the number of turns of the spiral. Since for resistances with a spiral threading the value of L_0 greatly increases, such resistances are not used in the nanosecond-range pulse networks.

In practice it is difficult to use the above-indicated substitution network in the calculations. It is considered that if the value of the re-

sistance $R>\sqrt{\frac{L_0}{C_0}}$, then the effect of L_0 may be neglected and the substitution network may be represented in the form of a parallel RC-circuit ($C=C_0 l$). In the case of smaller R the effect of C_0 is neglected and the substitution network is represented in the form of a series RL-circuit ($L=L_0 l$). The effect of L and C may be neglected if the respective time constants of L/R and RC are four or five times smaller than the duration of the leading edge.

The dependence of the value of resistance on voltage shows under the action of high voltages. In doing so, starting with a certain voltage the resistance R decreases and Ohm law is not observed. One of the reasons for the nonlinearity of the resistance are local overheatings of the conducting film, brought about by the nonuniformity of the distribution of current. In composition resistances the reason for nonlinearity of the resistance may be the effect of the conductance of the gap between the conducting grains, which with the field strengths of 10^5-10^6 volts/cm [101] bears a nonlinear character. The maximum permissible operating voltage is limited by electric breakdown and by sparking on the surface of the resistance. The voltage at which a breakdown occurs on the surface does not depend in practice on the type of the conducting coating and at a given pressure p is determined only by the distance between the lead-outs, their form and arrangement. The relationship of the voltage at which the breakdown occurs in resistances without threads (of the type MLT, VS, etc.) to the length of the resistance l and the pressure is expressed (for $pl>1$ mm of mercury column · ohms) with good approximation as follows [101]:

$$[U_{wp}=U_{pr}=U_{breakdown}] \qquad U_{wp}=300(pl)^{0.5} \text{ s. volts} \qquad (5.28)$$

If the effective voltage is 20-30 percent lower than U_{pr}, then in the absence of heating and outside temperature of 15-20°C a safe functioning of the resistance is guaranteed. It is necessary to bear in mind that the formula (5.28) is valid for pulses with a duration of the order of 10^{-6} sec, and for pulses with a duration of the order of 10^{-9} sec the value of U_{pr} is larger. The value of U_{pr} may be increased by placing the resistances in an insulating liquid.

The designs of the resistances operating in the nanosecond-range pulse networks are characterized by diverse shapes which are determined by the purpose of the resistances. Resistances are a part and even a component member of a structure. Disk and plate-like resistances are also used in addition to the cylindrical shapes. In Table 5.2 are given the basic parameters of some of the high-frequency cylindrical resistances of the type UNU with a carbonaceous coating [101].

Nichrome which is applied on the dielectric lining by spraying in vacuum is used as the surface coating in resistance of the metal-film type de-

Table 5.2

Type Тип	1 Номинальная мощность	2 Размеры, мм 3 длина	 4 диаметр	5 Величина сопротивления, ом	6 Предельные напряжения при $t_и$=1 мксек	7 Максимальная испытательная мощность в импульсе, квт
UNU УНУ-10	10	122	25	50,75	4000	212
УНУ-25	25	182	29	50,75	6500	570
УНУ-50	50	252	45	50,75	8700	1000
УНУ-100	100	352	64	75	12500	2000

Key: (1) Rated power
(2) Dimensions, mm
(3) Length
(4) Diameter
(5) Value of the resistance, ohms
(6) Maximum voltages with t_i=1 microsec
(7) Maximum testing power in a pulse, kilowatts

signed for operation in the area of high frequencies. Resistances with a composition coating (mixture of powdered conductor with a dielectric) are sometimes used to obtain high-frequency resistances of the order of 1 kilohm.

In the operation of resistances it is necessary to pay attention to the relationship of the value of resistance to the temperature which may rise in the process of operation of the resistance. To eliminate the overheating of resistances it is necessary to increase their surface or use forced air or water cooling. For example, resistances of the type UNU increase the rated power by 5-10 times with an intensive air cooling. The metal-film and carbonaceous resistances are sometimes made with water cooling. In doing so, their capacity reaches a few and even tens of kilowatts [102].

Aqueous solution of NaCl or of other salts may be used as the resistances in the case of pulse voltages of the order of hundreds of kilovolts. Such resistances have a low inductance and have a large thermal capacity. The surface effect is absent in such resistances if the diameter of the resistance

$$D < 0{,}1\delta. \tag{5.29}$$

Making use of the relationships (5.24) and (5.29) and taking into account that for water $\mu = \mu_0 = 4\pi 10^{-7}$ henries/meter we will find the following expression for a water resistance with which the surface effect will not appear:

$$R \geqslant 1{,}6 \cdot 10^{-4} f l \rho \text{ ом}, \tag{5.30}$$

where f is frequency, cps; l is the length of the resistance, meters.

Thus, knowing the upper limit of the frequency spectrum of a pulse f_m and the length of the resistance l, the necessary value of R is selected by the concentration of salt. A drawback of water resistances is the high dependence of R on the external factors, especially temperature, high self-capacitance and considerable change in R with time.

To match the long lines it is necessary to insert a resistance equal to the wave impedance of the line. If the usual lumped resistance is connected, then a pulse is distorted owing to the spurious parameters of the inductance and capacitance of the resistance and its feeds. Therefore, it is better to use a resistance of the disk type. An improvement in the frequency properties of the matching resistance may be achieved by placing cylindrical resistances with a diameter D and with a value of R equal to the wave impedance of the line into a cylindrical shield whose length considerably exceeds its diameter. In doing so, a line section with losses and with a certain wave impedance Z' is formed. The ratio between R and Z' may be selected from the equality $R=\sqrt{3Z'}$ [2]. However, a matching device with a cylindrical shield has a narrow frequency passband and may be recommended with a ratio of the length of the resistance l to the smallest wavelength λ_m of not more than 0.1.

For a better matching of the resistance with the transmitting line the profile of the shield surrounding the resistance is selected in such a manner that the wave impedance of the entire device in any cross section be equal to the resistance of the remaining portion of the resistance [10]. If the resistance has a uniform film coating, its value does not depend on the frequency and on the distance x from the end of the load $R_x=R_0x$ (see Figure 5.4) where R_0 is the resistance per unit of length. Wave impedance of the line without losses in this cross section is

$$Z_x=\sqrt{\frac{L_x}{C_x}}, \tag{5.31}$$

where L_x and C_x are inductance and capacitance per unit of length in the cross section x. Reflections will be absent if

$$\sqrt{\frac{L_x}{C_x}}=R_0x. \tag{5.32}$$

It may be assumed that on a small element Δx the diameter of the shield is constant; then

$$L_x=0{,}2\ln\frac{2y}{D}\ \underset{\text{microhenries/meter}}{\text{мкгн/м}},$$
$$C_x=\frac{55{,}5\varepsilon}{\ln\frac{2y}{D}}\ \underset{\text{picofarads/meter}}{\text{пф/м}}, \tag{5.33}$$

where ε is relative permittivity of the dielectric in the space between the resistance and the shield; D is the diameter of the resistance. On the basis of the equalities (5.32) and (5.33) we obtain

$$\frac{60}{\sqrt{\varepsilon}}\ln\frac{2y}{D}=R_0x \tag{5.33'}$$

or

$$y = \frac{D}{2} e^{\frac{R_0 x \sqrt{\varepsilon}}{60}}. \qquad (5.34)$$

The calculation of the profile of the shield given above takes into account only the radial components of an electric field and does not take into account the axial components. In spite of this, coaxial loads with an exponential shield give good frequency characteristics.

A further improvement of the frequency characterics of coaxial loads is achieved by making the shield with the profile of a tratrix, a detailed analysis of which is given in the work [102].

Par. 5.4. Capacitors for High-Voltage Pulse Devices

The chief requirement for capacitors used in high-voltage pulse devices is their low self-inductance. It is also necessary that the capacitor have small dimensions since with large dimensions of the capacitor the connecting wires will introduce considerable inductance into the discharge circuit.

Capacitors with a large capacitance are necessary to obtain pulses with a large current. Capacitors with paper-oil insulation have the largest capacitance from among the high-voltage capacitors. The calculation of the inductance of these capacitors is given in the works by P. N. Dashuk [103], and by Kuchinskiy and K. M. Irkayeva [104].

Capacitors with paper-oil insulation consist of separate sections wound into rolls and connected for increasing the capacitance into parallel groups which are series-connected to increase the operating voltage.

The inductance of one section L_s consists of the inductances of the plates L_0 and the leads L_v determined by their geometrical dimensions and arrangement of the leads on a section.

In the work [104] are given the data for the evaluation of L_s with the condition of a uniform flow of current over the conductors. Inductance is evaluated by formulas derived for busses of a rectangular cross section [105].

In Figure 5.5 are shown the possible arrangements of the leads on the capacitor plates. If the leads are arranged opposite each other (see Figure 5.5a), then

$$L_0 = \frac{\mu_0 l}{3b}(3a + 2d), \qquad (5.35)$$

where "a" is the distance between the plates determined by the thickness of the insulation; b, d, l are respectively the width, thickness and length of the metal plates.

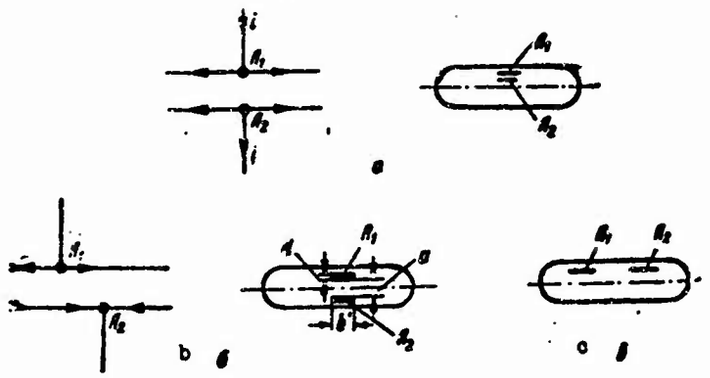

Figure 5.5. Methods of laying the leads in a capacitor section: the leads are placed one under the other on one layer of insulation (a); the leads are displaced (b, c).

Since usually $3a \gg 2d$, then

$$L_0 = \frac{\mu_0 a l}{b}. \tag{5.36}$$

If the leads are displaced to a certain distance l' relative to each other, then L_0 is made up of the inductance of the section with an opposite direction of the current $L_0' = \frac{\mu_0 a(l - l')}{b}$ and of the inductance of the section with a coinciding direction of the current L_0'' (see Figure 5.5b) The value of L_0'' depends on the arrangement of the leads relative to each other; if they are displaced along the length of the foil within the width of the section, then

$$L_0'' = \frac{\mu_0 l'}{2\pi}\left(\ln\frac{2r}{b} + \frac{1}{2}\right); \tag{5.37}$$

If the leads are displaced along the length of the foil by half a turn, then

$$L_0'' = \frac{\mu_0 l'}{3b'}(3a' + 2d), \tag{5.38}$$

where a' and b' are shown in Figure 5.5b. In the roll-type capacitors the leads are made in the form of copper busses and are arranged at one end to reduce the inductance. In this case the L_V of one lead is determined from the expression (5.35) where the linear quantities characterize the leads and their position relative to each other. Thus, $L_S = L_0 + 2L_V$. Experiments

on a rolled section with a capacitance C=1.0 microfarads and a=80 microns showed [104] that when the leads are placed opposite each other (see Figure 5.5a) the L_s depends little on the location of the leads and varies from 0.6 to 2.2 · 10^{-9} henries; with a displacement of the leads by 12 cm (half a turn), L_s increases from 2.5 · 10^{-9} to 16 · 10^{-9} henries upon the withdrawal of the leads from the start of the winding. This is explained by the increase of the dimension of the a' (see Figure 5.5b). With an increase of the distance the L_s rapidly increases owing to L_o". Therefore, the leads must be placed at a minimal distance from each other on the basis of the overlap of the insulation. It is noted in the work [104] that it is inexpedient to make several taps from one section since the current will flow mainly through the taps located at the start of the section owing to a lower value of L_o at this place. To decrease the inductance it is expedient to increase the number of parallel sections in a group since in doing so the dimensions of each section are reduced. The inductance of the capacitor decreases in proportion to the increase in the number of sections in a group and increases with an increase in the number of the groups. Ceramic capacitors of various types having two plates have a low inductance. From among the domestic ceramic capacitors, barrel capacitors of the type KOB having a comparatively high value of the capacitance are of the greatest interest.

Their characteristics are given in Table 5.3.

Table 5.3

	Параметр Parameter	КОБ-1 KOB	КОБ-2	КОБ-3
1	Емкость, *пф*	500	500	2500
2	Рабочее напряжение, *кв*	12	20	30
3	Высота, *мм*.	17	27	40
4	Диаметр, *мм*	20	33	62

Key: (1) Capacitance, picofarads (3) Height, mm
(2) Operating voltage, kv (4) Diameter, mm

When it is necessary to obtain a high-power pulse with a steep leading edge and a flat portion, it is expedient to use a parallel connection of a ceramic capacitor and of a capacitor with paper-oil insulation. In doing so, the value of the capacitance of the ceramic capacitor may be evaluated as indicated in Par. 3.1, on the basis of the value of the inductance of the capacitor with paper-oil insulation.

In Table 5.4 are given the values of the inductances of capacitors of different types [106].

Table 5.4

1 Тип конденсатора	9 Индуктивность, 10^{-9} гн
2 Воздушный образцовый:	
100 пф	10—20
1000 пф	30—50
3 Воздушный переменной емкости:	
малых размеров	6—20
средних размеров	10—60
4 Керамический дисковый:	
КДК-3	1—1,5
КДК-1,2	2—4
5 Керамический трубчатый:	
КТК-1,2	3—10
КТК-3, 4, 5	20—30
6 Слюдяной опрессованный:	
КСО-1	4—6
КСО-11, КСО-12, КСО-13	15—25
7 Слюдяной образцовый и блокировочный:	50—100
8 Бумажный:	
малых размеров КБГ-4	6—11
средних размеров КБГ-М, КБ	30—60
радиотипа Сольших размеров (ольшой емкости)	50—100
большой емкости с неправильным расположением выводов	200—150000

Key: (1) Type of capacitor
(2) Air reference capacitor:
100 picofarads
1,000 picofarads
(3) Air variable-capacitance capacitor of:
small dimensions
medium dimensions
(4) Ceramic disk capacitor:
KDK-3
KDK-1.2
(5) Ceramic tubular capacitor
KTK-1.2
KTK-3, 4, 5
(6) Mica molded capacitor:
KSO-1
KSO-11, KSO-12, KSO-13
(7) Mica reference and blocking capacitor
(8) Paper capacitor:
of small dimensions KBG-4
of medium dimensions KBG-M, KB
of radio type of large dimensions (of large capacitance)
of large capacitance with irregular arrangement of the leads
(9) Inductance, 10^{-9} henries

Par. 5.5. Spark Dischargers Triggered With Nanosecond Accuracy

When using spark dischargers in oscillographs for recording very short pulses, in the high-speed-photography devices, in circuits for the conversion of high-voltage pulses of nanosecond duration, etc. it is necessary that the time between the arrival of the triggering pulse and operation of the discharger amount to a value of the order of 10^{-8} sec, and stability -- to 10^{-9} sec. As a rule, three types of dischargers are used for this purpose: trigatrons, light (spark) relays and three-electrode dischargers. The trigatron T (Figure 5.6a) was suggested by I. S. Stekol'nikov [35].

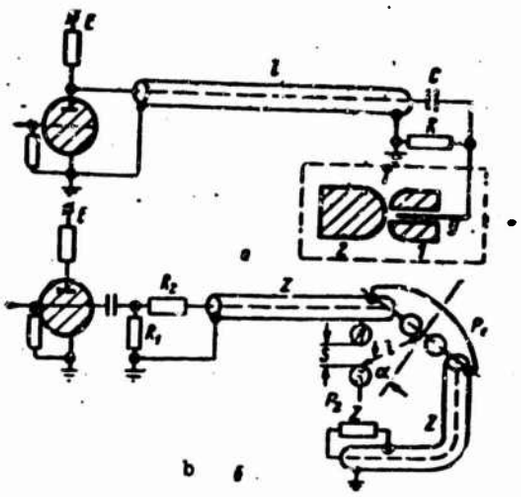

Figure 5.6. Circuit diagrams for triggering a trigatron (a) and a spark relay (b) with nanosecond precision.

After the arrival of the trigger pulse at the rod Y a discharge takes place between the rod and electrode 1. Ultraviolet irradiation of this discharge initiates a breakdown between the main electrodes 1 and 2. The operation time of the trigatron is usually equal to 10^{-6} sec with a spread of the order of 10^{-7} sec [10]. Theophanis [10] investigated the feasibility of triggering the trigatron with nanosecond precision. The trigatron was in a freon atmosphere with a pressure of 0.111 atmosphere. The maximum operating voltage was equal to 50 kv. Investigations showed that the operation time of the trigatron was shorter when the polarities of the trigger pulse and of the potential on the ungrounded electrode are opposite. A pulse with an amplitude of 15 kv and duration of the leading edge of $2 \cdot 10^{-8}$ sec appeared during the discharge of the capacitor through a thyratron [sic]. With a voltage in the trigatron with $\eta = 5$ percent lower than the breakdown voltage the spread in the operation time was equal to $5 \cdot 10^{-8}$ sec. With a decrease of η the spread decreased but spontaneous operations of the trigatron appeared owing to the random rises of the voltage.

When an open end of a line ($R \gg Z$, see Figure 5.6a) was connected to the electrode Y the amplitude of the trigger pulse doubled. In this case, for a $\eta \leqslant 10$ percent the operation time of the trigatron was equal to $2 \cdot 10^{-8}$ sec with a spread of not more than 10^{-9} sec. The operation time of the trigatron and its spread decrease with a decrease of the duration of the leading edge of the trigger pulse. This is connected with the creation of a large overvoltage between the electrodes 1 and Y.

A spark relay has two spark gaps (see Figure 5.6b): the main gap

P_1 and the initiating gap P_2 [P=gap]. Ultraviolet radiation of the spark in P_2 initiates a breakdown of P_1 (see Par. 1.1). For a stable operation of a spark relay the distance between the gaps must not exceed a few centimeters. Investigation of the operation of a spark relay was carried out by I. S. Stekol'nikov [35] who showed that with $\eta \leq 1$ to 2 percent and an operating voltage of about 10 kv the time between the breakdown of the initiating and the main gap is equal to $1 \pm 0.5 \cdot 10^{-8}$ sec. The initiating discharge in these [35] and later [20] investigations was created with a discharge of the capacitor in the spark gap.

Godlove [36] investigated the triggering of a spark relay with the insertion of P_2 in a break in the cable over which a trigger pulse (see Figure 5.6b) with an amplitude of about 7 kv and a duration of the leading edge $t_f = 10^{-8}$ sec comes in. Owing to the steep leading edge of the trigger voltage pulse the gap of P_2 was broken down in the case of overvoltage. In this process the steepness of the leading edge of the light pulse was greater than in a network with a capacitor discharge, and the stability of the time t_s between the breakdowns of the dischargers P_1 and P_2 was higher. In Figure 5.7 is shown the relationship of the time t_s to the value of the voltage U in the gap of the main discharger P_1 with spherical brass and stainless-steel electrodes and interelectrode distance S= =3.18 mm and different distances l between P_1 and P_2. It follows from Figure 5.7 that the material of the electrodes has little effect on the value of t_s.

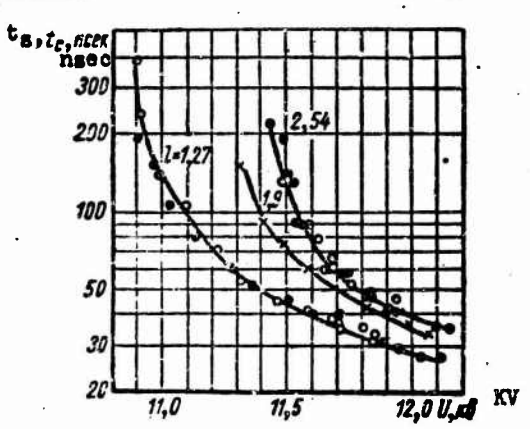

Figure 5.7. Relationship of the time between the operation of the dischargers P_1 and P_2 (see Figure 5.6b) to the voltage U on P_1 and to the distance l between the dischargers:

⊙ and × — stainless-steel electrodes;

● — brass electrodes.

With the constant values of S and with an increase of U the time t_s approaches a certain limit which may be evaluated by the following formula:

$$[t_{cm}=t_{sm};\ v_{av}=v_{avalanche}] \qquad t_{cm}=\frac{S}{v_a}=1{,}37\cdot10^{-6}\frac{S}{\sqrt{E}}. \tag{5.39}$$

where v_{av} is the velocity of the motion of avalanche in the gap; E — field strength at which the breakdown of the gap takes place. Depending on the S and l the time t_{sm} in Godlove's experiments [36] amounted to 10-60 nanoseconds with a variation of η in a range of 0-5 percent leading to a variation of $t_s=(1\text{ to }2)\ t_{sm}$ with spreads of about 10 percent of t_{sm}.

It is shown in the works [36] and [35] that cleaning of the electrodes of the main discharger hardly affects the value of t_s; the angle between the axes of P_1 and P_2 must not exceed 20°. It is not recommended to place barriers between P_1 and P_2 even when the barriers are made of the most transparent materials (LiF, etc.).

The advantages of a spark relay consist in a complete electric insulation between the firing and the main gap with short times of the spread (about 10^{-9} sec); the stability of the operating voltage is equal to 6 percent.

The main drawback consists in the small range of operating voltages when the interelectrode gap of P_1 is constant.

A three-electrode relay in the pulse circuits operates in the following manner (Figure 5.8a). The point A is connected to a source of direct voltage U_1 and the point B is grounded through a load. The length of the gap P_1 is selected to be such that no breakdown would occur with the voltage U_1, and P_2 — such that it would not break down under the action of the voltage U_2 of the trigger pulse. Upon the arrival at the point V of the trigger pulse U_2 with a polarity opposite of that of the U_1 the gap P_1 breaks down and the voltage U_1 is applied to P_2. The P_2 breaks down with an overvoltage the greatest magnitude of which may be created in the gaps P_1 and P_2 respectively and amounts to

$$\beta_1=\frac{U_1+U_2}{U_1},\quad \beta_2=\frac{U_1}{U_2}. \tag{5.40}$$

Investigations of the operation of a three-electrode discharger [35] showed the following. To decrease the initiation time of the discharger and increase the stability of this time the amplitude and the steepness of the leading edge of the trigger pulse should be increased. Spreads of the order of 10^{-8} sec are obtained with a steepness of 40-50 kilovolts/microsec and an amplitude of the trigger pulse equal to 50-70 percent of U_1. The operation of the discharger is considerably accelerated and stabilized if the gaps P_1 and P_2 are irradiated with ultraviolet rays.

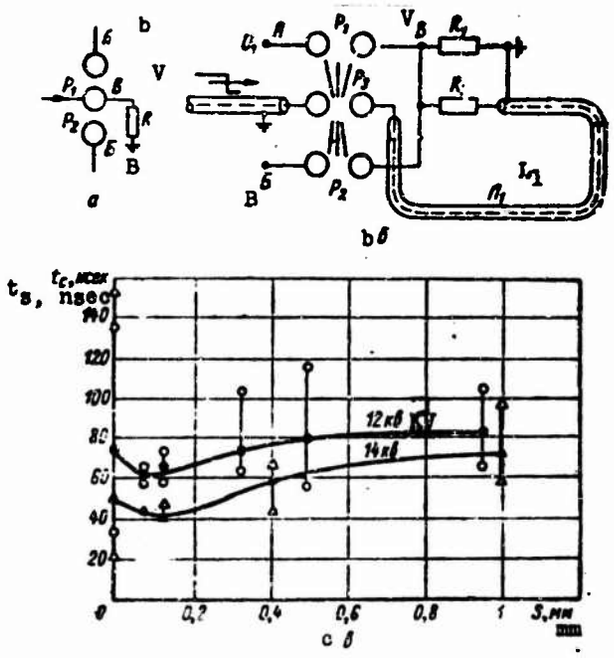

Figure 5.8. Circuit diagrams of a three-electrode spark discharger: the usual circuit diagram (a); with an additional discharger P_3; relationship of the operation time of the discharger to the length of the gap in P_3 (c).

In Figure 5.8b is shown a circuit diagram of a three-electrode discharger with an additional spark gap of the P_3 series-connected with the cable L_1 over which the trigger pulse arrives [108]. To irradiate two gaps simultaneously the center electrode is divided into two and the gaps P_1 and P_2 are arranged as shown in Figure 5.8b. The length of the spark gap P_3 can always be set so that the delay of the breakdown of this gap would be small. If $R_1 + R_2 \gg Z$ (Z is wave impedance of the cable L_1), then the steepensss of the leading edge of the trigger pulse is doubled owing to the doubling of the voltage at the end of the cable. For a normal operation of the discharger it is necessary to have $R_1 \gg R_3 \gg Z$.

We will determine the relationship between the voltages U_1 and U_2 assuming that statistical delay time in P_1 and P_2 is equal to zero and that the trigger pulse has a perpendicular leading edge. Under these conditions the triggering time of the discharger will depend only on the time for forming the discharge of the gaps P_1 and P_2. Then, the following may be written on the basis of the formula (1.21):

$$[t_c = t_s] \qquad t_c = \frac{1}{(\beta_1 - 1)^2} + \frac{1}{(\beta_2 - 1)^2}. \tag{5.41}$$

but it follows from the expression (5.40) that

$$\beta_2 = \frac{1}{\beta_1 - 1}. \tag{5.42}$$

If in the equality (5.41) β_1 is substituted with the quantity β_2, then from the condition that $\frac{dt_s}{d\beta_2} = 0$ we will determine the optimum value of the overvoltage β_{02} with which the operation time of the discharger will be minimal:

$$\beta_{20}(\beta_{20} - 1)^2 = 1. \tag{5.43}$$

It follows from the equations (5.43) and (5.42) that $\beta_{20} = 1.82$ and $\beta_{10} = 1.55$. Consequently, the optimum relationship between the operating voltage of the discharger U_1 and the amplitude of the trigger pulse is

$$U_2 = 0{,}55U_1. \tag{5.44}$$

In Figure 5.8c is shown the relationship of the operation time of a three-electrode discharger to the length S of the spark gap P_3 with a voltage of 14 and 12 kv with the distances between the electrodes in the gaps P_1 and P_2 remaining invariable. The duration of the leading edge of the trigger pulse is equal to 15 nanosec. The relationship between U_1 and U_2 approaches optimum relationship. With S=0 the discharger operates without irradiation. Vertical lines correspond to the spread of the values being observed. The best results were obtained with a U_1=14 kv and S=0.1 mm. In this case, the operation time $t_s = (42 \pm 1)$ nanosec. A decrease of the voltage to 12 kv (i.e. by 14 percent) leads to an increase of the time t_s to (62 ± 7) nanosec.

Works have recently appeared devoted to the investigation of vacuum dischargers and low-pressure dischargers, which make it possible to commutate the currents of up to hundreds of kiloamperes, have a long service life and a short triggering time.

A. A. Brish, Ab. Dmitriyev et al. [109] have developed small-sized vacuum dischargers of the type VIR. In these dischargers the breakdown of the main gap is initiated by an auxiliary breakdown on the surface of mica which separates the electrodes of the firing gap. The use of this insulation layer makes it possible to reduce the breakdown voltage of the firing gap,

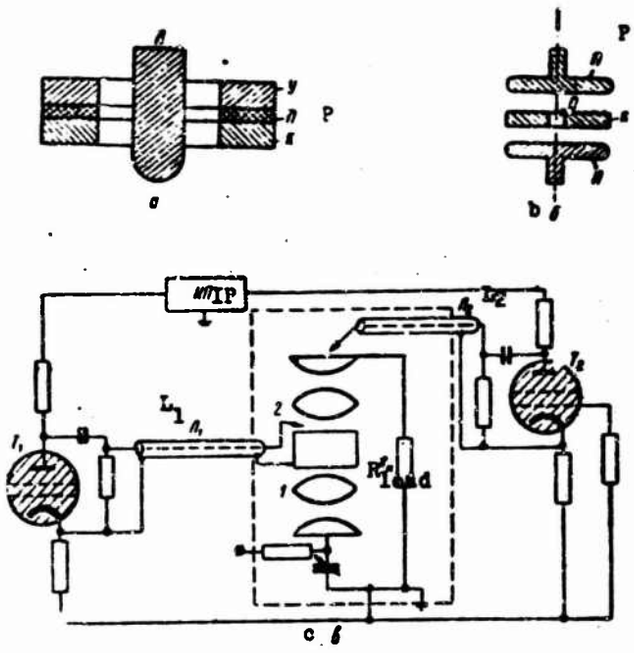

Figure 5.9. Coaxial make-up of a vacuum discharger (a): A — anode, K — cathode, P — mica layer, Y — controllable electrode; make-up of a low-pressure discharger (b) and circuit diagram of a high-power vacuum discharger (c).

and thereby also to reduce the amplitude of the trigger pulse. The dischargers of the type VIR have a large range of operating voltages. For example, VIR-7 operates reliably with a variation of the operating voltage from 10 kv to 100 volts. The triggering time of a discharger and its stability depend on the make-up of the discharger and the steepness of the leading of the trigger pulse. Coaxial make-up (Figure 5.9a) proved to be the best. With an amplitude of the trigger pulse of 2.2 kv and a steepness of the leading edge of 225 kv/microsec the triggering time is about $3 \cdot 10^{-8}$ sec with a spread of less than $1 \cdot 10^{-8}$ sec. A drawback of this discharger is the relatively small number of cut-ins and a large spread of the breakdown voltage of the firing gap. This sometimes limits their application.

The low-pressure dischargers developed by S. I. Lobov, V. A. Tsukerman and L. S. Eyg [75] do not have these drawbacks. The dischargers operate in a neon or argon atmosphere at a pressure p=0.1 to 0.7 mm of mercury column. The product of pS corresponds to the left branch of Paschen curve (see Par. 1.1). In this case the breakdown voltage decreases with an increase of the interelectrode gap.

A schematic arrangement of the electrodes in the discharger is shown in Figure 5.9b. The pressure and interelectrode distances in the discharger are set to be such that the main discharge gap A-K have a breakdown voltage which is on the left branch of Paschen curve and the voltage of the firing gap A-P be about the minimum. Until the arrival of the trigger pulse a "guard" discharge with a current of 10 microamperes burns between the trigger electrode P and the cathode K. After the arrival of a negative trigger pulse on the electrode P the gap P-K breaks down; in doing so, the electrodes rush to the anode through the opening O in the cathode and bring about the main discharge between the anode A and the cathode K. These dischargers operate in a range of operating voltages of 2-10 kv with an amplitude of the trigger pulse of 2 kv and a steepness of the leading edge of 5 kv/microsec. The delay time of the triggering amounts to 20-40 nanosec, the operatin current is 3-5 kiloamperes.

In Figure 5.9c is shown a diagram of the arrangement of the electrodes and a device for triggering the discharger with a current of up to 300 kiloamperes, developed by Mather and Williams [110]. The discharger consists of two identical sections 1 and 2 fastened inside a chamber out of which gas is continuously pumped out by a rough-exhaust pump. The pressure in the chamber is kept at a level of 0.05 mm of mercury column. After the operation of the thyratrons, trigger pulses with an amplitude of 20 kv and a duration of the leading edge of 10^{-8} sec arrive on the firing electrodes of both sections. The cable over which the trigger pulses arrive is not connected directly to the firing electrode. Owing to this, a doubling of the voltage of the trigger pulse takes place. The discharger operates in a range of voltages of 100 volts to 20 kv with a triggering delay time of $(5 \pm 2) \cdot 10^{-8}$ sec. Vacuum dischargers and low-pressure dischargers for currents of 1,000 to 2,000 kiloamperes [25] and a voltage of up to 100 kilovolts [111] are also known.

Par. 5.6. Series Dischargers

Several series-connected spark gaps are called a series discharger. Usually the voltage is distributed among the spark gaps by means of resistances. Sometimes each spark gap is shunted by a capacitance. A series discharger has small dimensions of the electrodes and can be made in smaller sizes than a single discharger for a full voltage.

G. A. Vorob'yov [112] proposed a circuit arrangement for obtaining pulses with a steep leading edge, where a series discharger is used (Figure 5.10a). The potentials of the upper electrodes of the dischargers relative to the ground amount respectively to U_1, U_2 and U_n. The first one to break down is usually the gap P_1 in which the "heating" capacitance C_1 discharges creating a conducting channel in the gap. Owing to the capacitance C_2 the potential at the point of its connection is kept practically constant. Therefore, the gap P_2 breaks down with an overvoltage $\beta_2 = \frac{U_1 + U}{U_{2pr}}$ where U_{2pr} is the breakdown voltage of P_2. The discharge of C_2 creates a conducting path

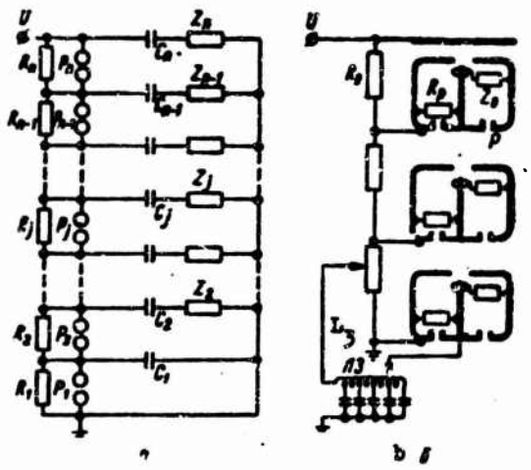

Figure 5.10. Circuit diagrams of a series multiple spark discharger (a) and of a pulse clipper (b).

in P_2 and maintains it in P_1. In this manner all of the n gaps successively break down with an overvoltage.

The number of spark gaps in a series discharger may be determined by setting a certain quantity

$$k_j = \frac{U_j}{U_0}$$

where j=1, 2, 3, ...n; U_0 is the potential of the upper electrode of the j-th gap. Under normal conditions the gap P_j must have a safety factor equal to

$$[U_{jnp} = U_{jpr}] \qquad \alpha_j = \frac{U_{j\,np}}{U_j - U_{j-1}}. \tag{5.45}$$

where U_{jpr} is the breakdown voltage of the j-th gap. The connection between α_j and the overvoltage β_j has the following form

$$\tau_j = (U_j - U_{j-1}) = \frac{U_j}{\beta_j}. \tag{5.46}$$

or

$$\tau_j = \frac{1}{\alpha_j \beta_j} = \frac{k_j - k_{j-1}}{k_j}. \tag{5.46'}$$

It follows from this expression that

$$k_1 = k_2(1-\gamma_2) = k_3(1-\gamma_3)(1-\gamma_2)\ldots = k_j(1-\gamma_j)(1-\gamma_2)\ldots\times \\ \times(1-\gamma_j)\ldots = \ldots = k_n(1-\gamma_2)(1-\gamma_3)\ldots(1-\gamma_n). \tag{5.47}$$

Three methods of voltage distribution over the dischargers are of interest.

1. Suppose $\gamma_j = \gamma = \text{const}$. In this case, when the factors α are equal all of the gaps break down with the same overvoltage β. Since $k_n = 1$, then it follows from the expression (5.47) that

$$\left.\begin{aligned} k_1 &= (1-\gamma)^{n-1}, \\ \text{or} \qquad n &= \frac{\ln k_1}{\ln(1-\gamma)} + 1 \end{aligned}\right\} \tag{5.48}$$

2. With a uniform voltage distribution over the dischargers

$$\gamma_j = \frac{1}{j} \quad \text{and} \quad n = \frac{1}{k_1} \tag{5.49}$$

3. Suppose the voltage is now distributed over the dischargers in such a manner that $k_3 - k_2 = k_4 - k_3 = \ldots k_n - k_{n-1}$ but $k_2 - k_1 \neq k$. In this case it is easy to show that

$$n = \frac{1-k_1}{k} + 1. \tag{5.50}$$

To explain the operation of a device with a series discharger it was assumed that in the process of the breakdown of the gaps the potentials of the electrodes of the gaps which did not break down remain unchanged, and that calculated overvoltages are attained in the gaps. Actually these conditions are not always observed.

In the time τ_j between the breakdowns of the gaps $P_j - P_{j-1}$ the capacitance C_j may discharge owing to the shunting of a portion of the active divider by the broken-down gaps. To eliminate the discharge of C_j it is necessary that

$$R_j C_j \gg \tau_j.$$

During the operation of the dischargers the potential distribution is affected by the self-capacitance of the dischargers C_{Pj}, onto which the C_j discharges after the breakdown of the P_{j-1}. Therefore, it is necessary that

$$C_j \gg C_{P_j}.$$

The value of the overvoltage at which the breakdown of the gaps takes place is also affected by the relationship between the commutation time $t_{k(j-1)}$

of the discharger P_{j-1} and by the delay τ_j of the breakdown of the gap P_j relative to the breakdown of P_{j-1}. If $t_{k(j-1)} > \tau_j$, then the potential difference in the gap will not have time to attain the maximum value of U_j since a breakdown of the gap P_j will take place. In doing so, the overvoltage in the gap P_j will be smaller than the calculated voltage. This increases the commutation time of a series discharger. An analysis of the time between the breakdown of adjacent gaps in the air in relation to the values of C_j, R_j and Z_j inserted in the discharge circuit of the "heating" capacitance was carried out in the work [47] with different arrangements of the gaps. Two different distributions of the voltage over the gaps were used. In the first case with the number of the dischargers $n=4$, $R_1=28.6$ megohms, $R_2=R_3=R_4=0.68$ megohm; in the second case -- with $n=3$, $R_1=R_2=R_3=10.2$ megohms. The dischargers were arranged in such a manner that a mutual irradiation of the gaps would occur.

In Figure 5.11 are shown the curves of the relationship of the time τ between the breakdown of the second and third and also of the first and second gap to the length of the gap in P_3 for the first and second distribution with different values of the heating capacitances and of the loads Z. Vertical lines indicate the spread of the values observed. The value of $C_j=\text{const}=C$.

The increase in the spreads of the value of τ with an increase in S is connected with a decrease of the overvoltage in the gap, and the increase of these spreads with a decrease of C_j is explained by an attenuation of the intensity of irradiation. Using the curves 1 and 3 in Figure 5.11c it is possible to determine the total time t_s of the discharger operation from three gaps: $t_s=\tau_2+\tau_3$. Thus, with a safety factor $\alpha=10$ percent and $S_2=S_3=1.4$ mm, $t_s=20$ nanoseconds. The value of t_s decreases and becomes more stable with a decrease of α, and it is also not sensitive to the value of C_j up to a certain minimum value of $C_{jm}\approx 30$ picofarads. With $C_j<C_{jm}$ the t_s greatly increases and also the spread of its value. With $C_j>C_{jm}$ the t_s is steplessly regulated by varying the distances of the gaps but up to a certain limit determined by the necessity of creating a certain overvoltage in the gap.

With certain additions the diagram in Figure 5.10a may also find another application. If a series discharger is installed as the first discharger of a pulsed-voltage generator using Arkad'yev--Marks circuit, then the synchronization of a GIN [pulsed-voltage generator] and electronic oscillograph may be made easier and stabilized.

If different circuits are connected to the gaps of a series discharger, then these circuits will operate at the instants which differ little from each other. This can also be achieved if the circuits are left uncoupled to each other and their dischargers are irradiated with sparks obtained in the gaps of the series discharger.

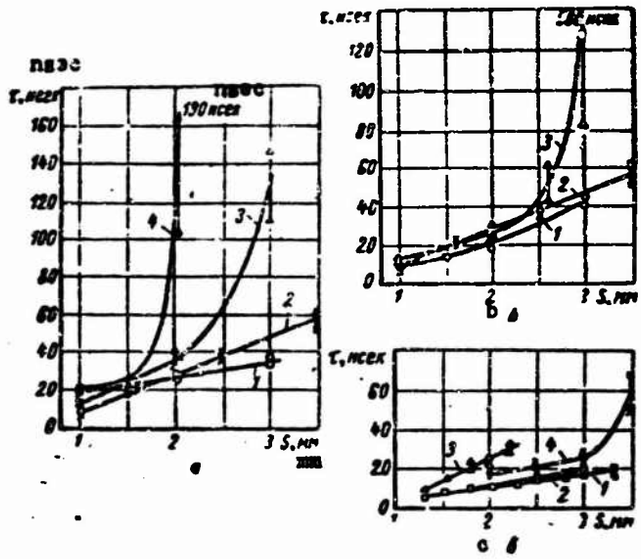

Figure 5.11. Relationship of the time τ between the breakdown of the dischargers to the length of the gap S in the first (a, b) and second (c) distribution of the voltage:

(a) $\tau_3(S_3)$ with S_2=3 mm, C_j=500 picofarads; 1 — Z_j= =0; 2 — Z_j=120 ohms; 3 — Z_j=10^4 ohms; 4 — Z_j=∞; (b) $\tau_3(S_3)$ with S_2=3 mm; Z_j=120 ohms; 1 — C_j= =2,500 picofarads; 2 — C_j=500 picofarads; 3 — C_j= =33 picofarads; (c) 1 — $\tau_3(S_3)$ with C_j=1,000 picofarads, Z_j=75 ohms; 4 — $\tau_3(S_3)$ with Z_j=∞.

If load impedances are placed in the circuit of the heating capacitances, then pulses repeating at a certain rate will be separated on these impedances. In order that these pulses be short, it is necessary to connect special circuits to the load impedance to clip a pulse to the necessary duration. The time between the pulses will be controlled by the length of the spark gaps. These pulses may find application in high-speed photography for taking frame-by-frame photographs with the aid of electronic-optical converters and electrooptical shutters.

Light flashes with a small controllable interval of their recurrence can be obtained with the aid of a series discharger. Flashes appear as a result of a breakdown of the spark gaps. A series discharger can serve as

a circuit for delaying high-voltage pulses with a steep leading edge. The pulse which has to be delayed for a time t_z is sent to trigger the discharger P_1. After the breakdown of the discharger P_n a new pulse will appear on Z_{load} with a certain delay t_z relative to the input pulse. The time is steplessly regulated by varying the length of the spark gaps P_j.

In the work [113] are given data on the use of a series discharger for obtaining clipped waves with an amplitude of 500 kilovolts and higher. The discharger (see Figure 5.10b) was connected to a pulse generator using Arkad'yev—Marks circuit. The distribution of the voltage over the gaps of the discharger was accomplished by means of an active divider with a total impedance of 39 kilohms. Each spark gap represented a trigatron. The discharge took place in each gap between the lower hemisphere and a segment of the upper electrode. In doing so, a potential difference would appear between the hemisphere and the firing electrode in the following gap with this potential difference bringing about the initiating discharge. Natural capacitances between the electrodes and between the electrodes and the ground are used as the heating capacitances. The pulse duration is set by the delay line LZ. Superimposition of several oscillograms with a clipping time of a few tenths of a microsecond showed a practically complete coincidence. The spread of the operation time of a series discharger is less than 10^{-7} sec.

Par. 5.7. Generators

In obtaining high-voltage pulses of nanosecond duration the main problem is to decrease the duration of the leading edge of the pulse. In the generators using the dischargers this is achieved by decreasing the spurious parameters of the discharge circuit and the commutation time. The commutation time t_k is decreased for many generators upon placing the discharger into a chamber with a high pressure and upon creating an overvoltage during the breakdown of the discharger.

A peaking spark discharger the theory of which was given in Par. 3.2 is often used in generators with a gap overvoltage.

In 1917 Herz [114] used for the first time a series connection of a long line with an oil-filled spark discharger to obtain short waves. Buravoy [3] created a generator with a peaking discharger in oil to obtain high-voltage pulses with a duration of the leading edge of about 10^{-9} sec and an amplitude of the order of 100 kv. This generator was used to investigate the delay of a pulsed breakdown of gases.

In Figure 5.12a is shown a diagram of one of the generators developed by Fletcher [27], in which a spark discharger under a pressure of about 100 atmospheres in nitrogen is used for peaking a pulse. The primary pulse is shaped by coaxial cable L_1 which is charged through the resistance R_1 from

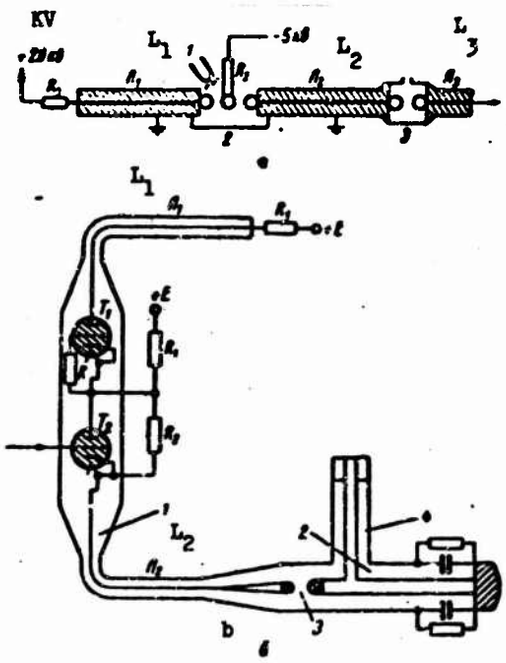

Figure 5.12. Diagram of a pulse generator with a peaking discharger in nitrogen under high pressure — a: 1 — mercury lamp; 2 — three-electrode discharger; 3 — peaker;
and diagram of a generator with a thyratron commutator — b: 1 — primary-pulses generator using thyratrons; 2 — coaxial device for pulse conversion; 3 — peaker; 4 — differentiating section.

a source having a voltage of 20 kv. A three-electrode discharger is used in the primary-pulses generator. After the arrival of a negative trigger pulse of -5 kv at the center electrode the discharger operates and a pulse with a t_{f_1} [f=leading edge] of about 20 nanoseconds is received in the cable L_2. After the peaking the duration of the leading edge decreases to t_{f_2} 0.3 nanosec. An important drawback of this generator is the large value of t_{f_1}. Owing to this, instability in t_{f_2} is observed and, in addition to this, it proved to be necessary to maintain a high pressure in the peaker to decrease the t_{f_2}.

In the generator developed by Heard [78] the value of t_{f_2} was decreased owing to the use of two series-connected hydrogen thyratrons with a steep commutation characteristic (see Figure 5.12b) as a commutator in the primary-pulses generator. The lower thyratron T_2 is triggered from the

trigger pulse and the thyratron T_1 proves to be energized by a double overvoltage and quickly operates. Voltage pulses with an amplitude of 25 kv and a duration of the leading edge of 1.7 nanoseconds are obtained at the output of the thyratron generator. Structurally the generator using thyratrons is made in the form of a coaxial line. This ensures a good matching with the shaping cable and connecting cables and makes it possible to reduce the spurious parameters of the generator. The peaking discharger is in the air at atmospheric pressure. After the peaking of the leading edge the pulse is shortened by a short-circuited section. The duration of the pulse at the output is controlled by the length of this section. After the peaker the duration of the leading edge of the pulses decreases to 0.6 nanosecond and the pulse duration is equal to 2.5 nanoseconds.

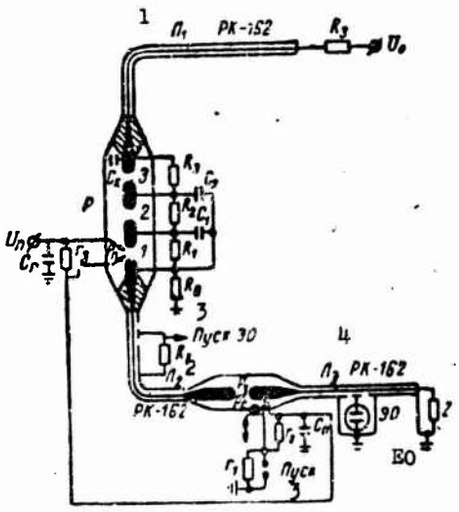

Figure 5.13. Diagram of a generator of pulses of controllable duration using a series spark discharger as the commutator.

Key: (1) L_1 (2) L_2 (3) Triggering of EO [electronic oscillograph] (4) PK-162 [type of cable].

In Figure 5.13 is shown diagram of a generator [115] in which a series discharger with three spark gaps described in Par. 5.6 is used as the commutator. The cable L_1 of three meters in length is charged from a direct-voltage (30 kv) source. After the operation of the discharger P a voltage pulse with an amplitude of 15 kv and a duration of 40 nanoseconds appears in

the cable L_2. The operation of the commutating device starts with the breakdown of the first gap. After this, the second and third gaps break down with an overvoltage.

The duration of the leading edge of a primary pulse t_{f_1} decreases with an increase of the overvoltage in P_3 but with a relative overvoltage $\beta \geq 2$ t_{f_1} it hardly decreases and with $C_1=C_2=30$ picofarads amounts to about 5 nanoseconds. A correcting capacitance $C_k=50$ picofarads is used to decrease the t_{f_1} to 2.5 nanoseconds. A peaking discharger P_z was used in the air under normal conditions for a further decrease of the duration of the leading edge of the pulse. The optimum length of the peaking gap is about 3 mm. After the peaker the duration of the leading edge of the pulse did not exceed 1 nanosecond. A "clipping" discharger P_s built-in into the chamber of the discharger P (see Par. 3.2) serves to decrease the duration of the pulse. The discharger P_s is irradiated with ultraviolet rays from a spark in a special gap P_0. The instant of the breakdown of the gap P_0 is synchronized with the triggering of the commutator in the following manner. The voltage is distributed among the P_0, P_p and the pushbutton "Triggering" in proportion to the values of the resistances r_1, r_2 and r_3. Upon depressing the pushbutton "Triggering" an overvoltage is created in the gap P_0 and it breaks down. The discharge of the capacitance C_0 through the P_0 creates a spark necessary to eliminate statistical delay in the gap P_s. After the breakdown of P_0 the gap P_p proves to be energized with an overvoltage and breaks down bringing about the operation of the commutator. The pulse duration is controlled by the length of the clipping gap in a range of not more than 0-40 nanoseconds.

A generator of pulses having an amplitude of 50 kv with the use of a peaking discharger was developed by Tucker [15]. The commutating discharger of the primary-pulses generator is under a pressure of 60 atmospheres in nitrogen atmosphere. The commutator operates upon a sudden decrease of the pressure in the discharger chamber. Pulse generators in which overvoltage in the spark gap is used to decrease the duration of the leading edge are described in the works [1, 11, 22, 23, 116].

The duration of the leading edge of a pulse obtained in a generator with a peaking discharger has a certain statistical spread owing to the fact that the delay in the breakdown of the peaker bears a statistical character. Generators with commutating dischargers under high pressure are used to correct this drawback. Such a generator was developed by Fletcher [27]. A three-electrode discharger under nitrogen pressure of 42 atmospheres was used as the commutator. The shaping element is a coaxial cable. When using a correcting capacitance the duration of the leading edge of the pulse at the output of the generator is equal to 0.4 nanosecond with an amplitude of 20 kv.

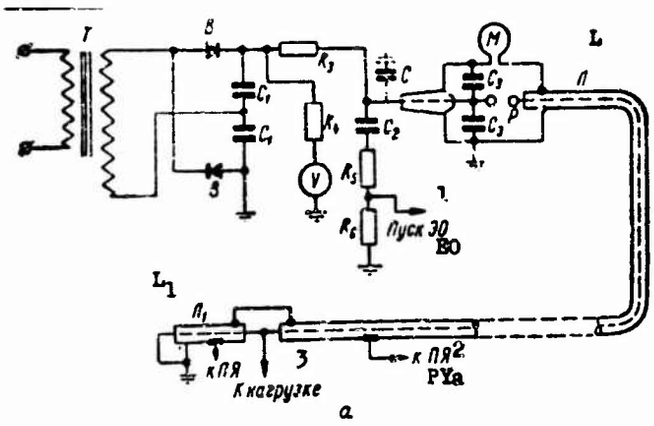

а

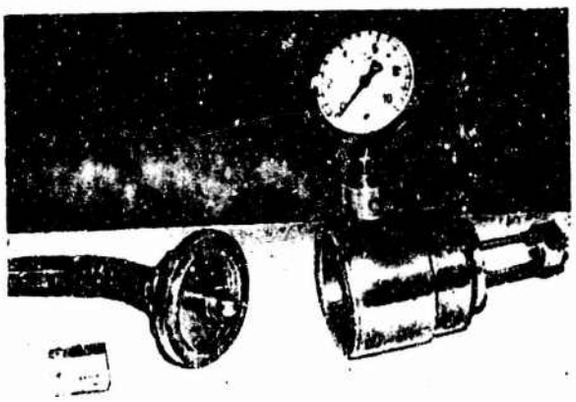

б

Figure 5.14. Basic diagram of a relaxation generator of short pulses: EO -- electronic oscillograph; PYa -- the plates of the event; capacitance C is inserted when obtaining pulses with a $t_i \geqslant 10^{-8}$ sec (a). Photograph of the discharging device of the generator (b).

Key: (1) The triggering of EO; (2) To the PYa; (3) To the load

In another generator with a commutating discharger at a high pressure a capacitor is used as the shaping element. Therefore, the ratio of the pulse amplitude to the charging voltage is about 1. The value of the shaping capacitance 2 C_3 is 1,000 picofarads (two parallel-connected capacitors of the type KOB-2) (Figure 5.14a). To decrease the inductance L of the discharge circuit the capacitors were placed inside a discharge chamber in which a pressure of 9.5 atmospheres was maintained. During the breakdown of the discharger the shaping capacitance discharged into the cable L. The load in the cable had an input capacitance of 10 picofarads. Therefore, it was necessary to calculate the optimum value of the wave impedance Z of the

load cable L. Since the duration of the leading edge without taking account of the commutation is determined from the expression:

$$t_{f_1}=2.2\frac{L}{Z},$$

the duration of the leading edge on the capacitive load C_n may be found from the following formula analagous to the formula (2.3)

$$t_0=\sqrt{\left(2.2\frac{L}{Z}\right)^2+(1.1ZC_n)^2}. \qquad (5.51)$$

where $1.1ZC_n$ is the duration of the leading edge of the pulse on C_n during the action of a rectangular pulse. From the condition $\frac{dt_f}{dZ}=0$ we will find the optimum value of the magnitude of the impedance Z at which the leading edge of the pulse will be the smallest,

$$Z_0=\sqrt{2\frac{L}{C_n}}. \qquad (5.52)$$

On the basis of these calculations a wave impedance of the line L equal to 37.5 ohms (two parallel-connected cables PK-3) was taken. The pulse duration was controlled by the length of the short-circuited section L_1. The pulse repetition rate was changed steplessly from 1 to 50 cps by changing the values of the charging resistance R_z and of the voltage of the charging device with a constant length of the discharger gap. With a constant pressure in the chamber the pulse amplitude was steplessly regulated from 4 to 18 kv. The pulse duration at the output was equal to 3 nanoseconds with a duration of the leading edge of less than 1 nanosecond. In Figure 5.14b is shown a photograph of the discharge device of the generator.

A generator with a shaping cable was developed to obtain pulses with and amplitude of 150 kv and a current of 5 kiloamp. The power for the generator is supplied by pulses with an amplitude of 300 kv from Arkad'yev-Marks generator. The shaping and the load lines were made of coaxial copper pipes, and transformer oil was used as the insulation. The discharger was in a hermetically sealed chamber under a gas pressure of 10 atmospheres. The adjustment of the length of the gap was accomplished by turning the inner conductor of the shaping line on the side of the charging voltage. Pulses with a duration of the leading edge of not more than 1 nanosecond and a flat top of $2 \cdot \cdot 10^{-8}$ seconds possibly appeared at the output of the generator.

Generators of high-voltage nanosecond pulses using high-pressure dischargers are described in the works [1, 4, 14, 22, 118].

Par. 5.8. Obtaining High-Voltage Pulses in Voltage Multiplying Circuits

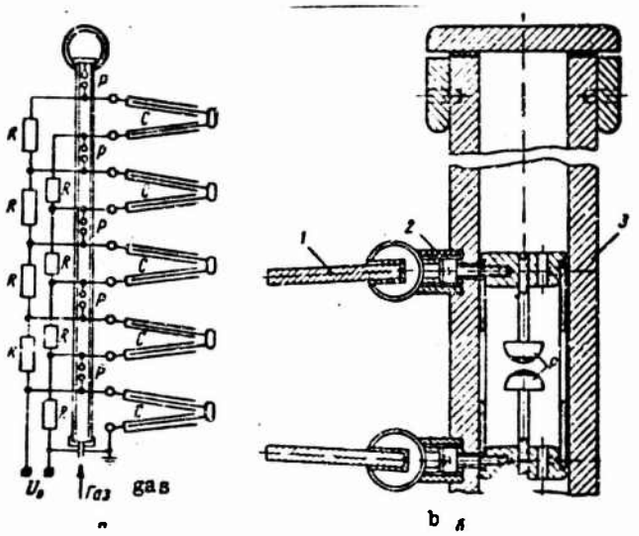

Figure 5.15. Simplified circuit diagram (a) and longitudinal section (b) of a GIN [voltage pulse generator] with dischargers in compressed gas:

1 -- capacitor; 2 — bushing; 3 -- bakelite pipe.

Voltage pulse generators GIN using Arkad'yev-Marks multiplying circuit are used in high-voltage laboratories to obtain pulses with an amplitude of hundreds and thousands of kilovolts and a duration of the leading edge on the order of 10^{-7} to 10^{-6} sec. Such pulses are necessary for high-voltage tests of power equipment and for carrying out certain experiments in physics [21, 22, 26]. The shortest possible duration of the leading edge of the pulses is limited by the capacitance C of the load and of the wiring of GIN and by the inductance of the discharge circuit L, which increase with an increase of the dimensions of GIN, i.e. with an increase of the operating voltage.

In Figure 5.15a is shown a simplified circuit diagram of a pulse generator built by Schering and Raske [4] for 500 kv. The generator uses a multiplying circuit; to reduce the commutation time the dischargers are placed in it in a chamber with carbon dioxide under a pressure of 13 atmospheres. There are five stages in the generator; two capacitors for 50 kv are series-connected in each stage. The capacitance of the GIN "in a stroke"

amounts to 0.0033 microfarad. The low-inductance plate capacitors consist of a larger number of parallel-connected plates of aluminum foil with paper insulation. The length of the capacitor is 108 cm, the width is 75 cm. To decrease the inductance of the discharge circuit the capacitors are "zigzag"-connected forming a bifilar conductor during the discharge. In Figure 5.15b is shown a longitudinal section of the generator. The length of the leading edge of the pulse with an amplitude of 375 kv is equal to $1.1 \cdot 10^{-8}$ sec. The dimensions of the generator are: height — 180 cm, the base — 140 x 90 cm.

Coaxial cables may be used as the shaping devices in order to decrease the inductance of the discharge circuit of the GIN. Rectangular pulses with an amplitude of 80 kc, pulse duration of 0.8 microsec and duration of the leading edge of 10^{-8} sec were obtained in such a generator with six coaxial cables. A voltage pulse generator with shaping cables is described in the work [22].

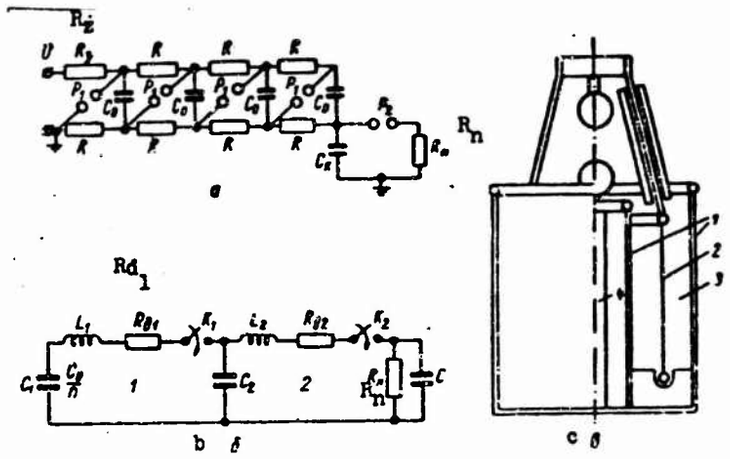

Figure 5.16. Simplified circuit diagram of a GIN with a compensating capacitance (a), a complete substitution network of the discharge circuit of the GIN (b) and arrangement of the compensating capacitor (c):

1 — capacitor plates; 2 — shield; 3 — transformer oil; 4 — the load R_n.

It follows from the foregoing that in order to decrease the leading edge of the pulse the commutation time t_k of all dischargers and the inductance L of the entire discharge circuit are decreased. If compensation of the inductance of the discharge circuit of the GIN by means of inserting a noninductive capacitance as shown in Figure 5.16a is used, then there is no need to decrease the t_k and L in the entire discharge circuit of the gen-

erator. It is sufficient to do this only for the circuit C, P_2, R_n. A similar decrease of the value of t_f in a single-stage GIN is described in the Par. 3.1.

The capacitor $C_2=C_k$ is selected with a low self-inductance and the circuit C_2, P_2, R_n which is energized by pulsed voltage alone has small dimensions and low inductance. In selecting the value of C_2 determining the quality of the flat portion of the pulse the characteristics of the operation of the circuit shown in Figure 5.16a are taken into account.

In doing so, the substitution network of the discharge circuit (see Figure 5.16b) of the GIN will consist of two circuits and two commutators K_1 and K_2: K_1 is the penultimate discharger and K_2 -- the last discharger of the GIN. The commutator K_2 operates following a certain time t_z after the operation of K_1. Upon the closing of the commutator K_1 oscillations are excited in the first circuit, which after the operation of K_2 may be transmitted to the load. If it is necessary to eliminate these oscillations, then the resistance R_{d1} is inserted in the first circuit. We will analyze the operation of the circuit when $C_1 \gg C_2$ assuming the capacitor C_1 as a source of direct voltage nU_0. If $Rd_1 < 2\sqrt{\frac{L_1}{C_2}}$, then upon the closing of K_1 the voltage across the C_2 and the current in the first circuit will vary in accordance with the following law:

$$h_c(t) = 1 - e^{-\beta t}\left(\cos\omega t + \frac{\beta}{\omega}\sin\omega t\right).$$
$$i_1(t) = \frac{1}{L_1\omega} e^{-\beta t}\cdot\sin\omega t, \qquad (5.53)$$

where

$$\omega = \sqrt{\frac{1}{L_1C_2} - \frac{R^2_{d_1}}{4L_1^2}}, \quad \beta = \frac{R_{d_1}}{2L_1}. \qquad (5.53')$$

The shape of the pulse will be different, according to the values of R_{d1} and t_z. To analyze the process at the top of the pulse we will consider that $L_2=0$; $C=0$; $R_{d2} \ll R_n$; $t_{k1}=0$.

Depending on the operator $q=\frac{L_1}{R_n}p$ the voltage across the R_n will assume the following form after the closing of K_2

$$h(q) = \frac{h_c(t_z)\,B\,q^2 + [h_c(t_z)\,b + A]\cdot q + 1}{B\,q^2 + (1+b)q + d}. \qquad (5.54)$$

where

$$B = \frac{R^2_n C_2}{L_1}; \quad b = \frac{R_{d_1} R_n C_2}{L_1}; \quad d = \frac{R_n + R_{d_1}}{R_n}; \qquad (5.54')$$
$$A = i(t_z)R_n.$$

If R_{d_2} is comparable in value with R_n, then $R_n + R_{d_2}$ instead of R_n should be written in the expressions for B, b, d, A. Since the parameter A may be ex-

pressed in terms of B, b, d, then h(q) depends only on these parameters.

The original of the representation (5.54) has the following form

$$h(\tau) = \frac{1}{d}\left[1 - \frac{h_c(t_3)d - 1}{\sin\varphi} e^{-\beta_1 \tau} \sin(\omega_1 \tau - \varphi)\right]. \qquad (5.55)$$

where

$$\tau = \frac{R_n}{L_1} t; \quad \beta_1 = \frac{1+b}{2B}; \quad \omega_1 = \sqrt{\frac{d}{B} - \frac{(1+b)^2}{4B^2}}; \qquad (5.55')$$

$$\operatorname{tg}\varphi = \frac{2B[h_c(t_3)d - 1]\omega_1}{-2d[h_c(t_3)b + A] + (1+b)[dh_c(t_3) - 1]}.$$

Three cases are of interest.

1. $$1.\ R_{\partial_1} = 0, \quad t_3 = \frac{\pi}{\omega_1}. \qquad (5.56)$$

In addition to this, it follows from the equation (5.54) that the pulse amplitude will amount to a value of $h_a=2$ (Figure 5.17a) when $\tau=0$, i.e. a doubling of the voltage takes place at the output of the GIN when the conditions (5.55) are observed. Moreover, it turns out that it is possible to obtain even a fourfold increase of the voltage. Indeed, suppose $R_{d2}=0$; $C \gg C_2$; $L_2 \ll L_1$; $R_n = \infty$, and $t_k=0$ (i.e. the damping action of the spark resistance does not show). Then, considering the voltage at the input of the second circuit (across the capacitor C_2) as a constant voltage and equal to 2, we will obtain

$$h(t) = 2\left(1 - \cos\frac{t}{\sqrt{L_2 C}}\right). \qquad (5.56')$$

Consequently, at the instant of time $t=\pi\sqrt{L_2C}$ we have h=4.

2. $$2.\ R_{\partial_1} = \sqrt{2\frac{L_1}{C_2}}, \quad t_3 = \infty. \qquad (5.57)$$

When the first condition is observed the voltage across C_2 increases nearly monotonically to h=1 (the horn at the top is less than 4 percent). No effort should be made to achieve a complete monotonicalness of h(t) since this leads to an increase of R_{d1} and a decrease of the pulse amplitude at the output. In this case the voltage h(t) depends only on the parameter B since

$$b = \sqrt{2B}; \quad d = 1 + \sqrt{\frac{2}{B}}; \quad \beta_1 = \frac{1+\sqrt{2B}}{2B}; \quad h_c(t_3) = 1;$$
$$A = 0; \quad \omega_1 = \frac{\sqrt{2B + 2\sqrt{2B} - 1}}{2B}; \quad \operatorname{tg}\varphi = \sqrt{2B + 2\sqrt{2B}}. \qquad (5.57')$$

The characteristic h(t) is shown in Figure 5.17b.

The parameter B may be limited below by a permissible quantity $\frac{1}{d}$ which is a steady-state value of the pulse voltage $h(\infty)$. In doing so,

$$B = \frac{2h^2(\infty)}{[1 - h(\infty)]^2}. \qquad (5.58)$$

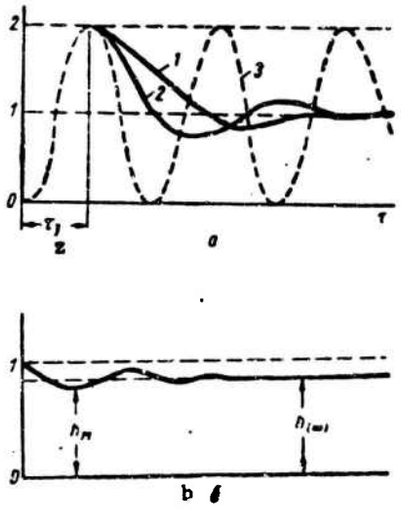

Figure 5.17. The shape of the voltage on the elements of GIN under different conditions:

a — $R_{d1}=0$; $t_z=\frac{\pi}{\omega}$; 1 — voltage across R_n in aperiodic process; 2 — voltage across R_n in oscillatory process; 3 — voltage across C_2 without the closing of K_2; b — $R_{d1}=\sqrt{2\frac{L_1}{C_2}}$; $\tau_z=\infty$.

To obtain a pulse approaching in shape a rectangular pulse the value of $h(\infty)$ must approach unity. For example, when $h(\infty)\geqslant 0.9$, the parameter $B\geqslant 162$. In order to have a complete notion of the characteristic $h(\tau)$ it is also necessary to know the value of Δ_0. For this purpose we will determine the smallest value of τ_m from the equation $\frac{dh(\tau)}{d\tau}=0$ and substitute this value into the equation (5.55). With the large values of B which are obtained from the equalities (5.57), h_m will be determined from the following simple relationship

$$h_m=h(\infty)\left(1-\frac{e^{-\frac{3\pi}{4}}}{\sqrt{B}}\right). \qquad (5.59)$$

where e is the base of a natural logarithm. With the values of B indicated the second term of this expression is much smaller than 1. Therefore, it may be neglected and then $h_m\approx h(\infty)$, i.e. the voltage at the top of the pulse decreases nearly monotonically from 1 to $h(\infty)$.

3. $3.\ t_3 = \infty,\ R_{d_1} \ll R_{кр} = 2\sqrt{\frac{L_1}{C_2}}.$ (5.60)

Processes taking place in the circuit in this case are similar to those in a single-stage GIN with compensation, which was examined in Par. 1.3. If C_2 is selected from the equation (3.8), then the shape of the pulse will approach rectangular shape and the amplitude will be equal to nU_0. In practice this case may be realized if the breakdown of the last discharger (the commutator K_2) is delayed for a time equal to 1 when the oscillations in the circuit will be damped. The aggregate resistance of the first circuit and the dischargers contained in it may serve as the R_{d_1}. In all of the three cases the duration and the steepness of the leading edge are determined by formulas (2.46) and (2.56).

Using the compensation method a GIN was built for obtaining pulses with an amplitude of 150 kv. The generator consisted of five stages with two-way charging with a voltage of 15 kv. Each stage consisted of two series-connected capacitors KBGP with a voltage of 15 kv. The parameters of the GIN were as follows: R_n=1,500 ohms; $L_1=2.7 \cdot 10^{-6}$ henries; $L_2=0.39 \cdot 10^{-6}$ henries; C_2=250 picofarads; C_p=4 picofarads; C_1=1,500 picofarads; R_{d_1}=100 ohms. A coaxial cylindrical capacitor filled with transformer oil (see Figure 5.16c) was used as the capacitor C_2. Copper pipes served as the capacitor plates: an outer pipe — grounded, an inner pipe — insulated. A glass tube with an aqueous solution of NaCL which was the load resistance R_n was built-in coaxially with the inner pipe. A discharger P_0 was built-in between the ungrounded end of the R_n and the inner plate of the capacitor. Such a design of the capacitor C_2 substantially decreased the value of L_2. The duration of the leading edge of the pulse obtained in this generator was 5 nanosec. Without the use of the compensating capacitor t_f was equal to 55 nanosec. Thus, the use of capacitive compensation of the inductance of the discharge circuit made it possible to decrease the duration of the leading edge by one order. In addition to this, it is important that t_f depends only on the processes in the circuit R_n, C_2, P_2 and, therefore, in order to obtain a pulse with a steep leading edge any laboratory GIN may be used regardless of the value of inductance in the discharge circuit.

Arkad'yev-Marks multiplying circuit has many spark dischargers. This has a bad effect on the stability of the parameters of the pulse and complicates the fabrication of the circuit and its handling. The voltage multiplying circuit with cable lines suggested by Lewis [121] has advantages in this respect. Several identical coaxial cables (in the general case n cables) are parallel-connected at the input and series-connected at the output (Figure 5.18a). If a pulse with an amplitude E is sent to the input of the cables, then an increase of the voltage by n times may be obtained across the resistance R_n=nZ with the impedance of the points on the sheathing of the load leads relative to the ground being $Z_S=\infty$. Actually the impedance $Z_S<\infty$. Therefore, it affects the value and shape of the voltage at the output of the

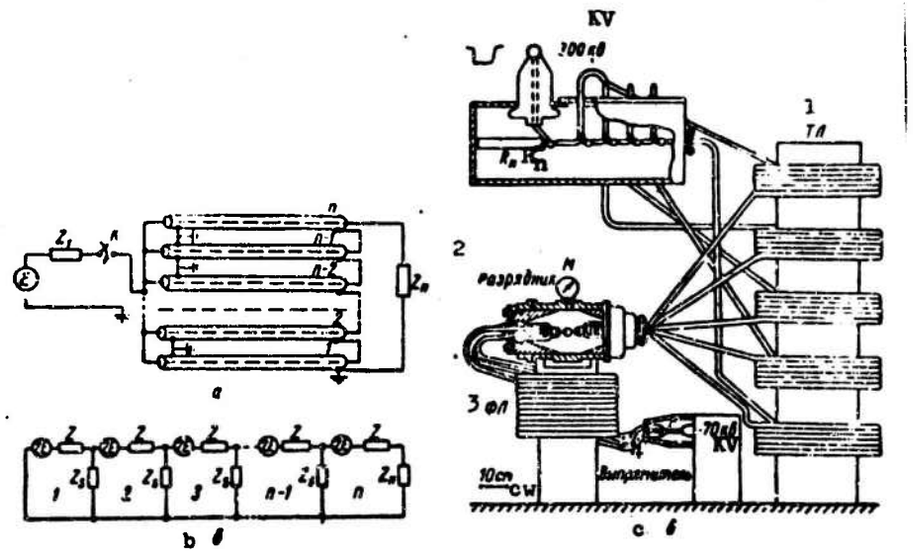

Figure 5.18. Simplified circuit diagram of a device with lengths of cables for multiplying the pulse voltage (a); substitution network of the device for time (b) and wiring diagram (c).

Key: (1) TL=transforming line; (2) Discharger; (3) FL=shaping line; (4) Rectifier.

device, as this follows from the substitution network in Figure 5.18b. The matching of the device may also be achieved with the condition $Z_1 = \frac{Z}{n}$, $R_n = \infty$. The length of the cable should exceed the length of the pulse. The impedance Z_S depends on the arrangement of the cable sheathing. To increase the Z_S the cable has to be twisted into a coil or wound on an insulating rod and inserted in a shielded housing. In the latter case the Z_S will be equal to the input impedance of a spiral coaxial line with the cable sheathing as the inner conductor.

With the aid of a network with n cables it is possible to obtain a multiplication of the voltage by 2n times if the condition $Z_1 = 0$, $R_n \gg nZ$ is satisfied. However, in this case the primary pulse will be accompanied by additional pulses brought about by multiple reflection of the pulse from the beginning and end of the cable. To eliminate these reflections the load may be shunted by a discharger which closes at the necessary instant of time.

An analysis of a ladder network of n active L-shaped two-terminal pair networks (see Figure 5.18b) shows that the voltage at the output of such a device [1]

$$U_{\substack{max \\ out}} = \frac{2E\frac{R_n}{Z}(1-\lambda^{2n})}{(1-\lambda)\left[\left(1+\frac{R_n}{Z}\right)(1+\lambda^{2n-1})+\frac{Z_S}{Z}(1-\lambda)(1-\lambda^{2n-2})\right]}. \qquad (5.61)$$

where

$$\lambda = 1+\frac{Z}{2Z_S}+\sqrt{\frac{Z}{Z_S}\left(1+\frac{Z}{4Z_S}\right)}. \qquad (5.61')$$

It follows from the expression (5.61) that with an infinite number of cables and a matched load $R_n = nZ$ the voltage

$$U_{max}^{out} = \frac{2E\lambda}{\lambda-1}. \qquad (5.62)$$

Consequently, the voltage at the output of the transformer will be determined by the ratio $\frac{Z_S}{Z}$ and not by the number of cables. For example, when $\frac{Z_S}{Z}=10$ the voltage U_{out} will amount only to 7.5 E. Consequently, with a specified $\frac{Z_S}{Z}$ it is always necessary to search for a certain optimum number of cables n with which U_{out} approaches the maximum (5.62) and their number is within reasonable limits. With an open end of the multiplier the voltage at the

1) It should be noted that the formula obtained by Lewis [121] for U_{out} is incorrect. This may be ascertained upon substituting $Z_S = \infty$.

output has the following form

$$U_{max} = \frac{2E(\lambda^{2n}-1)}{(\lambda-1)(1+\lambda^{2n-1})}. \qquad (5.63)$$

It is easy to show that with a very large number of cables n formula (5.63) will change into the equality (5.62).

The expression (5.61) was obtained without any preliminary conditions relative to the character of Z, Z_g and R_n. In the general case Z_g and R_n may be of the operator form. Therefore, formula (5.61) may be used to take account of the effect of reactances on the pulse shape. When rolling the cables into a coil it is necessary to consider that $Z_g = \frac{1}{Cp}$, where C is the capacitance of the coil relative to the ground, to analyze the leading edge of the pulse. In analyzing the top of the pulse it is necessary to consider that $Z_g = Lp$ where L is the inductance of the coil. In addition to this, the magnitude of the leading edge of the pulse will be affected by the inductance of the connections of the cables at the end, and also by the capacitance and inductance of the load. A. I. Pavlovskiy and O. V. Sklizkov [122] developed a device for obtaining high-voltage pulses with five sections of the cable RK-106 (see Figure 5.18c). The primary pulse is shaped by means of cable sections with a length of 25 meters (FL) connected in parallel. A length of the transforming line (TL) no smaller than the length of the pulse is selected. To increase the Z_g the line sections are wound into coils on an insulating pipe. A discharger of coaxial design operating under a pressure of several atmospheres was used as the commutator.

The authors state that with a charging voltage of 70 kv a pulse with an amplitude of 160 kv, a current of 600 amperes and a duration of 0.25 microsecond was obtained in such a generator using a matched load. A pulse with an amplitude of 300 kv and duration of the leading edge of 50 nanoseconds was obtained with a load resistance R_n=2 kilohms.

Par. 5.9. Obtaining Short Pulses in Networks With Nonlinear Inductance

In some of the ferromagnetic materials the curve describing the relationship of magnetic inductivity μ to the current i flowing through the coil has a clearly marked maximum (Figure 5.19a) with a certain current i_m. With the currents $i > i_m$ and $i < i_m$ the value of μ is several orders smaller than with $i = i_m$.

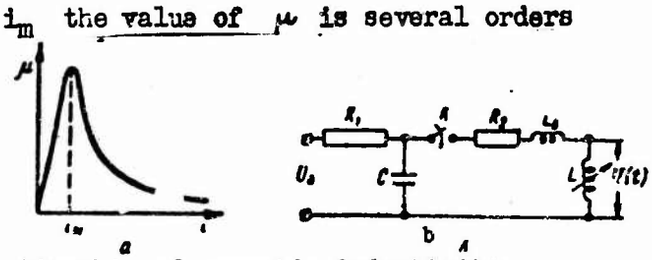

Figure 5.19. Relationship of magnetic inductivity to the current (a) and simplified circuit diagram for obtaining pulses (b).

Kult [8] suggested the use of this property to obtain high-voltage pike-shaped short pulses. He used a coil with a ferrite core. If such a coil is inserted into a circuit with a quick changing of current, then conditions are created for obtaining a short voltage pulse on the coil With an increase of the current the inductance of the coil L reaches its maximum value L_m at a certain instant of time t_m which corresponds to the current i_m. In doing so, L increases considerably faster than the current passing through the coil. This brings about a steep leading edge of the pulse. If the current increases further at the same rate, then the inductance decreases approximately in the same time to its minimum value L_0.

The voltage on the inductance is equal to

$$U_L = L(t) \frac{di}{dt}.$$

Consequently, to obtain a large pulse amplitude it is necessary to have a high degree of the steepness of the current $\frac{di}{dt}$ in the circuit. To satisfy this condition it is necessary to use a commutator with a short time t_k. For example, Kult used a high-voltage hydrogen thyratron. S. I. Andreyev, M. P. Vanyukov and V. A. Serebryakov [123] showed that an effect similar to that described may be obtained if a heavy-gage conductor with ferrite rings put on it is used. In doing so, the voltage pulse is taken off from the ends of the conductor. A circuit arrangement for obtaining short pulses by means of a coil of ferromagnetic material and a device with ferrite is shown in Figure 5.19b.

If the resistance R_2 is lower than the critical resistance R_{cr} corresponding to the values of the capacitance and inductance of the circuit, then one positive and one negative voltage pulse on the inductance L will correspond to each half-period of the current. The decrease of the amplitude of the pulse train forming in this process is determined by the parameters R_2, L and C of the circuit and by the voltage at the input U_0. When $R_2 > R_{cr}$ it is possible to obtain a single pulse if the steepness of the current on the rise is much greater than on the droop. The last is achieved by selecting the value of the resistance R_2.

An experimental investigation of the effect of the type of ferrite and of the parameters C, L_0 and R_2 of the discharge circuit on the amplitude and duration of pulses was carried out in the work [123]. A spark discharger was used as the commutator. A brass conductor on which ferrite rings were placed had a length of 40 mm and a diameter of 20 mm. Nickel-zinc ferrites (F-600, F-1000, F-2000), magnesium-zinc ferrites (MT-2000) and ferrites with a rectangular loop (K-27, K-65) were investigated. The pulses obtained in a network with ferrites of the first and third type differ little from each other. When using the ferrites of the brand MT-2000 a substantial difference of the pulse parameters in comparison with the other parameters was observed. The

amplitude of the pulses increases with the increase of the charging voltage U_0. In doing so, the duration of the pulses decreases. For the ferrites F-2000 and MT-2000 (with C=3,300 picofarads, L=0.1 microhenry) the amplitude of a single pulse (R_2=20 ohms) is considerably smaller than that of the pulse with the largest amplitude in the train (R_2=0).

The value of the capacitance C has little effect on the duration and amplitude of the pulses. However, by varying the value of C it is possible to control the frequency and the attenuation rate of the amplitude of the pulses in a train. An increase of the inductance L in the circuit leads to a decrease of the amplitude and increase of the duration of the pulses. An increase of the resistance R_2 from 20 to 160 ohms has practically no effect on the duration of a pulse and its amplitude.

It is necessary to bear in mind that the pulse parameters cannot be determined with the aid of static characteristics of the ferrites. For this purpose it is necessary to take into account the relaxation processes connected with the magnetic polarity reversal of the ferrites in a time of approximately 10^{-9} sec.

Pike-shaped pulses with an amplitude of up to 10 kv and a duration $t_i \approx 5 \cdot 10^{-9}$ sec were obtained in the works [8, 12] by means of a coil with a ferromagnetic core and a device with ferrite. In doing so, it proved to be possible to transform these pulses by means of a transformer with a ferromagnetic core [8]. The primary and secondary winding of this transformer was wound on the core in the form of a ring. The amplitude of the transformed pulse amounted to 30 kv and duration increased to 10^{-7} sec.

CHAPTER 6. MEASUREMENT OF PARAMETERS OF HIGH-VOLTAGE NANOSECOND PULSES

Introduction

Electronic oscillograph EO is the most suitable instrument making it possible to measure parameters of short pulses with acceptable accuracy. The voltage delivered to the plates of the event PYa of the electronic oscillograph is usually equal to 1-3 kv. Therefore, to measure pulses with a large amplitude a voltage divider DN is necessary which produces at the output a pulse with a lower amplitude. In Figure 6.1 is shown electric circuit of an apparatus for measuring the high-voltage pulses. The connecting wires be-

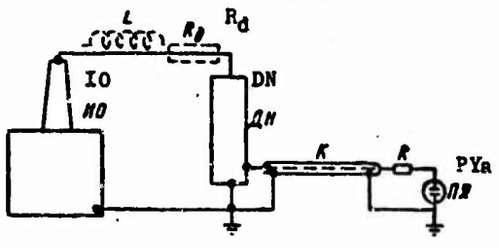

Figure 6.1. Simplified circuit diagram for measuring the pulse voltage:

IO -- the object being tested; DN -- voltage divider; K -- coupling cable; PYa -- the plates of the event; R and R_d -- damping resistances; L -- inductance of the connecting wires.

tween DN and IO create on DN a voltage different from the voltage on IO. The voltage at the output of DN differs in shape from the voltage acting on the DN owing to the influence of the spurious parameters of the DN. Attenuation of the wave in the cable connecting the DN and PYa leads to a smoothing of the leading edge and a decrease of the amplitude of the pulse propagating over the cable. With the effect of the capacitance of the PYa and inductance of the connecting wires the voltage appearing on the PYa differs from the voltage

at the output of the cable. All elements of the high-voltage measuring circuit must be selected in such a manner that the aggregate distortion of the pulse being investigated be within permissible limits.

Par. 6.1. Analysis of Errors Appearing During the Measurement of High-Voltage Pulses

The object of the analysis consists in determining the errors introduced by each element of the network (Figure 6.1) and by the entire network as a whole. Each element of the network may be represented as a two-terminal pair network the analysis of the transient process in which is carried out by the single-function method or by using the harmonic analysis.

1. Single-Function Method

The function h(t) — an expression of the signal at the output of the circuit upon the action of a single function on its input — is called the transfer characteristic of the circuit. Upon the action of the voltage U(t) on the input of the circuit the output signal is equal to the following if Duhamel integral is applied

$$S(t)=\int_0^t h(t)\,U'(t)\,dt, \tag{6.1}$$

where U'(t) is the time derivative.

Pulses used in nanosecond technique approach in shape the triangular or trapezoidal pulses. Thus, the functions with which we are most concerned are $U(t)=U_0$ and $U(t)=at$.

For a triangular pulse $U(t)=at$, $a=\frac{U_a}{t_f}$ where U_a is the maximum value of the voltage; t_f is the length of the leading edge $S(t)=a\int_0^t h(t)dt$. The maximum value of the signal $S_m=a\int_0^{t_f} h(t)dt$. The relative error in the measurement of the amplitude is equal to

$$\delta U=\frac{U(t=t_\phi)-S(t=t_\phi)}{U(t=t_\phi)}=\frac{a\int_0^{t_\phi}[1-h(t)]\,dt}{U_a}; \tag{6.2}$$

[ϕ=f]

δU will be positive if h(t) is a monotonic or weakly oscillatory function.

For a trapezoidal pulse, with $t \geqslant t_f$

$$U(t)=at-a(t-t_f)$$

and

$$S(t)=a\int_0^t h(t)\,dt-a\int_0^{t-t_\phi} h(t)\,dt=\int_{t-t_\phi}^{t_\phi} h(t)\,dt. \qquad (6.3)$$

If the pulse has an exponential form, then $U(t)=U_0(1-e^{-at})$

$$S(t)=U_0 a\int_0^t h(t)e^{-at}\,dt. \qquad (6.4)$$

After determining the S(t) it is possible to evaluate the distortion (lengthening) of the leading edge of the pulse.

Application of Harmonic Analysis

Every function may be expanded into a harmonic series

$$U(t)=A_1\sin(\omega t-\varphi_1)+A_2\sin(2\omega t-\varphi_2)+\ldots+ \\ +A_n\sin(n\omega t-\varphi_n). \qquad (6.4')$$

The signal at the output of a two-terminal pair network

$$S(j\omega)=A(\omega)F(j\omega), \qquad (6.5)$$

where $A(\omega)$ is a separate sinusoidal component; $F(j\omega)$ is a composite function ω called the transfer function and determined when the output of the two-terminal pair network is open. $F(j\omega)$ consists of two factors: real and imaginary. The former indicates the "transfer" of the amplitude, i.e. its change by the two-terminal pair network, the latter indicates the "transfer" of the phase. The expression for S(t) may be obtained after determining $S(j\omega)$ with respect to all components. However, as a rule the pulse voltages encountered in practice have a continuous harmonic spectrum, i.e. the number of harmonics approaches infinity, and the amplitudes of the harmonics become infinitely small. In doing so, the function U(t) and its spectrum $\varphi(j\omega)$ are connected by two Fourier transforms:

$$\varphi(j\omega)=\int_{-\infty}^{\infty} U(t)e^{-j\omega t}\,dt \qquad (6.5')$$

and

$$U(t)=\frac{1}{2\pi}\int_{-\infty}^{\infty}\varphi(j\omega)e^{j\omega t}\,d\omega. \qquad (6.5'')$$

In this case the operations are carried out not with a single harmonic but with a unit band of the spectrum. The expressions for S(t) resulting when using the harmonic analysis do not lend themselves to analytical solution and, therefore, the use of graphic methods is necessary, i.e. chiefly the single-function method is used. However, the effect of the circuit on the leading edge of the pulse determining the harmonic component with the greatest fre-

quency f_m is of interest. The connection between f_m and duration of the leading edge t_f is determined by the relationship (5.1). A more complete presentation of the analysis of distortions is given in the works [67, 124, 125].

If the transfer characteristic of the circuit h(t) has a monotonic character, then the lengthening of the leading edge of the pulse at the output of the circuit may be determined by making use of the principle of quadratic summing of the leading edges [74]

$$t_{\phi_1} = \sqrt{t^2_{\phi_1} + t^2_{o\phi_1}} \qquad (6.6)$$

where t_{f_1} and t_{f_2} are the duration of the leading edge of the pulse at the input and output of the circuit respectively; t_{of} is the duration of the leading edge at the output of the circuit during the action of the single function upon its input. The value of t_{of} may be determined by formula (2.5).

If n two-terminal pair networks are series-connected so that none of them affects the transfer of the pulse by the preceding two-terminal pair network, then

$$t_{\phi_1} = \sqrt{t^2_{\phi_1} + \sum_{k=1}^{n} t^2_{o\phi k}}. \qquad (6.7)$$

For the circuit shown in Figure 6.1 it may be considered that the impedance inserted at the output of the DN does not affect the transmission of the pulse of the DN and impedance inserted at the PYa does not affect the voltage at the output of the DN. The last is true if there are no reflections in the cable. In this case the duration of the leading edge of the pulse at the PYa

$$t_{\phi_1} = \sqrt{t^2_{\phi_1} + t^2_{1\phi} + t^2_{1\phi} + t^2_{2\phi}}, \qquad (6.8)$$

where t_{f_1} is the duration of the leading edge of the pulse on the IO; t_{1f} is the duration of the leading edge of the pulse appearing at the high-voltage lead-out of the DN and brought about by the impedance Z and by the lumped characteristics of the DN; t_{2f} is the duration of the leading edge of the pulse at the output of the DN; t_{3f} is the duration of the leading edge of the pulse on the PYa; t_{1f}, t_{2f} and t_{3f} are determined during the action of the single functiion on the input of the respective circuit. If necessary, the smoothing-out of the leading edge owing to the attenuation in the cable should be taken into account.

Suppose t_f exceeds t_{f_1} by k%. Then we find the following from the equation (6.8)

$$\sqrt{t^2_{1\phi} + t^2_{2\phi} + t^2_{3\phi}} = t_{\phi_1}\sqrt{\frac{2k}{100} + \left(\frac{k}{100}\right)^2} \approx t_{\phi_1}\sqrt{\frac{k}{50}}. \qquad (6.9)$$

In the case when the leading edge of the pulse at the output of the circuit is expressed by the exponential ($U=1-e^{-\frac{t}{T}}$) the length of the leading edge of the pulse defined by the points 0.1 and 0.9 is equal to 2.2T. In an oscillatory process an optimum case is considered that when the horn above the flat portion is equal to 4%. In this case the length of the leading edge defined by the points 0.1 and 0.9 is equal to $\frac{0.35}{f_0}$ where $f_0=\frac{1}{2\pi\sqrt{LC}}$ is the frequency of the natural oscillations of the circuit. The left term is determined by the expression (6.9) and the maximum permissible values for t_{1f}, t_{2f} and t_{3f} and the respective values of T or f_0 may be specified.

Par. 6.2. Voltage Dividers for High-Voltage Pulses of Nanosecond Duration

Many original and survey works [22, 67, 125-127] have been devoted to the development of voltage dividers producing small distortions and to the analysis of errors caused by them. We will endeavor to note the main features of the voltage dividers which may be used for the nanosecond range.

Active DN (made up of resistances), capacitive DN, and also DN utilizing certain features of wave propagation in a cable are used to measure the high-voltage nanosecond pulses. Each voltage divider consists of a high-voltage arm which takes up the greater portion of the voltage U_1 of a high-voltage pulse, and a low-voltage arm from which the divided voltage U_2 is taken off for the measuring instrument. The ratio $k=\frac{U_1}{U_2}$ is called the scaling factor and usually for the high-voltage voltage dividiers $k\gg1$. Therefore, the impedance of the low-voltage arm does not produce appreciable effect on the distribution of voltage on the DN, which had been created by the high-voltage arm. The elements of the high-voltage arm may have a longitudinal capacitance, capacitance relative to the ground and self-inductance. These spurious parameters explain in the main the errors introduced by a voltage divider.

In active DN the measurement errors are connected with the existence of self-inductance and capacitance relative to the ground C_z. Upon the action of a pulse with a perpendicular leading edge and a flat top on the voltage divider the voltage in the low-voltage arm is expressed by a composite relationship which in an aperiodic mode may be approximated by an exponential from the condition of the equality of the error, i.e.

$$[U_H=U_n;\ U_B=U_V] \qquad U_n=\frac{U_0}{k}\left(1-e^{-\frac{t}{T}}\right). \qquad (6.10)$$

where U_n is the voltage in the low-voltage arm; U_v is the voltage in the voltage divider. According to the data given in the work [124] the time constant T may be expressed as follows

$$[C_3 = C_z] \qquad T = \frac{L}{R} + \frac{RC_z}{6}. \qquad (6.11)$$

where R is the resistance of the voltage divider. The value of T may be reduced by means of decreasing the L and C_z. With the specified values of L and C_z the optimum resistance of DN $R_0 = \sqrt{6\frac{L}{C_z}}$.

The capacitance C_z is determined by the dimensions of the voltage divider and by its distance from the ground. Thus, the capacitance of a vertical cylinder with a length l and radius r, the lower end of which is removed to a distance "a" from the ground is defined in the following manner according to [126]:

$$C_z = 1{,}11\,\frac{l}{2\ln\frac{l}{r} - \ln\frac{3l-4a}{l+4a}} \qquad (6.12)$$

(linear dimensions are given in centimeters).

The length of the divider l is determined by the voltage U_v and by the permissible longitudinal gradient E_d which for the pulses of microsecond duration is equal to 3-5 kv/cm in the air and 15 kv/cm in the transformer oil. For the pulses of nanosecond duration E_d may be considerably increased but as yet there are no respective data for E_d.

Distortions caused by C_z may be decreased by using various methods of shielding the DN. With this aim, a shield usually in the form of a ring placed somewhat lower than the top of the DN is connected to the high-voltage end of the voltage divider. To avoid the appearance of oscillations brought about by the capacitance of the shield relative to the ground and by the inductance of the device the shield is connected with the high-voltage end of the DN through a resistance of appropriate value. In some of the DN placed in oil the high-voltage shield electrode made in the form of a solid of revolution covers a considerable portion of the DN.

In voltage dividers described in the works [128, 129] there were several (two or three) concentric columns with a resistance. In this case the outer columns were a shield and improved the distribution of voltage over the inner column which was the divider proper.

High-resistance alloys (constantan, nichrome, etc.) are usually used as the material of the voltage-divider resistance. Resistances made of aqueous electrolytes having low self-inductance and high thermal capacity are not used owing to their instability with time and temperature dependence. High-

resistance alloys are used in the form of wire, buses or thin strips. Non-inductive winding is used to decrease the inductance of the resistance. Carbon resistances are sometimes used. The existence of connecting wires between the IO and DN may cause undesirable oscillations brought about by the inductance of the connecting wires and by the capacitance of DN relative the ground. This also applies to the capacitive DN. To damp the oscillations a resistance of appropriate value should be inserted before the voltage divider. This leads to the smoothing-out of the leading edge of the pulse being investigated. Therefore, the connecting wires should be as short as possible.

In the work [13] is described an active voltage divider for a 1,400-kv installation, having a resistance of the high-voltage arm of 1,000 ohms and a resistance of the low-voltage arm of 1 ohm. The high-voltage arm is made up of ten identical elements of 100 ohms each. The length of the high-voltage arm is somewhat longer than 127 cm. Each element represented a polystyrene rod with a diameter of 1.27 cm and a length of 12.7 cm on which two insulated strips measuring 0.81 x 0.025 mm were wound in opposite directions. The strips were made of an alloy of nickel, chrome, aluminum and iron having a high resistivity and a small temperature coefficient. The low-voltage arm consists of four zigzag-shaped loops made up of 1.6 x 0.025-mm strips of the same high-resistance alloy. During the investigation of the breakdown of a spherical discharger the leading edge of the pulse with the shortest duration before the breakdown of 27 nanoseconds and a rapid fall-off during the breakdown was transmitted without distortion.

In the work [12] is described an active voltage divider for $2 \cdot 10^6$ volts; it has a center pipe with a height h=2 meters on which a high-resistance wire with a total resistance of 22.5 kilohms is wound. To improve the distribution of the voltage over the length of the DN, shielding was used consisting of two disks with a diameter D=0.4 and a height h=80 cm and four tori placed every 0.2 h over the length of the divider and not connected with the resistances of the voltage divider. The distribution of the field between the shielding electrodes, determined by means of an electrolytic bath approaches a uniform distribution. This contributes to the equalization of the field over the column with the high-resistance wire.

Upon sending a rectangular pulse to the input of the voltage divider an oscillatory voltage appeared at its output owing to the capacitance between the shielding electrodes and the inductance coupled with it. By adding a resistance in series with the upper shield the oscillations were damped and the pulse at the output of the voltage divider had a leading edge of 70 nanoseconds in length. It was possible to reduce the length of the leading edge to 30 nanoseconds by adding into the low-voltage arm a small inductance consisting of several turns of copper wire. Taking into account the high resistance of the voltage divider its characteristics should be considered good. Probably the phase error could have been reduced to a few nanoseconds by decreasing the resistance of such a divider [12].

If the pulse moves over a cable, then it is expedient to use a voltage

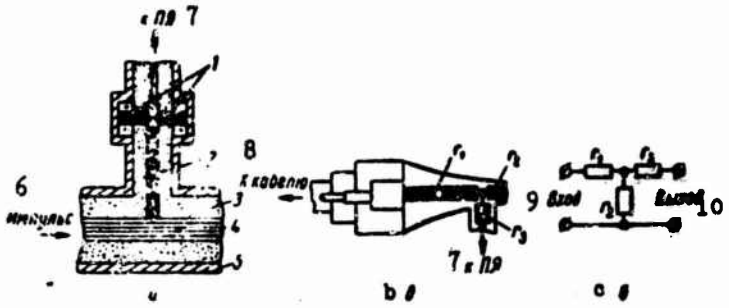

Figure 6.2. Active voltage divider built-in into a cable (a); load resistance NS-1 (b) and diagram of the connection of resistances in NS-1 (c):

1 — resistance of the low-voltage arm; 2 — resistance of the high-voltage arm; 3 — cable insulation; 4 — conductor; 5 — sheathing; 6 — pulse; 7 — to the PYa; 8 — to the cable; 9 — input; 10 — output.

divider with a closed wiring, built-in into the cable. Dividers of this type are shown in Figure 6.2. In Figure 6.2a is shown an active voltage divider designed by Fletcher [27] for recording pulses with an amplitude of 20 kv. The high-voltage arm consists of three series-connected resistances of 330 ohms each; the low-voltage arm consists of two parallel-connected resistances of 20 ohms each. The limiting factor is the capacitance of the high-voltage arm relative to the ground. In this case, a pulse with a length of the leading edge of 5 nanoseconds was recorded with a 10-percent error. A certain limitation is also imposed by the heating of the resistance of the voltage divider owing to the dissipation of a portion of the pulse energy. As a result of this the value of the resistance decreases and the scaling factor changes.

In Figure 6.2b is shown the arrangement and diagram of connections of the load resistance of the type NS-1 which is at the same time also a DN for pulses with an amplitude on the order of kilovolts. Resistances of the type UNU which represent a thin layer of carbon applied on a ceramic rod (see Par. 5.3) are used as the resistances r_1, r_2 and r_3 ($r_1=r_2=58$ ohms, $r_3=17$ ohms). The divider is adapted for connection to a cable with a wave impedance of 75 ohms and is enclosed in a shield the calculation of which is described in Par. 5.3.

In capacitive voltage dividers the main factor causing the distortion is self-inductance. Therefore, the length of the high-voltage arm of the divider should be short. Capacitive dividers which are used or can be used for measuring the high-voltage nanosecond pulses are shown in Figure 6.3.

For a voltage divider shown in Figure 6.3a the high-voltage arm is formed by the high-voltage electrode and receiving electrode connected to

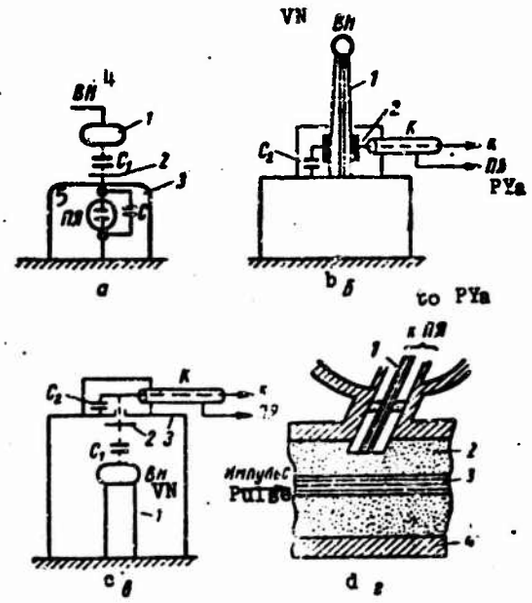

Figure 6.3. Capacitive voltage dividers: (a) 1 — high-voltage electrode; 2 — receiving electrode; 3 — shield; 4 — VN=high voltage; 5 — PYa=plate of the event; C — capacitance for adjusting the scaling factor; (b) 1 — partition insulator; 2 — capacitive ring; K — cable; (c) 1 — high-voltage source; 2 — receiving electrode; 3 — shield; (d) 1 — wire and PYa; 2 — cable insulation; 3 — conductor; 4 — sheathing.

one plate of the event, and the low-voltage arm is formed by the capacitance of the plate of the event. The scaling factor can be controlled by connecting to the plate of the event additional capacitances. Capacitors with air or mica insulation in which the dielectric constant at the pulsed and constant voltage is the same or nearly the same may be used as the additional capacitances. It is necessary that the high-voltage electrode and the receiving electrode have no corona discharge.

A capacitive voltage divider may be placed on the insulation lead-out of the object being tested, as shown in Figure 6.3b. The high-voltage arm is formed by the capacitance of the rod inside the insulator and by an additional ring placed on the outer surface of the insulator; C_2 is the capacitance connected additionally. It is impossible to place the PYa close to such a divider. Therefore, a coupling cable is necessary.

The voltage in the low-voltage arm

$$U_н = U_0 \frac{C_1}{C_1 + C_2} e^{-\frac{t}{T}}. \qquad (6.13)$$

where $T=Z(C_1 + C_2)$. If a permissible drop of k% on the flat portion of the pulse is assumed, then the necessary value of C_2 with the condition that $\frac{k}{100} \ll 1$ is defined as follows:

$$C_2 \approx \frac{100\tau}{kZ} - C_1 \approx \frac{100\tau}{kZ}. \qquad (6.14)$$

If the source of high voltage and IO are in the same tank (for example, the high-voltage source and the accelerating tube), then a voltage divider shown in Figure 6.3c may be used. In order that the receiving electrode do not disturb the uniformity of the field, it should not be moved out far from the metal wall of the tank. The scaling factor can be regulated both by the value of C_2 and by the size of the receiving electrode.

In Figure 6.3d is shown a capacitive voltage divider fitted on a cable [27], for recording pulses of 20 kv. The conductor touching the cable insulation and running to the PYa of the microoscillograph formed with the cable conductor a capacitance of 0.01 picofarad. The capacitance of the PYa is 1 picofarad so that k=100. The voltage divider had a frequency of natural oscillations of 3,800 Mc and recorded a pulse with a length of the leading edge $t_ф = \frac{10}{\pi f_0} = 0.8$ nanosecond. The voltage divider described in the work [131] is based on this principle.

In Figure 6.4 are shown voltage dividers for recording 20-kv pulses. These voltage dividers make use of the characteristics of wave propagation in a line [27].

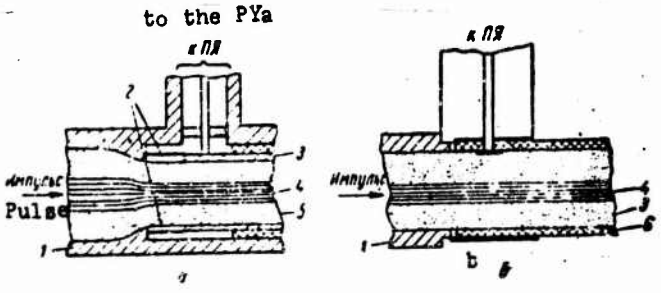

Figure 6.4. Diagrams of an active cable (a) and a cable (b) voltage divider:

1 — sheathing; 2 — insulation cylinder with a layer of metal; 3 — ungrounded cable sheathing; 4 — conductor; 5 — cable insulation; 6 — tube made of Ti_2O.

In Figure 6.4a is shown a diagram of a voltage divider of an active cable type [27]. On the cable section occupied by the DN and further beyond it following the course of the pulse motion the outer sheathing of the cable

was not grounded but was connected to the ground through a resistance of 0.5 ohm. With a wave impedance of the cable of 50 ohms the scaling factor of the divider is equal to 100. The resistance of 0.5 ohm consisted of a thin layer of gold-platinum alloy applied on the outer surface of a glass cylinder with a length of 1 cm and a diameter of 1 cm. An oscillogram obtained with the aid of this divider had a horn on the top with a following nearly linear droop. The resistance of the low-voltage arm proved to be unstable owing to an overheating with the flowing current. As a result of this, the resistance first decreased owing to a redistribution of the atoms and then increased owing to the evaporation of the metal. This was observed by an increase in the transparency of the layer. When the thickness of the layer and its length were increased twofold to increase the thermal stability of this resistance, then the oscillogram showed an increase in the width of the horn. This confirmed the supposition that the horn on the top of the pulse was caused by the inductance of the resistance of the low-voltage arm. This inductance limited the shortest length of the leading edge of the pulse being recorded to 25 nanosecond with an error of 10 percent. As the author of [27] points out, the measurement error can be considerably reduced if a semiconductor of very small length is used as the resistance of the low-voltage arm.

In Figure 6.4b is shown a diagram of a voltage divider consisting of two coaxial lines [27]. The inner line represented a usual cable with polyethylene insulation and wave impedance of 50 ohms; the outer line represented a tube made of rutile with silver electrodes on the outer and inner surface, with a wave impedance of 0.5 ohm. Transients distorting the pulse take place in such a system when the insulation of the lines has considerably differing dielectric constants. However, when a cable running to the PYa and to the outer line near its beginning was used the error should not exceed 10 percent when recording a pulse being investigated having a length of the leading edge of $4 \cdot 10^{-10}$ sec.

When using a DN it is necessary to know the range of the frequencies or of the steepness of the leading edges within which it can function with a small error. This is achieved by testing the DN with a pulse having a very steep leading edge or a high-frequency voltage.

In the work [124] it is pointed out that to test the divider a pulse generator was used which generated pulses with an amplitude of 150 volts, a duration of 0.5 micrsecond and a length of the leading edge of 1 nanosecond. An amplifier from the output of which the voltage was sent to an electronic oscillograph was connected to the output of the divider. An amplifier with a wide frequency passband is necessary for such tests. A comparison of the shapes of the pulses sent to the divider and taken off from the output of the amplifier made it possible to determine the error introduced by the divider.

In testing with a high-frequency voltage a wide-band amplifier with

a measuring device at the output [124] was also connected to the output of the divider. The scaling factor was measured at different frequencies of the acting voltage; usually in a certain frequency range the value of k remains constant and then increases with the increase of f. The connection between the upper permissible frequency f_m and the shortest duration of the leading edge t_f was determined by the expression (5.1).

Par. 6.3. Basic Characteristics of Electronic Oscillograph

The development and perfecting of electronic oscillography contributed to the successful development of many branches of science and engineering and, in particular, the nanosecond technique.

Some of the features of oscillographic recording chiefly of the single pulses of nanosecond duration will be briefly examined in this chapter. This problem is set forth in detail in the books and survey articles [1, 2, 22, 35, 127, 132].

Oscillographs with a cold cathode gained wide use in the 1930's and in the 1940's and later — oscillographs with a hot or heated cathods. These oscillographs were rapidly perfected and gained the widest use. Owing to their dimensions and complexity of handling oscillographs with a cold cathode are used comparatively seldom.

Oscillograph consists of two basic elements: electron-beam tube and electric circuit. Heated cathode emitting the electrons is surrounded by a cylinder called modulator and has a narrow opening for the passage of the electron beam. Next, the electrons reach a strong electric field created by the voltage applied between the cathode and grounded anode and equal to 10 kv and more. After acceleration, with account taken of the relativistic effect the velocity of electron

$$v_x = \sqrt{\frac{2eU}{m_0}} \sqrt{\sqrt{1+\frac{4e^2U^2}{m_0^2c^4}} - \frac{2eU}{m_0c^2}}. \qquad (6.15)$$

The calculated data are given in Table 6.1.

Table 6.1

U, kv	10	15	20	25	30	40	50
v_x, 10^{10} cm/sec	0,587	0,75	0,822	0,916	1,002	1,156	1,278
$\frac{v_x}{c}$	0,196	0,25	0,274	0,305	0,334	0,385	0,426

In an electron-beam tube with electrostatic focusing the accelerating system is combined with the focusing system, i.e. after acceleration the electron beam is focused while with magnetic focusing (microoscillographs, etc.) the electron beam is focused by a magnetic lens after acceleration. Next, the electrons of the beam pass successively between the plates of the event PYa and the time plates PV and undergo appropriate deflection in the transverse vertical and horizontal directions.

For the plane and parallel deflecting plates, electron velocity in the transverse direction acquired at the outlet from the transverse field of the plates is defined as follows:

$$\left[v_n = p;\ U_n = U_p\right] \qquad v_y = \int_t^{t+\tau_n} \frac{e \cdot U_n}{m_0 d}\, dt, \tag{6.16}$$

where U_p is voltage applied to the deflecting plates; d is distance between the plates; τ_p is electron transit time in the field of deflecting plates, called transit factor.

$$\tau_n = \frac{l}{v_x}$$

where $l = l_p + (0.4 \text{ to } 0.5)d$; l_p is the length of the deflecting plates. An increase of l in comparison with l_p takes into account that electric field of the deflecting plates extends beyond their boundaries.

For a deflecting voltage changing insignificantly in the time τ_p we find

$$v_y = \frac{el}{m_0 d} \cdot \frac{U_n}{v_x}. \tag{6.17}$$

If the distance from the deflecting plates to the screen $L \gg l$, the deflection of the beam on the screen of the tube is equal to

$$h = \frac{1}{2} \cdot \frac{lL}{d} \cdot \frac{U_n}{U}. \tag{6.18}$$

The quantity

$$h_0 = \frac{h}{U_n} = \frac{1}{2} \cdot \frac{lL}{Ud} \tag{6.19}$$

is called sensitivity of the deflecting plates and is determined by the geometry of the electron-beam tube and by the accelerating voltage U.

Often sensitivity is defined not in units of length but by the number

of diameters of the spot on the oscillograph screen by which the beam deflected upon the application of a voltage equal to one volt to the deflecting plates.

The second definition of the sensitivity is more essential than the first. To obtain a sharp oscillogram it is necessary that its linear dimensions exceed the diameter of the spot at least by one order. The absolute dimensions of oscillogram are not important inasmuch as an oscillogram can be magnified by optical means to the dimensions required.

After passing the deflecting plates the electrons impinge on the luminescent screen and bring about its luminescence. The brilliance of the luminescence J of the luminophore is determined by the density of the current in the electron beam and by the energy of the electrons, i.e. by the accelerating voltage,

$$[U_H = U_n] \qquad J = A f(j)(U - U_n)^n. \qquad (6.20)$$

where n=1 to 3; f(j) is a function approaching a linear function; A -- some constant; U_n -- initial potential amounting to several tens of volts. The image on the screen must be a contrast image. The contrast of an image may be reduced by the external light reaching the screen, owing to the phenomenon of complete internal reflection in the glass of the screen and owing to a bombardment of the screen by the secondary-emission electrons from the electrodes of the deflecting systems.

An important characteristic of oscillograph is the maximum recording speed v_m at which the image on the photolayer still comes out sharp. In this process the photographic density of the blackening defined as the logarithm of the ratio luminous flux passing through the layer of photographic emulsion before the development to the luminous flux passing through the blackened layer after development must be at least 0.1.

The value of v_m should be determined under the following conditions: magnification of the image M=1, the aperture ratio of the objective 1:F=1, photographic film -- highly sensitive; the developer -- sharp-contrast developer. Usually $M \leqslant 1$ and $1:F \leqslant 1$. The value of the maximum recording speed v'_m is determined in this process. Scaling is accomplished by using the following formula

$$v_m = v'_m F^2 \frac{1 + M^2}{4}. \qquad (6.21)$$

where v_m is measured in cm/sec or diameter of the spot/sec. The last is more essential and characterizes the oscillograph as a whole. An increase of v_m may be easily obtained by means of increasing the accelerating voltage. However, in doing so, the deflection sensitivity decreases as may be seen from the expression (6.18). This is of no material significance for

measuring the high-voltage pulses. A decrease in sensitivity is undesirable when recording weak signals. Therefore, electron-beam tubes with post-acceleration are used in which the electrons of the beam undergo additional acceleration after passing the deflecting plates.

With the use of pulsed power supply in the 13LO-2S tube designed chiefly for the microsecond range it was possible to achieve a recording speed of $3.4 \cdot 10^{10}$ cm/sec=13c where c is the velocity of light, with 1:F=1:2 [133]. Oscillations with a frequency f=9,500 Mc were recorded with a tube designed for the investigation of short-duration processes. In doing so, maximum recording speed was $6.6 \cdot 10^{10}$ cm/sec=2.2c with 1:F=1:1.

Microoscillographs make it possible to record short-duration processes at a comparatively low linear recording speed which is achieved owing to a small transverse dimension of the electron beam. Therefore, considerable linear movements of the beam on the screen are not necessary to obtain a sharp oscillogram. Microoscillographs have a hot tungsten cathode. The accelerating voltage reaches 30-60 kv. The small transverse dimension of the electron beam is obtained by means of patterning it with diaphragms having small apertures and by means of focusing with magnetic lenses made and installed with high precision. In the Ardenne [135] microoscillograph the transverse dimension of the electron beam is equal to 2 microns. The focusing of the beam is done under a microscope. To record an event the photographic plate is placed inside the oscillograph where a vacuum of 10^{-4} to 10^{-5} mm of mercury column must be created. The tube of the microoscillograph requires continous exhaustion. Not more than 10-15 minutes are required to replace a photographic plate and create vacuum in modern microoscillographs. As many as 100 oscillograms are accomodated on one photographic plate placed in microscillograph. In processing the oscillograms by optical means their dimensions are magnified by 50-100 times. Oscillations with a frequency f=9,500 Mc and good sharpness of the image have been recorded by means of microoscillograph. Microoscillographs are also used for the investigation of processes of longer duration. By magnifying the separate sections of oscillograms it is possible to trace the details of a process which were imperceptible on a conventional electron-beam tube.

"Memory" electron-beam tubes based on the property of dielectrics to retain electric charge for a long period have been of late in the process of development. The main element of such tubes "with memory" is a luminescent screen; a "memory" target placed inside the tube in front of the screen and consisting of a grid on which bits of a hard dielectric are fastened in the form of a mosaic; and two systems for forming the electron beams: a recording system and a scanning system. The recording system consists of the elements of a conventional electron-beam tube (accelerating focusing and beam deflecting elements). The beam of the recording system describes on the "memory" target a curve corresponding to the event being investigated. As a result of considerable secondary electron emission the sections of the mosaic where the recording beam had passed are positively charged. The elec-

tron beam of the scanning system travels over the entire "memory" target but passes through it chiefly where the elements of the mosaic have a positive charge. Thus, a stationary image of a single process is obtained on the screen. This image can be reproduced after several hours or days. The minimum duration of the process which a tube with "memory" can reproduce depends on the current density of the beam of the recording system and on the secondary emission ratio of the elements of the mosaic. At the present time there are electron-beam tubes with "memory" having a speed of up to 10 cm per microsecond [136].

Par. 6.4. Effect of Transit Factor on the Reproduction of Quickly Passing Processes

The electron transit time τ_p in the field of deflecting plates is equal to 10^{-9}—10^{-10} sec for the usual high-voltage oscillograph and may introduce an error when recording quickly passing processes. The effect of τ_p on the measurement error may be determined by using the integral (6.16).

For parallel plane deflecting plates when recording a sinusoidal voltage having an angular frequency ω the sensitivity of deflecting plates decreases in accordance with the following law:

$$h'_0 = h_0 \frac{\sin \frac{\omega \tau_p}{2}}{\frac{\omega \tau_p}{2}} = h_0 \sigma, \qquad (6.22)$$

where h_0 is sensitivity without the effect of τ_p; the function $\sigma = f(\omega)$ is a damped sinusoidal function. The fall-off of the amplitude of the sinusoid by 2 percent ($\sigma = 0.98$) takes place when the frequency $f = \frac{1}{16 \tau_p}$.

The distortion of a short pulse will be the greater the higher the upper limit of the frequencies ω_m usually determined by the leading edge of the pulse. The distortions of a rectangular and triangular pulse may be determined from the expression (6.16). The former is recorded as a pulse with oblique-angled leading edge having a duration τ_p.

In a triangular pulse the initial and the end portion -- each with a duration τ_p -- are distorted, the duration of the leading edge increases, the amplitude decreases and a tail appears. The center portion of the leading edge of the pulses with a duration $(t_f - \tau_p)$ is transmitted without distortion.

The deflecting plates are bent away at the ends to increase the deflection sensitivity. Therefore, it is of interest to determine the effect of τ_p in the case of nonparallel diverging plates. This question was examined theoretically in the work [137].

The author of [137] considers that electric field between the plates remains uniform but decreases along the length of the plate

[illegible] $E_n = \frac{U_n}{d_1 + (d_2 - d_1)\frac{x}{l}}$. (6.23)

where d_1 and d_2 are the minimum and maximum distances between the plates respectively.

For the sake of simplicity we will operate with the quantity v_y inasmuch as deviation on the screen $h \equiv v_y$.

Substituting the equality (6.23) into the expression (6.16) we will find

[illegible] $v_y = \frac{l}{m_0} \int_t^{\tau_n} \frac{U_n\, dt}{d_1 + (d_2 - d_1)\frac{t - t_0}{l} v_x}$. (6.24)

where t_0 is the time before the entrance of electron into the field of deflecting plates.

Inasmuch as $\frac{l}{v_x} \approx \tau_p$, then

[illegible] $v_y = \frac{l}{m_0} \int_t^{t+\tau_n} \frac{U_n\, dt}{d_1 + (d_2 - d_1)\frac{t - t_0}{\tau}}$. (6.25)

We will examine the effect of the transit factor for pulses with a perpendicular leading edge and with a linearly rising leading edge and with a flat top. For a rectangular pulse $U_p = 0$ for $t < 0$ and $U_p = U_0$ for $t \geqslant 0$. If $\tau_p > t_0 > 0$, then

$$v_y = \frac{l}{m_0} \cdot \frac{l \tau_n \ln \frac{d_2}{d_1}}{(d_2 - d_1)\left[1 - \left(\frac{d_2}{d_1} - 1\right)\frac{t_0}{\tau_n}\right]}. \quad (6.26)$$

If $t_0 \geqslant 0$, then v_y reaches a steady-state value

[illegible] $v_{yc} = \frac{l}{m_0} U_0 \frac{l \tau_n}{d_2 - d_1} \ln \frac{d_2}{d_1}$. (6.27)

For a pulse with a linearly rising leading edge having a duration t_f we have:

$$\text{with } t = 0 \quad U_p = 0;$$

$$\text{with } 0 < t < t_f \quad U_p = \frac{U_0}{t_f} t;$$

and with $t \geqslant t_f$ $\quad U_p = \frac{U_0}{t_f} t - \frac{U_0}{t_f}(t - t_f) = U_0$.

With $\tau_p < t_0 < 0$

$$v_y = \frac{l}{m_0} \cdot \frac{U_0}{t_\phi} \cdot \frac{\tau_n}{d_2 - d_1} \left[\tau_n + t_0 - \frac{d_1 \tau_n}{d_2 - d_1} \times \right.$$
$$\left. \times \ln \frac{d_1 + (d_2 - d_1) \frac{\tau_n + t_0}{\tau_n}}{d_1} \right]. \qquad (6.28)$$

With $t_0 > 0$

$$v_y = \frac{l}{m_0} \cdot \frac{U_0}{t_\phi} \cdot \frac{\tau_n}{d_2 - d_1} \left[\tau_n - \frac{d_1 \tau_n}{d_2 - d_1} \times \right.$$
$$\left. \times \ln \frac{d_1 + (d_2 - d_1) \frac{t_0 + \tau_n}{\tau_n}}{d_1 + (d_2 - d_1) \frac{t_0}{\tau_n}} \right]; \qquad (6.29)$$

with $t_0 > t_f$

$$v_y = \frac{l}{m_0} \cdot \frac{U_0}{t_\phi} \cdot \frac{\tau_n}{d_2 - d_1} \times$$
$$\times \ln \frac{\left[d_1 + \frac{(d_2 - d_1)(\tau_n + t_0)}{\tau_n} \right] \left[d_2 + (d_2 - d_1) \frac{t_0 - t_\phi}{\tau_n} \right]}{\left[d_1 + (d_2 - d_1) \frac{t_0}{\tau_n} \right] \left[d_1 + (d_2 - d_1) \frac{t_0 - t_\phi + \tau_n}{\tau_n} \right]}. \qquad (6.30)$$

In Figure 6.5 are shown the beam deflections on the screen calculated in the work [137] for some of the values of t_f and d_2/d_1. The following may be found from Figure 6.5:

1) error increases with an increase of d_2/d_1;
2) the effect of the value of d_2/d_1 decreases with an increase of t_f;
3) increase of the length of the leading edge τ_p does not depend on d_2/d_1.

For plates with the edges bent outward and having a parallel and a divergent section the effect τ_p will be an intermediate effect between the effect produced by τ_p on the parallel and divergent plates, and it will also depend on l_1/l_2 where l_1 and l_2 are the lengths of the parallel and divergent section respectively.

The value of τ_p may be decreased by reducing the length of the deflecting plates, and a deflecting system in the form of two small parallel wires results at the limit. Rudenberg [138] calculated the sensitivity of such a deflecting system.

$$h_0 = \frac{L \operatorname{tg} \alpha}{U_a}. \qquad (6.31)$$

The angle of deflection of the electron beam

$$\alpha = \frac{\pi l'_n}{2U \operatorname{ch}^{-1}\left(\frac{d}{2r}\right)} = \frac{\pi U_a}{2U \ln \frac{d}{r}}, \qquad (6.32)$$

where r is the radius of the small wire and d is the distance between the wires.

Thus, with r=3 mm, d=6mm, L=250 mm and U=20 kv the value of h_0=0.015 mm/volt, and wave impedance z=160 ohms. This type of deflecting system is completely acceptable when recording high-voltage events. But such a deflecting system is useless for recording weak signals because of the low value of h_0.

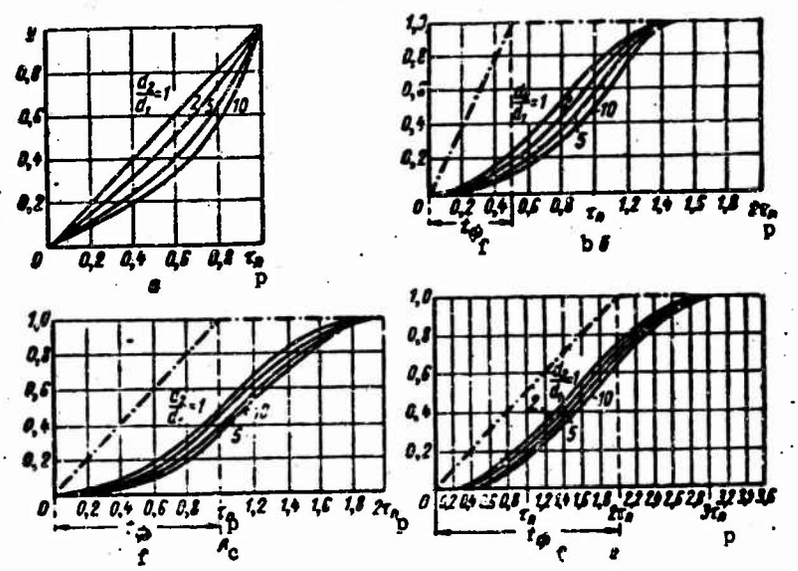

Figure 6.5. Time dependence of deflection on the screen y; t_f — duration of the leading edge of the acting pulse: a — t_f=0; t_f/τ_p=0.5; c — t_f/τ_p=1; d — t_f/τ_p=2.

A deflecting system with traveling wave was created to obtain high sensitivity of the deflecting system with a small value of τ_p. The value of τ_p for a deflecting system made up of coaxial cylinders is small. Such a system is easily matched with the cable over which the event is transmitted. Inasmuch as electric field in such a system is a diverging field, the sensitivity decreases with the withdrawal of the opening in outer cylinder — through which the electron beam passes — from the inner cylinder.

The duration of the time scanning is several times longer than the

duration of the event being investigated and considerably exceeds the τ_p. Therefore, the usual plane deflecting plates with the edges bent outward are used as the time plates.

For the periodically repeating pulses the effect of τ_p may be eliminated by stroboscopic methods of recording. The use of microwave semiconductor triodes and tunnel diodes made it possible to create a stroboscope for recording periodic nanosecond pulses [139]. The pulses being investigated were sent to a gallium-arsenous crystal which became a conducting crystal upon the action on it by another pulse whose duration was much less than the duration of the pulse being investigated. The frequency of the trigger pulses is somewhat lower than the frequency of the plates being investigated. Therefore, the events transmit by turn different portions of the pulse being investigated. The scanning rate is determined by the difference in the repetition rate of the pulses being investigated and the trigger pulses and is low. The stroboscope being described made it possible to record pulses with the shortest rise time of 0.2 nanosecond determined by the duration of the trigger pulse.

Gaddy [140] described a method of measuring the parameters of nanosecond pulses of trapezoidal shape with a high repetition rate without the use of gating pulses. A superposition of the incident and reflected pulse takes place with the aid of a short-circuited cable section. The resultant voltage is defined by the time shift of both pulses, set by the length of the cable section. An RC circuit is connected to the place of superposition of the pulses. The voltage across the capacitor may be measured with a direct-current instrument. The following pulse parameters are determined from the curve of voltage variation on the capacitor according to the time shift of the pulses: the length of the leading edge, the duration of the flat portion, the duration of the voltage fall-off. Time resolution is equal to 10^{-10} sec.

Par. 6.5. Errors Introduced by L and C Parameters of the Tube Plates

Deflecting plates have capacitance C and self-inductance L which bring about oscillations with a natural frequency $f_0 = \frac{1}{2\pi\sqrt{LC}}$. Usually it is considered [2] that a resistance the value of which is defined as $R = \sqrt{2\frac{L}{C}}$ has to be inserted in the circuit of one of the deflecting plates to damp the oscillations.

However, A. I. Sokolik [141] showed that such a simplified approach does not bring to light the optimal conditions for connecting the cable, and proved experimentally that the form of an image on the screen of the tube

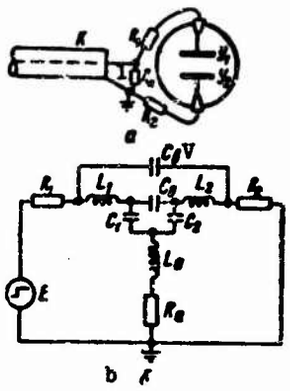

Figure 6.6 Diagram of connection of the cable to the event plates of oscillographic tube (a) and diagram of the substitution network of the recording system (b).

1 -- R_n=load resistance.

depends on where the damping resistance is inserted: in the circuit of the plate to which voltage is supplied and which the author calls "active", or in the circuit of grounded plate (Figure 6.6a). A. I. Sokolik suggested a substitution network for the deflecting system, shown in Figure 6.6b. In this network R_1, L_1 and C_1 are parameters pertaining to the "active" plate, and R_2, L_2 and C_2 — to the grounded plate; C_0 is capacitance between the plates; C_v is capacitance between the inputs; C_1 and C_2 — capacitance of the plates relative to the grounded anode; L_a and R_a — inductance and resistance of the circuit connecting the anode with the "ground" contact. A. I. Sokolik made up a model according to the diagram in Figure 6.5b with an increase of parameters by 1,000 times as against the actual parameters. By selecting the R_1 and R_2 parameters of the model it was possible to obtain the same shapes of the pulses as in the tube (13LO-5A) being tested. This indicates the soundness of the network (see Figure 6.6b). Investigations on the model showed that L_1 and R_1 bring about the distortions to a greater degree than L_2 and R_2. Therefore, first of all it is necessary to decrease L_1, perhaps even by means of a certain increase of L_2. In doing so, it may turn out that cable resistance is sufficient for an active plate. As a rule, a damping resistance is necessary for a grounded plate. The small value of C_v (of the order of picofarads) contributes to the smoothing of oscillations which follow the leading edge of the pulse but a further increase of C_v brings about the appearance of undesirable spike on the flat portion.

Investigations carried out made it possible to select optimum conditions for connecting PYa [plate of the event] of the tube 13LO-5A. In doing so, a pulse with a steep leading edge of 1.1-nanosec duration was recorded. In recording on a tube with a deflecting system in the form of a traveling wave with f_0=5,000 Mc this same pulse had a duration of the leading edge of 0.8 nanosecond.

The frequency of natural oscillations of a deflecting system in the form of two plates brought out to the lateral surface of the tube is equal to 250-600 Mc. For deflecting systems in the form of a two-wire coaxial line or of the traveling-wave type it reaches up to 10,000 Mc.

G. A. Mesyats [14] carried out the calculation of the distortion of the leading edge of a pulse, described by the equation $U=U_0(1-e^{-\alpha t})$ and sent to the PYa [plate of the event] through a capacitive voltage divider (see Figure 6.3d). If the frequency of natural oscillations of the DN [voltage divider] exceeds the f_0 for PYa, then the frequency of the DN-PYa system will exceed the f_0. According to data cited in the work [14] the shortest duration of the leading edge t_{fm} which will be recorded with an error of not more than 10 percent is defined as

$$[t_{\phi m}=t_{fm}] \qquad t_{\phi m}=\frac{9{,}2\,ZC}{k\left[1-\sqrt{1-16\,(0{,}05\sqrt{a}-0{,}01)}\right]}. \qquad (6.33)$$

where k is the scaling factor of the voltage divider; $a=\frac{4\pi^2 Z^2 C^2 f_0^2}{k\,k_L}$.

C is capacitance of PYa; Z — wave impedance of the cable over which the pulse is fed to the divider; k_L -- the ratio of the inductance of the voltage divider-plate of the event (DN-PYa) system to the inductance of PYa.

It is necessary to watch the correctness of matching the cable at the place of its connection to the event plates. A resistance equal to the wave impedance of the cable and inserted between the conductor and sheathing of the cable is ordinarily used for this purpose. Wave impedance of the cable is a function of frequency with a change in which the resistance and inductance of the cable change owing to the appearance of the surface effect and conductance of the cable insulation changes owing to a change in dielectric losses. According to the data in the work [13], for cables with polyethylene insulation and wave impedance of 50 ohms the actual value of the latter at a frequency $f \leqslant 100$ kc is equal to 55 ohms, with $f=10^5$-10^7 it varies from 55 to 50 ohms and with $f \geqslant 10^7$ it remains equal to 50 ohms. Therefore, if a resistance of a certain value is connected to the cable, then complete matching is possible only with a certain frequency. The largest error in measuring the amplitude is equal to five percent. Requirements demanded in regard to the matching resistance are indicated in Par. 5.3. Difficulties in matching increase with a decrease in the duration of the pulse being investigated. Therefore, in recording short pulses, instead of a matching resistance at the event plates it is more expedient to connect a length of cable of the same type as the coupling cable. If the double time of the pulse motion over the cable section exceeds the duration of the pulse, then no especially exact matching of the cable section at the end is necessary.

Par. 6.6. Circuitry of High-Voltage Oscillographs

High-voltage oscillograph consists of the following units: power-supply unit, time-base unit, beam-intensifier unit and external-pulse-conversion unit. Before the arrival of the trigger pulse the electron beam is absent owing to a higher negative potential on the modulator than on the cathode. The trigger pulse acts on the external-pulse-conversion unit which generates a positive-polarity pulse and ignites the beam-intensifier and time-base units. The beam-intensifier unit generates a rectangular pulse of positive polarity and a certain duration, which by acting on the modulator reduces its negative potential. Owing to this, an electron beam appears. The time-base unit generates voltage varying in time and necessary for the time base.

Some of the features of the circuitry of high-voltage oscillographs brought recently to light will be examined in this paragraph. A detailed description of the circuitry of high-voltage oscillographs may be found in the works [1, 2, 22, 35, 127]. Continuous and pulsed voltage is used to supply the electron-beam tubes. Continuous voltage of 10-25 kv for the sealed tubes and that of 30-60 kv for a microoscillograph is received from the rectifier system. Voltage doubling, tripling and quadrupling circuits are used to reduce the dimensions of the last one. The distribution of potentials over the electrodes of electron-beam tube is done with the aid of an active voltage divider whose value $R_d=(0.5-1)U$ megohms, where U is accelerating voltage expressed in kilovolts. Usually pi-shaped filters are employed to decrease pulsation of the supply voltage. Separate parts of the divider may be shunted by capacitances to improve the voltage stability on this section.

The pulsed method of supplying power for electron-beam tubes was suggested and proven by I. S. Stekol'nikov [35]. With a continuous power supply the highest voltage determining the maximum recording rate is limited by discharges within the deflecting system. When supplying the electron-beam tubes with voltage pulses of the order of microseconds they can withstand a voltage which considerably exceeds the permissible continuous voltage. In his experiments I. S. Stekol'nikov applied pulses with an amplitude of 8-27 kv to electron-beam tubes with a rated voltage of 2-3 kv and obtained record-breaking recording speeds: 150 to 200 x 10^3 kilometers/sec. Modern sealed-off high-voltage electron-beam tubes withstand pulsed overvoltages exceeding by 1.5-2 times the permissible continuous voltage.

Capacitance discharge onto an active voltage divider is sometimes used for pulsed supply of the tubes. The value of this capacitance is determined from the following condition

$$[t_н=t_i;\ R_э=R_d] \qquad C=\frac{100\,t_i}{k\,R_\theta}. \qquad (6.34)$$

where t_i is the length of the pulse; k is permissible voltage drop at the

end of the pulse expressed in percent. However, in this case the dimensions of the capacitor and step-up device turn out to be large. I. S. Stekol'nikov, A. Ya Inkov and A. M. Chernushenko [133] used as a pulsed-supply source a pulse transformer with a modulator using a stepped-down voltage. The secondary winding of the pulse transformer consisted of two branches. This made it possible to heat the cathode with a transformer having a low-voltage insulation. However a pulse of accelerating voltage with an amplitude of 35-40 kv had a flat portion small in duration. This made synchronization with the time base difficult.

G. A. Vorob'yov [144] used as a pulsed-supply source a GIN [voltage-pulse generator] employing Arkad'yev-Marks circuit arrangement. A pulse of accelerating voltage with an amplitude of 30-40 kv had a flat portion considerable in duration, and the power-supply unit has small dimensions.

A partial discharge of capacitance through a high-power electron tube may also be used for the same purpose. A. M. Chernushenko used this in creating a high-speed oscillograph.

One of the main requirements in regard to the external-pulse-conversion unit is the short operating time of this unit. Thyratron circuits operate in 100 nanoseconds or more. For this, the pulse being investigated is delayed by means of inserting a cable with a length of 15-20 meters which may bring about a smoothing of the leading edge and attenuation of the pulse being investigated. Tubes with a secondary electron emission have a much shorter operating time.

N. A. Uvarov [146] used a vacuum tetrode with a secondary electron emission; its operating time is about 20 nanoseconds and does not depend on the duration of the trigger pulse in a range of 10-300 nanoseconds with an amplitude of 10 volts.

According to Martin's data [147] the operating time of a tube with secondary emission decreases with an increase of the trigger-pulse amplitude and with a value of the latter of 12 volts the operating time is equal to about 5 nanoseconds.

Two commutators are used in the usual beam-intensifier circuit. Upon the operation of the first commutator the capacitance discharges onto a resistance on which a long-duration pulse is separated. Upon the operation of the second commutator the duration is limited. The minimal duration of the intensifier pulse in this process is determined by the operating time of the second commutator. If however the duration of the intensifier pulse nevertheless exceeds the duration of the time base, then the triggering of the latter is delayed so that the time base would coincide in time with the end of the intensifier pulse. In doing so, it is possible to avoid the gating of the screen from the flyback of the beam.

A short intensifier pulse may be obtained if the resistance onto which

the capacitance discharges through the first commutator is shunted by a short-circuited section of cable. In doing so, the pulse duration will be equal to the double electrical length of the cable section. The triggering time of the beam intensification generator may be short if a tube with secondary emission is used as the commutator. Linear scanning, i.e. the event being investigated is scanned in rectangular coordinates, is usually employed in high-speed oscillographs. In this process the voltage on the time plates PV should change monotonically, without fluctuations. Most desirable of all is a uniform time base when the voltage on the PV changes linearly in time. The degree of nonlinearity of the scanning

$$\delta = \frac{\left(\frac{dU}{dt}\right)_{max} - \left(\frac{dU}{dt}\right)_{min}}{\frac{1}{2}\left[\left(\frac{dU}{dt}\right)_{max} + \left(\frac{dU}{dt}\right)_{min}\right]} 100\%, \qquad (6.35)$$

where $\left(\frac{dU}{dt}\right)_{max}$ and $\left(\frac{dU}{dt}\right)_{min}$ are the maximum and minimum value of the derivative on the time base section.

It is simplest of all to obtain a time-base pulse with a discharge of capacitance onto the resistance through a discharger or thyratron. It is described by the expression $U=U_0 e^{-\frac{t}{RC}}$.

In the time from 0 to t=0.2 RC the value of δ amounts to 20 percent but only about 20 percent of the discharge voltage are used in this process. The necessary voltage for the time base may be obtained by amplification. The linearity of the time base may be considerably improved by inserting appropriate inductance parallel to the resistance. Other networks are also used to obtain more linear time bases. One of such networks is shown in Figure 6.7a. The trigger pulse is amplified by the transformer and brings about the operation of the thyratron. In doing so, the line and capacitance connected to the anode discharge through the thyratron. A rectangular voltage pulse is separated on the resistance, a portion of which is supplied for the intensification of the beam of the tube. Capacitance connected to Z_0 discharges through the line. The paraphase voltage appearing on the connected capacitances is utilized for the time base. The smallest nonlinearity is when $\frac{L}{R^2C}$=0.7 to 0.8. The L, R and C parameters were determined in the calculation; the smallest nonlinearity was achieved in the process of tuning by a slight varying of R and L. The network under consideration made it possible to obtain two scanning rates: 130 cm/microsecond and 400 cm/microsecond. In the former case $R=R'=250$ ohms, $C_1=C_1'=500$ picofarads and $L_1=L_1'=12.5$ millihenries; in the latter case $C_2=C_2'=200$ picofarads, $L_2=L_2'=3.2$ millihenries. The operating instability of this network does not exceed $2 \cdot 10^{-11}$ sec.

Networks with the discharging and charging of capacitances through the

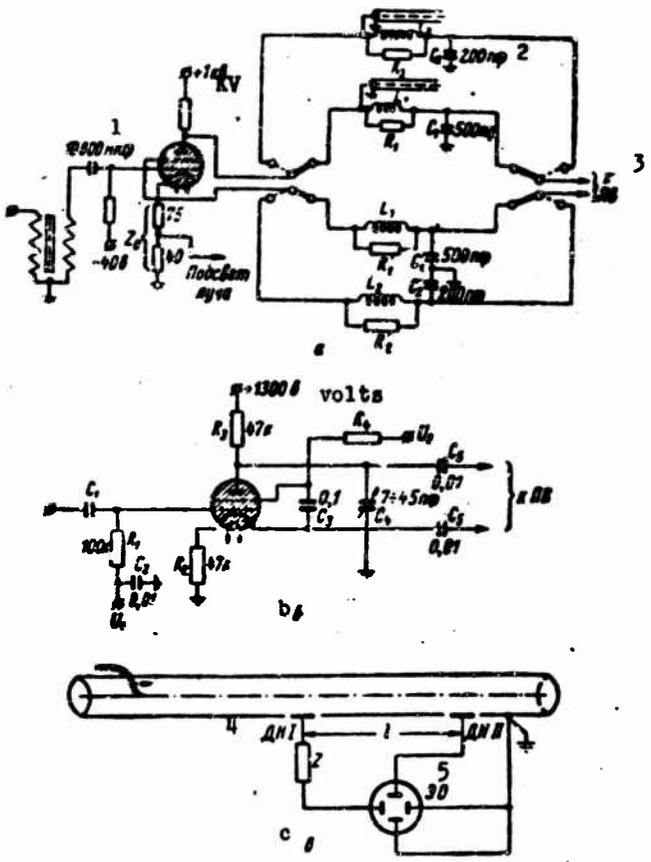

Figure 6.7. Linear-scanning networks (a, b) and diagram of synchronization of event and time base with the aid of a cable and capacitive dividers (c).

Key: (1) Microfarads
(2) Picofarads
(3) To the PV [time plate]
(4) DN=voltage divider
(5) EO=electron-beam oscillograph

vacuum tubes (tetrodes and pentodes) are often used. The voltage on the capacitance changes linearly if the charging or discharge current $I_C = C\frac{dU_C}{dt} =$ =const. The constancy of the current passing through a tetrode or pentode can be achieved if the voltage between the control grid and the cathode remains constant. Therefore, the scanning network using vacuum tubes includes a rectangular-pulse generator and the time-base generator proper.

The scanning rate is determined and controlled by the value of the discharging capacitance. The scanning time is defined as $t_r = \frac{U_0 C}{I_a}$ where

U_0 is the voltage on the capacitance before the discharge, and I_a is the anode current of the tube. The shortest scanning time results when a wiring capacitance equal to 20 piccfarads is inserted as the discharging capacitance. Thus, the shortest duration of scanning is determined by the maximum discharge current I_a of the tube. The tetrode 6P3 provides a current of 1.66 amp, and the pentode GU-50 — a current of 10 amp.

In Figure 6.7b is shown a simplified circuit diagram of the time base of oscillograph described by Martin [147]. The trigger pulse of the necessary duration is shaped by means of a tube with secondary electron emission and is sent through the pulse transformer and capacitance C_1 to the control grid of the tetrode. The latter is triggered and the variable capacitance C_5 (7-45 picofarads) discharges onto R_2 and capacitance of the cathode in relation to the ground. The voltage varying on C_5 is used for the time base.

It was found from experiments that the fastest scanning of 1 nsec/cm results with a zero potential difference between the control grid and the cathode when sending the trigger pulse.

The linearity of scanning was checked in the following manner. The pulse sent to the event plates was delayed by cable sections of different length. Experimental points of the characteristic between the distance from the edge of the screen of the electron-beam oscillograph to the beginning of the pulse and electrical length of the delaying cable fitted well on a straight line. Judging from these data the nonlinearity of the scanning did not exceed a few percent.

Fast scannings may be obtained with the use of commutation characteristic of a spark discharger or thyratron. In doing so, the time plates are connected through the separation capacitances parallel to the commutating device or resistances onto which the capacitances discharge through the commutating devices. In the latter case, the leading edge of the pulses appearing on the resistances is used for scanning. As shown in the preceding chapters, pulses with a length of the leading edge of 10^{-10} to 10^{-9} sec are obtained with the aid of spark dischargers. The use of these pulses will make it possible to obtain scannings with a time on the screen of 10^{-9} sec and less.

L. S. Bartenev, G. V. Glebovich and K. N. Ptitsyn [148] described a high-speed oscillograph. The time-base circuit includes a shaping capacitance of 0.013 microfarads, a tetrode as a commutator, and two lines. Upon sending a trigger pulse through the transformer to the grid of the tetrode the latter is triggered and the shaping capacitance discharges onto one of the connected lines. A pulse with an amplitude of 3 kv, duration of 50 nanoseconds and a length of the leading edge t_f=15 nanoseconds is shaped in this process. A delay cable RK-400 providing the necessary delay of the initia-

tion of the time base. To obtain the fastest scanning the pulse is sent to an artificial line with nonlinear inductances. The principle of operation of the artificial line is described in Par. 3.3. A pulse with an amplitude of 2.8 kv and t_f=1.7 nanoseconds is obtained at the output of the line. Balanced voltage is obtained owing to the grounding of the center tap of a matching resistance inserted at the end of the line. An important component of oscillographic tube is the installation of a diaphragm with a slit behind the deflecting systems. Owing to this, the necessary portion of the leading edge of the pulse arriving at the time plates is selected for the time base. The remaining portion of the leading edge of the pulse is cut off by the diaphragm and in doing so the screen is not lit up. Owing to the transit factor in PV the above-mentioned pulse with a steep leading edge acquires nonlinear sections at the beginning and at the top. Therefore, only a linear section with a drop of 1 kv is utilized out of the entire pulse. Owing to the stabilization of all supply voltages and design measures it was possible to reduce the scanning instability to $1.5 \cdot 10^{-11}$ sec. Using the oscillograph described it was possible to record a pulse with a duration of the leading edge of 1 nanosecond, which occupied the greater portion of the screen.

In recording single processes the synchronization of the oscillograph and of the event must ensure the event's reaching a specified region of the screen. It is difficult to provide proper synchronization when recording periodically repeating pulses. In this process, the spread in the appearance of separate pulses on the time axis must not exceed the width of the spot on the screen.

The method of synchronizing the oscillograph and the process being investigated depends on the controllability or uncontrollability of event. In the latter case the instant of action of the pulse being investigated on the PVa has to be delayed for the period of operation of the oscillograph circuit. In doing so, it is important that the operating time of the oscillograph circuit be stable and short as far as possible since distortions of an event in the cable increase with the length of the latter. In this sense, tubes with secondary electron emission are preferable in comparison with thyratrons.

Different methods of synchronization are employed when recording controllable processes. A high-voltage testing apparatus in which several types of synchronization of the events and electronic oscillograph were tested is described in the work [130] (Figure 6.8). The apparatus contains a GIN using Arkad'yev-Marks circuit and generating a voltage of up to 1,400 kv, an active voltage divider, a shielded room with electronic oscillograph, and a generator for triggering the GIN and oscillograph. Three types of synchronization were investigated.

1. Light Synchronization. A trigger generator was used in this case. A breakdown of the discharger P_1 takes place upon energizing the solenoid. In this process, C_2 discharges onto R_3 and the pulse which

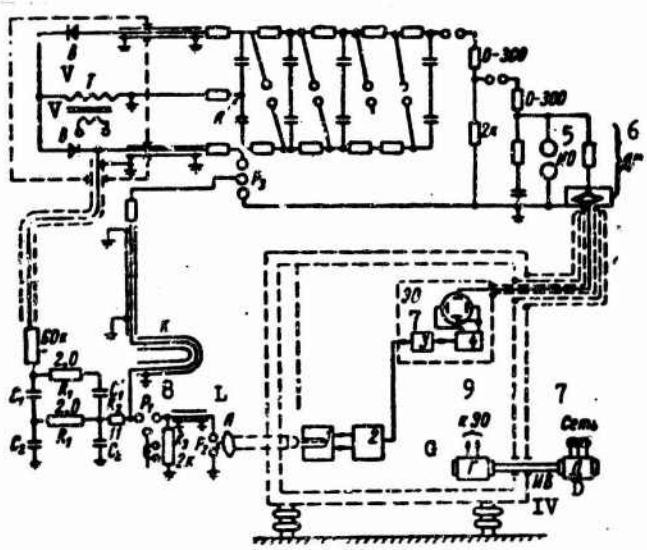

Figure 6.8. Circuit diagram of a high-voltage apparatus for investigating discharger breakdown:

D — motor; G — generator; IV — insulated shaft; L — lens; L — FEU [photoelectronic multiplier]; 2 — amplifier; 3 — 0-15 microsec triggering delay; 4 — time-base unit; 5 — IO=the object being investigated; 6 — DN=voltage divider; 7 — network; 8 — P=discharger; 9 — to the EO [electronic oscillograph]; T — step-up transformer; V — rectifiers; K — delay cable.

appears brings about the breakdown of P_2. The luminescence of the spark in P_2 reaches through the lens L a photoelectronic multiplier placed in a shielded room. The pulse from the output of FEU [photoelectronic multiplier] is amplified and triggers the electronic oscillograph. After the breakdown of P_2 the potential of the center electrode in the three-electrode discharger P_3 of the GIN drops to zero in 0.4 microsecond. This brings about the operation of P_3 and GIN. This synchronization provided a maximum spread of not more than 0.1 microsecond.

2. Delay-Cable Installation. A pulse arriving from the divider triggered the oscillograph and was sent through a 0.4-microsecond delay cable to the event plate. Very stable synchronization resulted. However, delay cable brings about an attenuation of the pulse amplitude by 18 percent.

3. Triggering of Oscillograph from GIN. After the breakdown of P_3 a voltage pulse appears at the point A, which was sent through a resistance and triple-shield cable to the oscillograph and triggered it. The time spread in the appearance of the pulse on the oscillograph screen is smaller than in the first case. However, undesirable oscillations were induced on the leading edge of the pulse on the oscillograph screen in this type of synchronization. Therefore, the authors of [130] selected the first type of synchronization.

An attempt was made in the work [130] to get rid of various inductions which appear with the voltages of hundreds and thousands of kilovolts. Oscillograph is in a separate room with double shielding. The cable running from the divider to the oscillograph has three shields connected together and grounded at the place of connection to the divider. Two external shields are connected respectively to the shields in the room and the inner shield — to the housing of the oscillograph. Power for the oscillograph was supplied from a motor-generator with the generator being in the shielded room and the motor -- outside the room. The generator and motor are connected by a shaft made of electroinsulation material. Displacement of zero line and distortion of the droop during the breakdown of the discharger being tested were discovered when supplying the oscillograph from a separation transformer.

The grounding of the entire apparatus was done at the location of the object being tested. In the absence of a separate ground connection the shielded room acquired a potential of up to 35 kv during the operation of GIN. Therefore, the shielded room was connected by a separate conductor to the common ground. This did not affect the quality of oscillographic recording.

To reduce the effect of currents flowing in the grounding conductors on the quality of oscillographic recording the floor of the high-voltage room was sometimes [149] covered with metal sheets or metal netting which are reliably grounded, and the objects to be grounded are connected by means of short conductors to the grounded floor.

G. A. Vorob'yov, A. I. Golynskiy and G. S. Korshunov suggested a method of oscillographic recording (see Figure 6.7c) of the leading edge of a high-voltage pulse moving over a cable [150]. The pulse being investigated is sent by means of DN II to the event plates PYa, and the voltage taken off from DN II is sent through a certain impedance Z to the time plates. Thus, voltage appears on the PV sooner than on PYa by a time determined by the length of the cable l. Stability of this type of synchronization depends on the properties of the cable and is very high. This is especially important when recording pulses that are repeated at a high rate.

BIBLIOGRAPHY

1. G. V. Glebovich, L. A. Morugin — Formirovaniye Impul'sov Nanosekungdoy Dlitel'nosti /Shaping of Pulses of Nanosecond Duration/. Moscow, Sovetskoye Radio Publishing House, 1958.

2. I. Lewis, F. Wales — Millimikrosekundnaya Impul'snaya Tekhnika /Millimicrosecond Pulse Technique/. Moscow, Izd-vo Inostr. Lit. /Foreign Literature Press/, 1956.

3. O. Burawou — Arch. Elektrotechnic, 16, 3, 205 (1926).

4. H. Schering, W. Raske — ETZ, 56, 27, 751 (1935).

5. L. Binder — Bluzhdayushchiye Volny v Elektricheskikh Setyakh /Stray Waves in Electric Networks/. Moscow — Leningrad. ONTI /Associated Scientific-Technical State Publishing House/, 1935.

6. W. Beindorf — Arch. Elektrotechnic, 32, 10, 634 (1928).

7. O. S. Kolotov Yu. N. Lobanov, N. I. Tulinova — Zh. Tekh. Fiz. /Journal of Technical Physics/, 29, 9, 1173 (1959).

8. K. Kult — Slaboproudy Obzor, 19, 5, 48 (1958).

9. Electronics, 33, 3 (1960).

10. O. E. Delange — Bell System Techn. J., 31 No 1 (1952).

11. K. R. Allen, K. Phillips — Rev. Scient. Instrum., 30, 4, 230 (1959).

12. L. Loeb — Osnovnyye Protsessy Elektricheskikh Razryadov v Gazakh /Basic Processes of Electrical Discharges in Gases/. Moscow, Izd-vo Inostr. Lit., 1950.

13. J. M. Sommerville, J. F. Williams -- Proc. Phys. Soc., 74, 3, 477 (1959).

14. E. Rose — Ann. Phys., 5, 1-5, 15 (1959).

15. T. J. Tucker -- Rev. Scient. Instrum., 31, 2, 165 (1960).

16. A. A. Vorob'yov, G. A. Vorob'yov, G. A. Mesyats, K. K. Sonchik -- Radiotekhnika i Elektronika /Radio Engineering and Electronics/, No 8, 1217 (1959).

17. R. C. Fletcher — Phys. Rev., 76, 10, 1501 (1949).

18. G. A. Mesyats, G. A. Vorob'yov — Izv. Vuzov. Ser. Fiz. /News of Higher Educational Institutions. Physics Series/, No 3, 21 (1962).

19. M. A. Mel'nikov — Elektrichestvo /Electricity/, No 2, 14 (1959).

20. D. Meek, D. Craigs — Elektricheskiy Proboy v Gazakh /Electrical Breakdown in Gases/. Moscow, Izd-vo Inostr. Lit., 1960.

21. L. S. Sirotinskiy — Tekhnika Vysokikh Napryazheniy /High Voltage Technique/, Part 1. Moscow, Gosenergoizdat, 1953.

22. A. A. Vorob'yov, G. A. Vorob'yov et al. — Vysokovol'tnoye Ispytatel'noye Oborudovaniye i Izmereniya /High-Voltage Testing Equipment and Measurements/. Moscow, Gosenergoizdat, 1960.

23. H. Cones — J. Res. Nat. Bur. Standards, 57, 3 (1956).

24. A. Asner — Brown Boveri Mitt., 47.7, 473 (1960).

25. W. R. Baker — Rev. Scient. Instrum., 30, 8, 700 (1959); D. Hagerman, A. Williams — Rev. Scient. Instrum., 30, 3, 182 (1959).

26. A. A. Vorob'yov — Sverkhvysokiye Elektricheskiye Napryazheniya /Super-High Electric Voltages/. Moscow, Gosenergoizdat, 1955.

27. R. C. Fletcher — Rev. Scient. Instrum., 20, 12, 861 (1949).

28. T. A. Voronchev -- Impul'snyye Tiratrony /Pulsed Thyratrons/. Moscow, Sovetskoye Radio Publishing House, 1958.

29. G. I. Skanavi -- Fizika Dielektrikov /Physics of Dielectrics/, Part 2. Moscow Fizmatgiz, 1958.

30. I. S. Stekol'nikov — Priroda Dlinnoy Iskry /The Nature of a Long Spark/. Moscow, Izd-vo AN SSSR /Published by Academy of Science USSR/, 1960.

31. A. A. Vorob'yov — Tekhnika Vysokikh Napryazheniy. Moscow, Gosenergoizdat, 1945.

32. N. A. Kaptsov — Elektricheskiye Yavleniya v Gazakh i Vakuume /Electrical Phenomena in Gases and Vacuum/. Moscow, Gostekhteorizdat, 1950.

33. B. M. Gokhberg — Izv. AN SSSR. Ser. Fiz., 16, 4, 425 (1946).

34. B. M. Gokhberg, E. Ya. Zandberg — Zh. Tekhn. Fiz., 12, 2-3, 65 (1942).

35. I. S. Stekol'nikov — Impul'snaya Ostsillografiya i yeyo Primeneniye /Pulsed Oscillography and its Application/. Moscow, Izd-vo AN SSSR, 1949.

36. T. F. Godlove — J. Appl. Phys., 32, 1589, 8 (1961).

37. M. Druyvesteyn, F. Penning — Rev. Mod. Phys., 12, 2, 87 (1940).

38. M. Steenbek — Wiss. Veröff. Siemens-Werk, 9, 42 (1930).

39. F. Heyman — Proc. Phys. Soc., 63, 1, 361B, 25 (1950).

40. H. Raether — Z. Phys., 117, 5-6, 375 (1941); 117, 7-8, 524 (1941).

41. H. Raether — Ergebn. Exakt. Naturwiss., 22, 73 (1949).

42. H. Raether — Z. Phys., 107, 1-2, 91 (1937).

43. R. Wilson — Phys. Rev., 50, 11, 1082 (1936).

44. M. Newman — Phys. Rev., 52, 6, 652 (1937).

45. G. A. Mesyats — Izv. Vuzov. Ser. Fiz. , No 4, 229 (1960).

46. A. A. Vorob'yov, G. A. Vorob'yov, V. A. Kostrygin — Zh. Tekhn. Fiz., 21, 9, 1135 (1961).

47. G. A. Mesyats, U. Ya. Predneks — Izv. Vuzov. Ser. Energ. /News of Higher Educational Institutions. Power Series/, No 3, 17 (1961)

48. G. A. Mesyats — Elektronnye Uskoriteli. Trudy Tret'yey Mezhvuzovskoy Konferentsii /Electron Accelerators. Works of the 3rd Conference of Higher Educational Institutions/. omsk, TGU Publishing House, 1961.

49. M. Toepler — Ann. Phys., 21, 193 (1906).

50. M. Toepler — Arch. Elektr., 18, 6, 630 (1927).

51. J. Krutzsch — ETZ., 49, 16, 607 (1928).

52. G. Sahner, Z. Wiss — T. H. Dresden, 7, 6, 1225 (1957-1958).

53. S. I. Andreyev, M. F. Vanyukov — Zh. Tekhn. Fiz., 31, 1, 68 (1961).

54. G. A. Mesyats — Pribory i Tekhnika Eksperimenta /Instruments and Technology for Experiments/, No 1, 89 (1963).

55. W. Rogowski, E. Flegler, R. Tamm — Arch. Elektr., 18, 5, 506 (1927).

56. R. Tamm — Arch. Elektr., 19, 3, 235 (1928).

57. K. Buss — Arch. Elektr., 26, 3, 266 (1932).

58. O. Mayr — Arch. Elektr., 24, 1, 15 (1930).

59. B. Knün — Ann. Phys., 3, 5-6, 241 (1959).

60. I. S. Marshak — Usp. Fiz. Nauk /Successes in Physical Sciences/, 77, 2, 229 (1962).

61. W. Rogowski, R. Tamm — Arch. Elektr., 20, 5-6, 625 (1927).

62. B. Gänger — Arch. Elektr., 39, 5, 508 (1949).

63. G. A. Mesyats, Yu. P. Usov — Izv. Vuzov. Ser. Fiz., No 2, 38 (1963).

64. A. A. Vorob'yov, G. A. Vorob'yov, G. A. Mesyats, Yu. P. Usov — Izv. Vuzov. Ser. Fiz., No 5, 174 (1961).

65. G. A. Mesyats — Izv. Vuzov. Ser. Elektromekhan. /News of Higher Educational Institutions. Electromechanics Series/, No 10, 128 (1960).

66. G. A. Mesyats, Yu. P. Usov — Izv. Vuzov. Ser. Energ., No 12, 35 (1961).

67. K. Berger, A. Asner — ASE, No. 51, 769 (1960).

68. W. Weizel, R. Romple — Z. Phys., 122, 9-12, 636 (1944).

69. W. Weizel, R. Rompl — Ann. Phys. 1, 6, 285 (1947).

70. W. Weizel — Z. Phys., 135, 5, 639 (1953).

71. I. S. Abramson, I. S. Marshak — Zh. Tekhn. Fiz., 12, 10, 632 (1942).

72. A. V. Rubchinskiy — Investigations in the Field of Electrical Discharge in Gases. Trudy VEI. M., GEI /Works of All-Union Electrical Engineering Institute. Moscow, GEI/, 63, 1950, p 54.

73. Components and Elements of Radar Systems. Sovetskoye Radio Publishing House, 1952.

74. I. G. Mamonkin — Impul'snyye Usiliteli /Pulse Amplifiers/. Moscow, Gosenergoizdat, 1958.

75. S. I. Lobov, V. A. Tsukerman, L. S. Eyg — Pribory i Tekhnika Eksperimenta, No 1, 89 (1960).

76. B. Gross — Brit. J. Appl. Phys., 1, 10, 259 (1950).

77. G. A. Mesyats — Izv. AN SSSR. Ser. Energet. i Avtomat. /News of the Academy of Sciences USSR. Power Engineering and Automation Series/, No 4, 68 (1962).

78. H. Heard — Rev. Scient. Instrum. 25, 5, 454 (1954).

79. A. V. Gaponov, G. I. Freydman — Zh. Tekhn. Fiz., 36, 3, 957 (1959); Izv. Vuzov. Ser. Radiofiz. /News of Higher Educational Institutions. Radiophysics Series/, 3, 1, 79 (1960).

80. I. G. Katayev — Author's Certificate No 118859. 1959. Udarnyye Elektromagnitnyye Volny /Electromagnetic Shock Waves/. Moscow, Sovetskoye Radio Publishing House, 1963.

81. A. M. Belyantsev, L. A. Ostrovskiy — Izv. Vuzov. Ser. Radiofiz., 5, 1, 183 (1962).

82. A. M. Belyantsev, Yu. K. Bogatyrev — Izv. Vuzov. Ser. Radiofiz., 5, 1, 116 (1962).

83. Ya. S. Itskhoki — Impul'snaya Tekhnika /Pulse Technique/, Moscow, Sovetskoye Radio Publishing House, 1960.

85. Yu. V. Vvedenskiy — Izv. Vuzov. Ser. Radiotekhn. /News of Higher Educational Institutions. Radio Engineering Series/, No 1 (1959).

86. V. A. Auslender, O. G. Il'in, A. M. Shenderovich — Pribory i Tekhnika Eksperimenta, No 3, 81 (1962).

87. N. I. Belorussov, I. I. Grodnev — Radiochastotnyye Kabeli /Radio-Frequency Cables/. Moscow, Gosenergoizdat, 1959.

88. L. N. Loshakov, Ye. B. Ol'der — Radiotekhnika /Radio Engineering/, 3, 2, 12 (1948).

89. E. Williams, E. Schatz — PIPE, 39, 1, 84 (1951).

90. G. Kuchel, E. Williams — Voprosy Radiolokatsionnoy Tekhniki /Radar Engineering Problems/, 5, No 23 (1954).

91. Yu. S. Belozerov — Izv. Vuzov. Ser. Radiotekhn., No 1, 58 (1962).

92. O. N. Litvinenko — Radiotekhnika, 17, 2, 42 (1962).

93. A. T. Starr — Radiotekhnika i Radiolokatsiya /Radio Engineering and Radar/. Moscow, Sovetskoye Radio Publishing House, 1960.

94. Kh. Meynke and F. Gundlakh — Radiotekhnicheskiy Spravochnik /Radio Engineering Handbook/, Vol 1. Moscow, Gosenergoizdat, 1960.

95. G. A. Mesyats — Advanced Scientific-Technical and Production Experience. GOSINTI, Issue 11, No P-62-61/11, 1962.

96. P. Bening — Elektricheskaya Prochnost' Materialov i Konstruktsiy /Electric Strength of Materials and Structures/. Moscow, Gosenergoizdat, 1960.

97. R. W. Cornes — Proc. Inst. Radio Eng., 37, 1, 94 (1949).

98. Kaden H. G. Ellenberg. Arch. Electr. Ubertrag., H. 3, 313 (1949).

99. D. W. Peterson — PIRE, 37, 11, 1294 (1949).

100. V. M. Gorbachev, N. A. Uvarov, L. D. Usenko — Pribory i Tekhnika Eksperimenta, No 2, 92 (1962).

101. B. S. Gal'perin — Neprovolochnyye Soprotivleniya /Nonwire Resistances/. Moscow, Gosenergoizdat, 1958.

102. V. V. Slutskaya — Tonkiye Plenki v Tekhnike Sverkhvysokikh Chastot /Thin Films in Super-High-Frequency Technique/. Moscow, Gosenergoizdat, 1962.

103. P. N. Dashuk — Izv. Vuzov. Ser. Energ., No 3 (1961).

104. G. S. Kuchinskiy, K. M. Irkayeva — Vestnik Elektropromyshlennosti /Herald of Electrical Industry/, No 11, (1961).

105. P. L. Kalantarov, L. A. Tseytlin — Raschet Induktivnostey /Calculation of Inductances/. Moscow, Gosenergoizdat, 1955.

106. V. T. Renne — Elektricheskiye Kondensatory /Electric Capacitors/. Moscow, Gosenergoizdat. 1959.

107. G. A. Theophanis — Rev. Scient. Instrum., 31, 4, 427 (1960).

108. G. A. Mesyats, G. S. Korshunov — Pribory i Tekhnika Eksperimenta, No 4, 123 (1963).

109. A. A. Brish, A. B. Dmitriyev et al. — Pribory i Tekhnika Eksperimenta, No 5, 53 (1958).

110. I. W. Mather, A. H. Williams — Rev. Scient. Instrum., 31, 3, 297 (1960).

111. A. M. Rodin, V. V. Surenyants — Pribory i Tekhnika Experimenta, No 6, 62 (1960).

112. G. A. Vorob'yov — Author's Certificate No 120876, 1958.

113. F. H. Airey — Electr. Rev., 166, 11, 450 (1960).

114. H. Herz — ETZ, No 36, 398 (1917).

115. A. A. Vorob'yov, G. A. Vorob'yov, G. A. Mesyats, A. I. Golynskiy — Pribory i Tekhnika Eksperimenta, No 1, 96 (1962).

116. G. A. Vorob'yov, G. A. Mesyats, Yu. P. Usov — Pribory i Tekhnika Eksperimenta, No 3, 165 (1961).

117. G. A. Vorob'yov, G. A. Mesyats, G. S. Korshunov — Pribory i Tekhnika Eksperimenta, No 2, 93 (1963).

118. G. A. Mesyats, Yu. P. Usov — Izv. Vuzov. Ser. Energ. , No 12, 39, (1961).

119. D. H. Goodman, D. H. Sloan, E. A. Trau — Rev. Scient. Instrum., 23, 12, 766, (1952).

120. G. A. Mesyats, V. V. Kremnev — Izv. AN SSSR. Ser. Energ. i Transp. /News of the Academy of Sciences USSR. Power Engineering and Transportation Series/, No 2, 199 (1963).

121. I. Lewis — Electronic Engng., 27, 332 (1955).

122. A. I. Pavlovskiy, G. V. Sklizkov — Pribory i Tekhnika Eksperimenta, No 2, 98 (1962).

123. S. I. Andreyev, M. P. Vanyukov and V. A. Serebryakov — Pribory i Tekhnika Eksperimenta, No 3, 89 (1962).

124. H. Arribe, Cl. Gary — Bull. Soc. Franc. Électriciens, 2, 21, 494 (1961).

125. B. Geller, A. Veverka — Volnovyye Protsessy v Elektricheskikh Mashinakh /Wave Processes in Electrical Machines/. Moscow, Gosenergoizdat, 1960.

126. P. R. Govard — Tochnyye Elektricheskiye Izmereniya /Exact Electrical Measurements/. Moscow, Gosenergoizdat, 1959.

127. I. Craggs, I. Meck — High-Voltage Laboratory Technique, Lond., 1954.

128. W. Raske — Arch. Techn. Messen., No 90, 166 (1938).

129. I. Ye. Balygin — Elektrichestvo /Electricity/, No 4, 53 (1940); Zh. Tekhn. Fiz., No 10, 12 (1940).

130. C. I. Miller, I. F. Wittibschlager — Commun. and Electronics, No 37, 262 (1958).

131. V. M. Kul'gavchuk, N. A. Protopopov — Pribory i Tekhnika Eksperimenta, No 1, 85 (1960).

132. V. I. Voznesenskiy, N. V. Korotkikh, A. V. Chernetskiy, A. S. Koporskiy — Usp. Fiz. Nauk, 62, 497 (1957).

133. I. S. Stekol'nikov, A. Ya. Inkov, A. M. Chernushenko — Izv. AN SSSR, OTN /News of the Academy of Sciences USSR. Division of Technical Sciences/, 98, 6, 959 (1954).

134. D. R. Hardy, B. Jackson, Feinberg — Electronic Engng, 28, 335, 8 (1956).

135. M. Ardenne — Hochfrequenztechn. und Elektroakust., 54, 6, 181 (1939).

136. A. E. Cawkell, R. Reeves — Electro-techn., 37, 2, 50 (1960).

137. Lotsch H. Frequenz, 15, 5, 163 (1961).

138. H. I. Rudenberg — J. Appl. Phys., 16, 5, 279 (1945).

139. Bell Labs. Rec., 38, 7, 272 (1960).

140. O. L. Gaddy — IRE Trans., 1-9, 3, 326 (1960).

141. A. I. Sokolik — Radiotekhnika i Elektronika, No 10, 1718 (1961).

142. G. A. Mesyats — Izv. Tomskogo Politekhn. In-ta /News of Tomsk Polytechnic Institute/, 122, 145 (1962).

143. I. H. Park — Commun. and Electronics, 37, 343 (1958).

144. G. A. Vorob'yev — Izv. Vuzov. Ser. Fiz., No 4, 174 (1958).

145. A. M. Chernushenko — Radiotekhnika i Elektronika, No 1, 3 (1956).

146. N. A. Uvarov — Pribory i Tekhnika Eksperimenta, No 5, 178 (1961).

FTD-HC-23-643-70

147. E. Martin -- Bull. Eng. Archit., No 43, 19 (1959).

148. L. S. Bartenev, G. V. Globovich, K. N. Ptitsyn -- Pribory i Tekhnika Eksperimenta, No 6, 80 (1961).

149. N. Hylten -- ASEA Journal, 30, 5, 75 (1957).

150. G. A. Vorob'yov, A. I. Golynskiy, G. S. Korshunov -- Pribory i Tekhnika Eksperimenta, No 5, 115 (1963).

1561
CSO: R-12330-D